



**NAVAL
POSTGRADUATE
SCHOOL**

MONTEREY, CALIFORNIA

THESIS

**THE DESIGN AND IMPLEMENTATION OF A
PROTOTYPE SURF-ZONE ROBOT FOR
WATERBORNE OPERATIONS**

by

Manuel Ariza

December 2015

Thesis Advisor:
Second Reader:

Richard Harkins
Fabio Alves

Approved for public release; distribution is unlimited

THIS PAGE INTENTIONALLY LEFT BLANK

REPORT DOCUMENTATION PAGE			Form Approved OMB No. 0704-0188	
Public reporting burden for this collection of information is estimated to average 1 hour per response, including the time for reviewing instruction, searching existing data sources, gathering and maintaining the data needed, and completing and reviewing the collection of information. Send comments regarding this burden estimate or any other aspect of this collection of information, including suggestions for reducing this burden, to Washington headquarters Services, Directorate for Information Operations and Reports, 1215 Jefferson Davis Highway, Suite 1204, Arlington, VA 22202-4302, and to the Office of Management and Budget, Paperwork Reduction Project (0704-0188) Washington, DC 20503.				
1. AGENCY USE ONLY <i>(Leave blank)</i>		2. REPORT DATE December 2015	3. REPORT TYPE AND DATES COVERED Master's thesis	
4. TITLE AND SUBTITLE THE DESIGN AND IMPLEMENTATION OF A PROTOTYPE SURF-ZONE ROBOT FOR WATERBORNE OPERATIONS			5. FUNDING NUMBERS	
6. AUTHOR(S) Ariza, Manuel				
7. PERFORMING ORGANIZATION NAME(S) AND ADDRESS(ES) Naval Postgraduate School Monterey, CA 93943-5000			8. PERFORMING ORGANIZATION REPORT NUMBER	
9. SPONSORING /MONITORING AGENCY NAME(S) AND ADDRESS(ES) N/A			10. SPONSORING / MONITORING AGENCY REPORT NUMBER	
11. SUPPLEMENTARY NOTES The views expressed in this thesis are those of the author and do not reflect the official policy or position of the Department of Defense or the U.S. Government. IRB Protocol number ____N/A____.				
12a. DISTRIBUTION / AVAILABILITY STATEMENT Approved for public release; distribution is unlimited			12b. DISTRIBUTION CODE	
13. ABSTRACT (maximum 200 words) Three dimensional (3D) simulation, Fused Deposition Modeling (FDM) technology and Computer Numerical Control (CNC) milling are used to design and implement a waterborne surf-zone robot prototype. This robot is an autonomous platform meant to be a test-bed for sensors and algorithms for future developments; a key enabler is its modular design. It combines the capabilities of an untethered Remotely Operated Vehicle (ROV) and an Unmanned Ground Vehicle (UGV), being able to transition between the maritime and ground environments. Components for the robot are modeled using Solidworks and later 3D printed or CNC milled in aluminum. A five-spoke Whег variant is used for mobility on land, and three thrusters in a typical ROV configuration (one vertical, two lateral) provide water mobility. Channels to direct water flow around the waterproof cylinder are implemented as a novel way to avoid a through hole for the vertical thruster. Modular design enables platform design modifications and sensors to be changed or added for different missions. All sensible actuators, sensors, cabling and parts are waterproofed to withstand the difficult conditions of the surf zone.				
14. SUBJECT TERMS surf-zone, robot, vehicle, unmanned, autonomous, platform, 3D printing, CAD, robotics, FDM technology, Solidworks, CNC milling, waterproof.			15. NUMBER OF PAGES 173	
			16. PRICE CODE	
17. SECURITY CLASSIFICATION OF REPORT Unclassified	18. SECURITY CLASSIFICATION OF THIS PAGE Unclassified	19. SECURITY CLASSIFICATION OF ABSTRACT Unclassified	20. LIMITATION OF ABSTRACT UU	

THIS PAGE INTENTIONALLY LEFT BLANK

Approved for public release; distribution is unlimited

**THE DESIGN AND IMPLEMENTATION OF A PROTOTYPE SURF-ZONE
ROBOT FOR WATERBORNE OPERATIONS**

Manuel Ariza
Lieutenant, Colombian Navy
B.S., Escuela Naval de Cadetes "Almirante Padilla," 2005
B.E., Escuela Naval de Cadetes "Almirante Padilla," 2012

Submitted in partial fulfillment of the
requirements for the degree of

MASTER OF SCIENCE IN APPLIED PHYSICS

from the

**NAVAL POSTGRADUATE SCHOOL
December 2015**

Approved by: Richard Harkins
Thesis Advisor

Fabio Alves
Second Reader

Kevin B. Smith
Chair, Department of Physics

THIS PAGE INTENTIONALLY LEFT BLANK

ABSTRACT

Three dimensional (3D) simulation, Fused Deposition Modeling (FDM) technology and Computer Numerical Control (CNC) milling are used to design and implement a waterborne surf-zone robot prototype. This robot is an autonomous platform meant to be a test-bed for sensors and algorithms for future developments; a key enabler is its modular design. It combines the capabilities of an untethered Remotely Operated Vehicle (ROV) and an Unmanned Ground Vehicle (UGV), being able to transition between the maritime and ground environments. Components for the robot are modeled using Solidworks and later 3D printed or CNC milled in aluminum. A five-spoke Wheg variant is used for mobility on land, and three thrusters in a typical ROV configuration (one vertical, two lateral) provide water mobility. Channels to direct water flow around the waterproof cylinder are implemented as a novel way to avoid a through hole for the vertical thruster. Modular design enables platform design modifications and sensors to be changed or added for different missions. All sensible actuators, sensors, cabling and parts are waterproofed to withstand the difficult conditions of the surf zone.

THIS PAGE INTENTIONALLY LEFT BLANK

TABLE OF CONTENTS

I.	INTRODUCTION	1
A.	BACKGROUND	2
1.	Previous Designs.....	2
a.	<i>Mobility over Non-trivial Terrain–MONTe</i>	<i>2</i>
b.	<i>Durable Autonomous Robotic Crustacean– DARc</i>	<i>3</i>
c.	<i>DARcII and AXV 5WGen Wheg.....</i>	<i>3</i>
2.	COTS and Research Designs.....	4
B.	CONCEPT OF OPERATIONS (CONOPS).....	6
1.	Constraints.....	9
C.	MOSART DESIGN CONCEPT	10
II.	THEORY AND MAIN COMPONENTS SELECTION.....	13
A.	CONSIDERATIONS FOR MARITIME MOBILITY	13
1.	Pressure (kPa).....	13
a.	<i>Waterproof Cylinder for Internal Electronics</i>	<i>14</i>
2.	Water Tank Test	17
a.	<i>Materials Selection.....</i>	<i>17</i>
3.	Hopkinson Bar and Instron Tests.....	18
4.	Absorption Test	20
5.	Viscosity and Drag.....	25
a.	<i>Skin Friction Drag</i>	<i>27</i>
b.	<i>Form Drag.....</i>	<i>29</i>
6.	Thruster Selection and Configuration	31
7.	Buoyancy and Stability	35
a.	<i>Hydrostatic Equilibrium.....</i>	<i>36</i>
b.	<i>Transverse Stability</i>	<i>38</i>
c.	<i>Water Density and Buoyancy</i>	<i>39</i>
B.	CONSIDERATIONS FOR LAND MOBILITY	40
1.	Land Motors	40
2.	Chain Drives.....	44
3.	Pitch and Speed Ratio	44
4.	Center Distance and Chain Length.....	44
5.	Chain Pitch, Chain Velocity and Platform Velocity.....	45
6.	Power Capacity of Roller Chains.....	46
7.	5WGen Wheg Modification.....	49

III.	DESIGN	51
A.	DESIGN THEORY	51
1.	Power Sources	51
2.	Autonomy Levels for Unmanned Systems (ALFUS)	51
3.	Communications	52
4.	Photo/Video Transmission	53
B.	MOSART DESIGN	53
1.	Water Section	57
a.	<i>Bow End Cap</i>	59
b.	<i>Stern End Cap</i>	61
c.	<i>Middle Section Bottom/Top</i>	61
d.	<i>Electronics Rack</i>	64
e.	<i>Doppler Cone</i>	66
f.	<i>Sail</i>	67
2.	Land Section	68
a.	<i>Bottom Land Skid</i>	71
b.	<i>Upper Land Skid</i>	73
c.	<i>Drive Train</i>	74
d.	<i>Tail Assembly</i>	76
e.	<i>Component Holders and Mounts</i>	77
IV.	CONSTRUCTION AND INTEGRATION	79
A.	PARTS PRODUCTION	79
1.	FDM Parts	79
2.	CNC Milled Parts	80
B.	INTEGRATION	82
1.	Drive Train	82
2.	Sensors, Electronics and Electric Components	84
3.	Waterproofing	86
V.	CONCLUSION	91
A.	PHYSICS	91
1.	Physics Motivated and Drove the Design	91
2.	Pre-production Models	91
3.	Material and Component Selection	91
B.	TECHNIQUE	92
1.	CAD Modeling	92
2.	Component Production	92
3.	Strength Tests	92
C.	EFFICIENT DESIGN	92

1.	Space Efficiency	92
2.	Modularity	92
3.	Amphibious and Terrestrial Capabilities.....	93
4.	Water Protection	93
D.	FUTURE WORK AND RECOMMENDATIONS	93
APPENDIX A. COMPONENTS SPECIFICATIONS.....		95
A.	THRUSTERS	95
B.	MATERIALS	97
1.	ABSplus-P430 (Production Grade Thermoplastic)	97
2.	PC-Polycarbonate (Production Grade Thermoplastic)	98
3.	PH4857 Lab 1 by Garcia and Palacios.....	99
C.	LAND MOTORS.....	109
D.	SPROCKETS	111
APPENDIX B. SKETCHES		113
LIST OF REFERENCES		147
INITIAL DISTRIBUTION LIST		151

THIS PAGE INTENTIONALLY LEFT BLANK

LIST OF FIGURES

Figure 1.	AXV LAB Robot Designs (2001–2015). Platform Design Approaches for the Surf Zone.....	2
Figure 2.	AXV Lab–Wheel-Legs (Whegs) Designs. Different Approaches on Whег Design for the Surf Zone.....	4
Figure 3.	COTS and Research Designs–Terrestrial Propulsion Types. Various Platforms and its Propulsion Type on Land.	5
Figure 4.	COTS and Research Designs–Aquatic Propulsion Types. Various Platforms and their Propulsion Type on Water.....	6
Figure 5.	The Nearshore Environment.....	7
Figure 6.	<i>MOSARt</i> CONOPS.....	9
Figure 7.	<i>MOSARt</i> Concept.....	11
Figure 8.	Pressure in Atmospheres from Various Levels	14
Figure 9.	Waterproof Vessel by CrustCrawler.....	14
Figure 10.	Aviation Waterproof Connectors	15
Figure 11.	Connectors Added on Waterproof Cylinder End Caps	16
Figure 12.	Waterproof vessel test.....	17
Figure 13.	Hopkinson Bar and Instron Tests Results.....	19
Figure 14.	Sparse and Solid FDM Samples T1 and T2 for Test.....	20
Figure 15.	Coating Process on FDM Part T5.....	23
Figure 16.	Drop Test for Doppler Cone T6	24
Figure 17.	Doppler Cone Assembly	25
Figure 18.	Drag Coefficients for Various Shapes.....	26
Figure 19.	Basic Shape and Actual Front Cross-Sectional Area of the Robot	26
Figure 20.	Ideal Form with Skin Surface Detail.....	28
Figure 21.	Drag Curves	29
Figure 22.	CrustCrawler Inc. 400HFS-L Hi-flow Thruster and ESC.....	32
Figure 23.	Thrust (kg) vs. Current (A) Rating at 24V (130W max)	33
Figure 24.	Various Thruster Configurations for ROVs.....	33
Figure 25.	Effects of Vehicle Geometry and Thruster Location on Stability....	34
Figure 26.	Degrees of Freedom (DOF).....	36

Figure 27.	Vehicle’s Longitudinal Righting Moment	37
Figure 28.	Longitudinal Righting Moment Detail	37
Figure 29.	Lateral Righting Moment	38
Figure 30.	Change in Lateral Stability.....	39
Figure 31.	Specific gravity (SG) and vehicle buoyancy.....	40
Figure 32.	Land Motor Waterproofing Scheme and Test	42
Figure 33.	Effects of Motor Heat on Wax Waterproofing.....	43
Figure 34.	Motor Encoder Shaft Cap	43
Figure 35.	Hitachi #25SS Roller Chain–3.048m (10 ft)	48
Figure 36.	<i>MOSARt</i> sprockets.....	49
Figure 37.	Flanged Double Sealed Ball Bearing (Rendered Version)	49
Figure 38.	5WGen(1.5)–(Rendered Version).....	50
Figure 39.	Initial Design Approaches	54
Figure 40.	<i>MOSARt</i> - Final Design (Rendered Version)	55
Figure 41.	<i>MOSARt</i> ’s Principal Axes	56
Figure 42.	Water Section (Rendered Version)	57
Figure 43.	Bow End Cap (Rendered Version).....	59
Figure 44.	Bow End Cap–Back view (Rendered Version).....	60
Figure 45.	Bow End Cap–Front view (Rendered Version)	60
Figure 46.	Bow End Cap Components (Rendered Version).....	61
Figure 47.	Stern End Cap Main Features and Components (Rendered Version).....	61
Figure 48.	Middle Section Features and Components (Rendered Version) ...	62
Figure 49.	Top Middle Section Features (Rendered Version).	63
Figure 50.	Bottom Middle Section Features (Rendered Version).....	63
Figure 51.	Designed Interior Electronics Rack.....	65
Figure 52.	Electronics Rack with all Features (Rendered Version)	66
Figure 53.	Doppler Cone Design Evolution (Rendered Version).....	66
Figure 54.	Doppler Cone Sensor and Features (Rendered Version)	67
Figure 55.	Sail Features (Rendered Version)	68
Figure 56.	Land Section (Rendered Version)	69
Figure 57.	Land Section Sensors and Actuators (Rendered Version).....	71

Figure 58.	Bottom Skid (Rendered Version)	72
Figure 59.	Power Bus Main Components	73
Figure 60.	Upper Skid	74
Figure 61.	Drive Train with Components (Rendered Version).....	75
Figure 62.	Chain Protection Covers.....	76
Figure 63.	Tail Assembly with Components (Rendered Version)	76
Figure 64.	Component Holders and Mounts (Rendered Version)	77
Figure 65.	FDM Process for Stern End Cap	79
Figure 66.	Tool Path Generation and Milling Simulation	80
Figure 67.	CNC Milling Process for Bottom Skid	81
Figure 68.	Top and Bottom Land Skid Fitting Test.....	81
Figure 69.	Drive Train Without Chain–Parts and Assembly	82
Figure 70.	Sprockets Machining to Fit Design	83
Figure 71.	Drivetrain Integration Lab Test	84
Figure 72.	Sensors and Electronics Testing and Characterization.....	84
Figure 73.	Integration Process for Internal Electronics and Sensors.....	85
Figure 74.	Electronic Components Schematic	86
Figure 75.	Cable Connection Potting Process	87
Figure 76.	<i>MOSARt</i> in Final Integration Stage	88
Figure 77.	ABSplus-P430 Properties	97
Figure 78.	PC - Polycarbonate Properties	98
Figure 79.	Maxon Motor RE35 Specifications.....	109
Figure 80.	Planetary Gearhead GP 32 HP	110
Figure 81.	45 Teeth Sprocket Specifications	111
Figure 82.	13 Teeth Sprocket Specifications	112

THIS PAGE INTENTIONALLY LEFT BLANK

LIST OF TABLES

Table 1.	CONOPS Constraints.....	10
Table 2.	CrustCrawler Waterproof Vessel Specifications.....	15
Table 3.	Selected Materials.....	18
Table 4.	FDM Samples Deposition Structure and Absorption Test Results.....	21
Table 5.	Cubes T3 and T4 Absorption Test Results with Coating.....	22
Table 6.	FDM Part T5 Absorption Test Results.....	23
Table 7.	Volumes for Reynolds Number Estimation.....	29
Table 8.	Vehicle Performance Parameters for Different Velocities.....	35
Table 9.	Waterproofing Methods for Land Motors.....	41
Table 10.	Center Distance and Chain Length Calculations.....	45
Table 11.	Vehicle Speed Estimation on Land.....	46
Table 12.	Service Factors (K_1) for Single Strand Roller Chains.....	47
Table 13.	Multiple-strand factors (K_2) for roller chains.....	47
Table 14.	<i>MOSARt</i> Calculated Parameters.....	50
Table 15.	Information Types and Linkages.....	52
Table 16.	<i>MOSARt</i> General Properties.....	56
Table 17.	Bulk Aluminum Material.....	80
Table 18.	<i>MOSARt</i> Milestones.....	89
Table 19.	Thruster Specifications.....	95

THIS PAGE INTENTIONALLY LEFT BLANK

LIST OF ACRONYMS AND ABBREVIATIONS

AAV	Autonomous Amphibious Vehicle
ALFUS	Autonomy Levels for Unmanned Systems
AXV-#WGen	AXV-Number (1 st , 2 nd , 3 rd , 4 th) Wheg Generation
CAD	Computer-aided Design
CJCS	Chairman of the Joint Chiefs of Staff
CB	Center of Buoyancy
CG	Center of Gravity
CNC	Computer Numerical Control
CONOPS	Concept of Operations
COM	Center of Mass
CRUSER	Consortium for Robotics and Unmanned Systems Education and Research
CSA	Crawler Skid Attachment
DARc	Durable Autonomous Robotic Crustacean
DR	Dead reckoning
EC	Environmental Complexity
ESC	Electronic Speed Controller
DOD	Department of Defense
DOF	Degrees of Freedom
FDM	Fused Deposition Modeling
GVW	Gross Vehicle Weight
HDU	High Density Urethane
HRI	Human Robot Interaction/Interphase
HI	Human Independence
IMU	Inertial Measurement Unit
IR	Infrared
MC	Mission Complexity
MONTe	Mobility over Non-Trivial Terrain
MOSART	Mobile Surf-zone Amphibious Robot
NIST	National Institute of Standards and Technology

LBC	Little Benthic Crawler
LOA	Levels of Autonomy / Length Overall
PC	Polycarbonate
PWM	Pulse Width Modulation
RHIB	Rigid-hulled Inflatable Boat
ROV	Remotely Operated Vehicle
SS	Stainless Steel
STL	Stereo Lithography
UGV	Unmanned Ground Vehicle
UMS	Unmanned Systems
UUV	Unmanned Underwater Vehicle/Vessel
vLBC	Vectored Little Benthic Crawler
WP	Waterproof
WW	Weight on each drive wheel

ACKNOWLEDGMENTS

To my Lord and Savior Jesus, for all the blessings, guidance, wisdom and strength that could have only come from you. I have grown personally, spiritually and professionally during this time held in your hands.

Alexandra, my princess, Day and night you were there supporting me and bearing with me; your unconditional and supportive love and encouragement made this possible. You are truly and angel from God.

To my parents, Oscar and Ada Lucia, for allowing my mind to dream and pursue those dreams since I was a child. To Sean, Judith, Tatiana, David and Sebastian, your love and support were always a reason to keep going.

To Oscar Garcia, for being a great friend and co-researcher. I wish you and your family the best for the future.

I give special thanks to the following for their support in the development of this thesis and the time and efforts invested in it: Richard Harkins, Fabio Alves, Steven Jacobs and Daniel Sakoda.

For the knowledge shared in class and labs and the experience, expertise and excellence as professors in the Physics Department: Peter Crooker, Brett Borden, Bruce Denardo, Andres Larraza, Gamani Kurunasiri, Robert Armstead, Richard Harkins and Fabio Alves—all of you contributed in one way or another to the success of this work.

To all my classmates who made this experience a richer and fulfilling one.

To Jhonna and Hanna, for the hours and efforts invested on machining pieces for the robot.

And last but not the least, to Cotecmar and the Colombian Navy for thinking of me as worthy of these privileges and trusting my capabilities as a navy officer and professional.

THIS PAGE INTENTIONALLY LEFT BLANK

I. INTRODUCTION

Robotics, since its first mention in the science fiction short story “Liar!” by Asimov in 1941, have provided a set of unique capabilities to the consumer. These include the ability to automate the production of commercial goods, and in more recent years, have changed the way humans interact with challenging and difficult environments. Additionally, progress in the disciplines of computer science and engineering have made automated manipulators, personal assistants, toys and vehicles nearly ubiquitous to commercial-industry and consumers.

Important users and developers of robotic systems include the military and academia. Both conduct research and development (R&D) as a primary focus. For nearly four decades the results of these efforts have been made available to the private industry and have spurred the rise of private commercial of-the-self (COTS) initiatives resulting in reduced procurement, development and maintenance costs.

Platforms with different modes of operation, and different sensors have been developed for a variety of missions in space, air, surface, underwater and land environments. It is of special interest for the military to have robots operate in various and difficult scenarios, including the transition between land and water for reconnaissance and mine operations, among others.

For more than a decade the Naval Postgraduate School (NPS)–AXV lab has explored the autonomous surf-zone robot as a research topic. Under NPS CRUSER sponsorship and in collaboration with Case Western University, NPS has pursued the development of an amphibious autonomous surf-zone robot capable of operations at land and sea with the mobility to transition between both. Different approaches generated platforms as test beds in an effort to explore an understanding of mobility, communications and autonomy in the harsh

surf zone. The amphibious capability is one of the major design challenges for the surf-zone robot and is the genesis of the work that we now continue.

A. BACKGROUND

1. Previous Designs

Through the years, the approach in design and the levels of autonomy for the NPS prototypes has changed (see Figure 1). Recent designs including MONTe and DARc are discussed below.

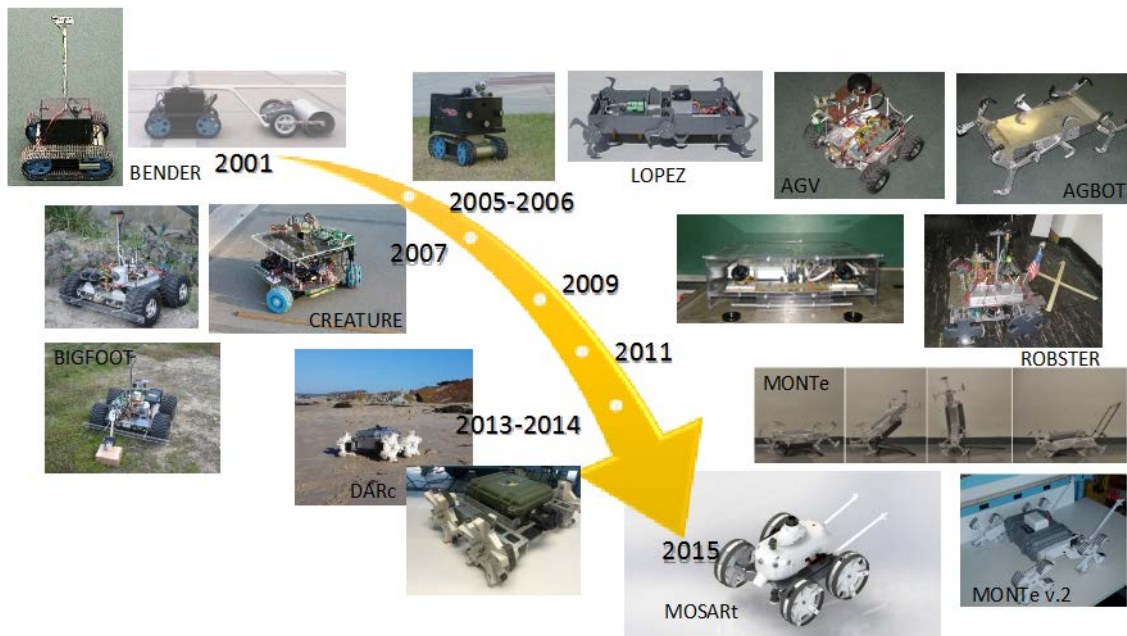


Figure 1. AXV LAB Robot Designs (2001–2015). Platform Design Approaches for the Surf Zone.

a. *Mobility over Non-trivial Terrain–MONTe*

As part of Halle and Hickie’s [1] and Slatt’s [2] theses, a semi-autonomous vehicle was designed, modeled and tested for deployment and operation in coastal environments [1]; Whegs–AXV 3WGen and 4WGen, as shown in Figure 2, and a tail were implemented to provide better mobility with climbing capabilities for obstacles (15.24–19.05 cm) and self-righting using the tail.

In general, the MONTE prototype performed well on hard surfaces and the sand portion of the surf zone; its self-righting and climbing obstacles capabilities proved effective. But waterborne mobility was not possible given the platform had up to 22 breach points [2].

b. *Durable Autonomous Robotic Crustacean–DARc*

As part of Fitzgerald's thesis [3], a Surf-Zone Robot was used for the identification and characterization of rotational inertia and wheel slip parameters. These, in turn, were used to validate the Shuey Dynamic Model [4]. Different scenarios like benign flat terrain and more complicated beach runs were used for the collection of data. Track lengths spanned from 10 to 80 meters, turns up to 180 degrees and inclines of less than 2 degrees. The Shuey model proved reliable for short runs of no more than 10 meters. Including closed loop heading input resulted in significant improvement to the model [3].

c. *DARcII and AXV 5WGen Whег*

As part of Bells' thesis [5], a remote controlled exoskeleton platform was developed and tested for mobility in a beachfront environment. Three wheel-designs were tested during fixed pattern tests on grass, concrete and sand. The Whег–AXV 5WGen, as shown in Figure 2, proved to be the most versatile on various terrains, while the sparse print round wheel showed promise in heavy vegetation. This suggests that a Whег wheel with improved round wheel characteristics would be optimal for various beachfront terrains [5].

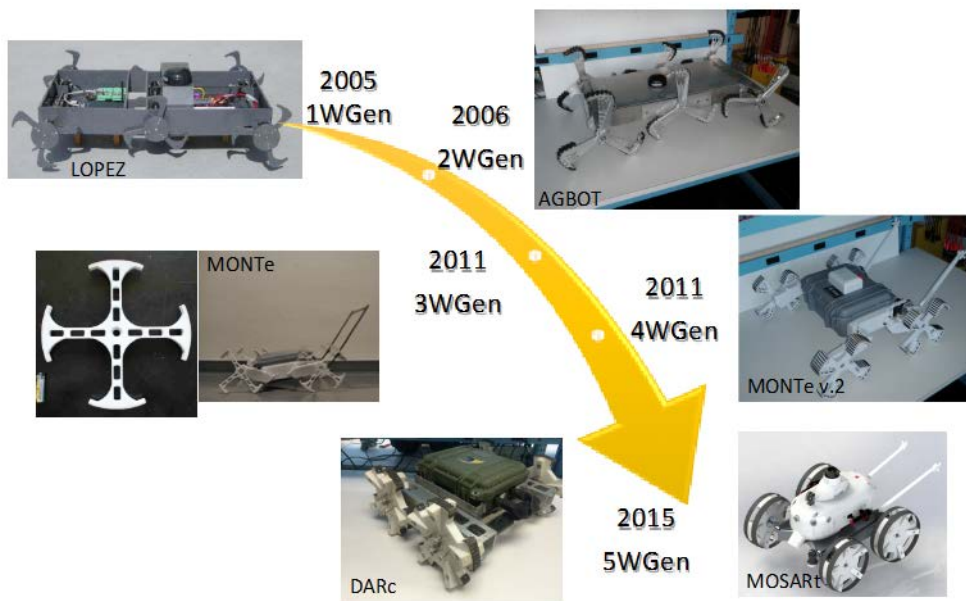


Figure 2. AXV Lab–Wheel-Legs (Whegs) Designs. Different Approaches on Whieg Design for the Surf Zone.

In general, previous designs addressed mobility solutions at shore with some degree of autonomy. Previous designs were not able to enter the surf zone and had limited or no sensors to provide information that would have enabled this capability.

2. COTS and Research Designs

The type of robots developed in the last five to ten years for the surf-zone or marine environment vary in size, means of mobility, levels of autonomy, application, construction and materials, among others.

Many designs are available as platforms and others are still in the concept stage. Figure 3 and Figure 4 show some of the most relevant designs characterized by the type of mobility they use on land and water. Some robots have a combination of terrestrial and aquatic propulsion while others use only terrestrial propulsion, as is the case for most crawlers.

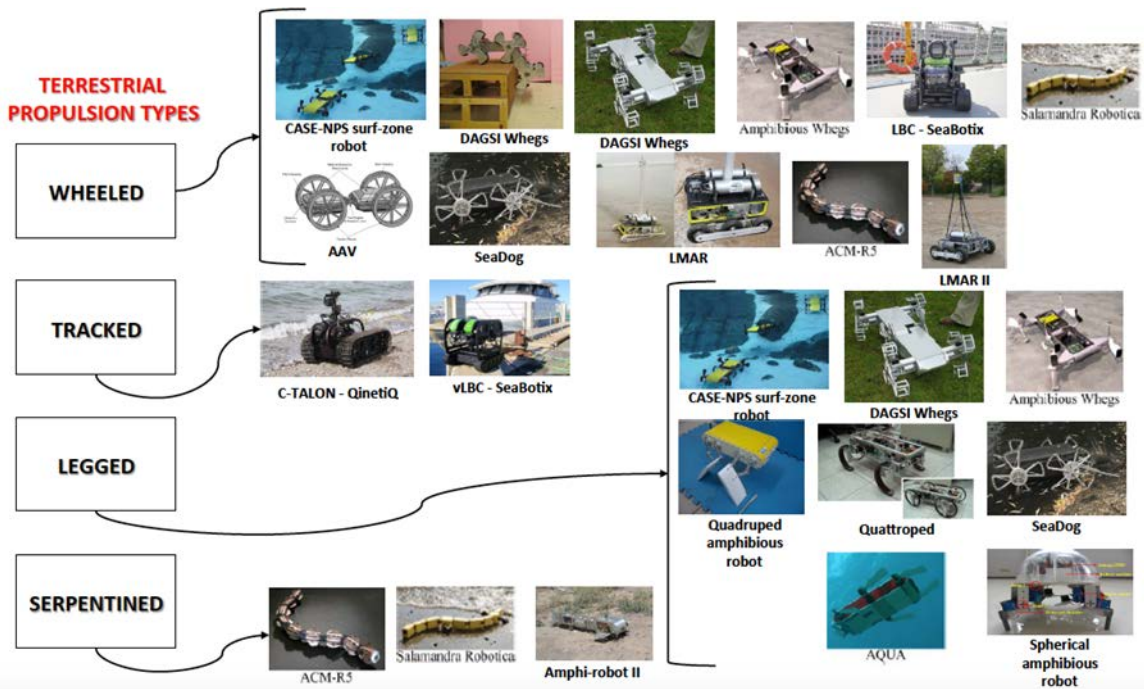


Figure 3. COTS and Research Designs–Terrestrial Propulsion Types. Various Platforms and its Propulsion Type on Land.

Two robotic platforms are in current use for naval, military applications;

- The LBC - Little Benthic Crawler and vLBC - vectored Little Benthic Crawler shown in Figure 3 and Figure 4. Both of these are tethered and are produced by Teledyne SeaBotix [6, 7]. These combine a ROV mounted on a Crawler Skid Attachment (CSA) that uses vortex suction to adhere to surfaces in currents up to 5 knots [6, 7].
- The second design is the C-Talon by QinetiQ North America shown in Figure 3 and Figure 4. This design has been used for years in the U.S. military as Talon and is now suited for the surf zone as a crawler. The robot has a disposable optical fiber spool (up to 3km) for communications with the operator console [8].

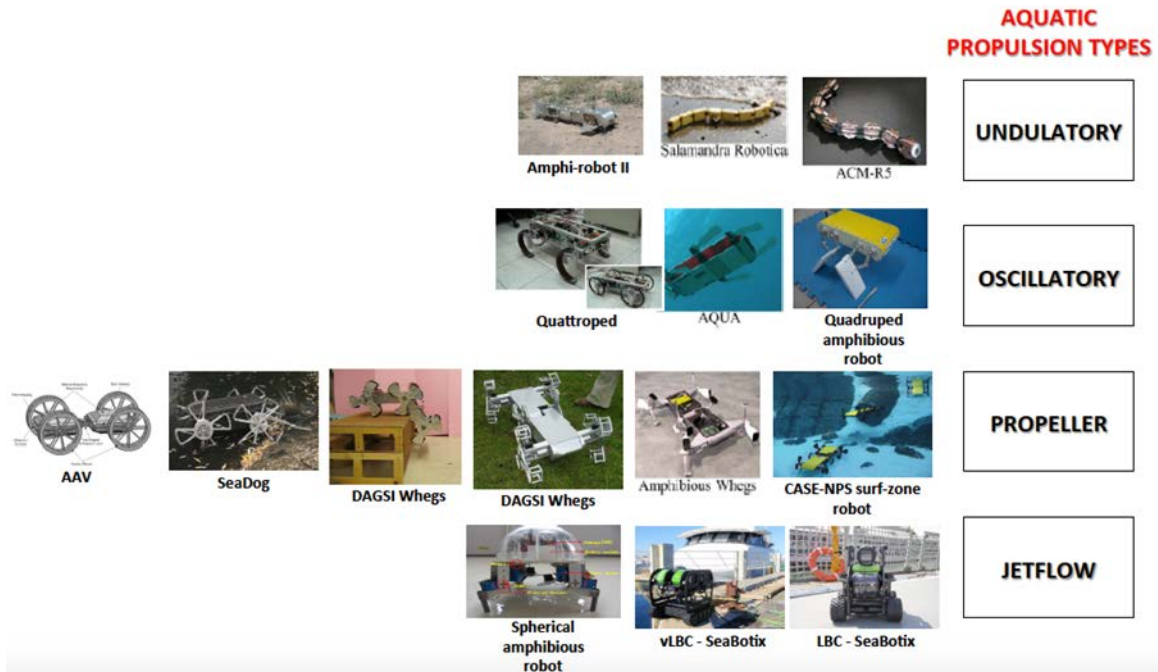
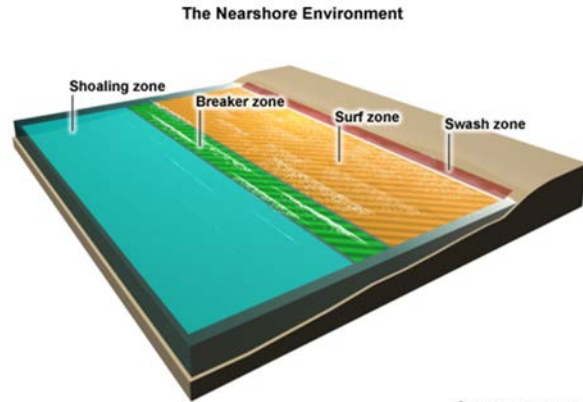


Figure 4. COTS and Research Designs—Aquatic Propulsion Types. Various Platforms and their Propulsion Type on Water.

B. CONCEPT OF OPERATIONS (CONOPS)

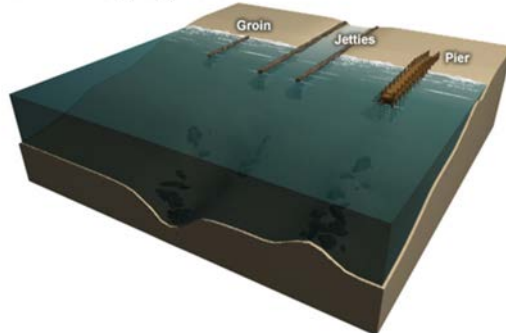
As defined in Joint Publication 1–02 “DOD Dictionary of Military and Associated terms,” the surf line is “the point offshore where waves and swells are affected by the underwater surface and become breakers” [9]. The surf zone is “the area of water from the surf line to the beach” [9]. Both are depicted in Figure 5.



©The COMET Program

(a)

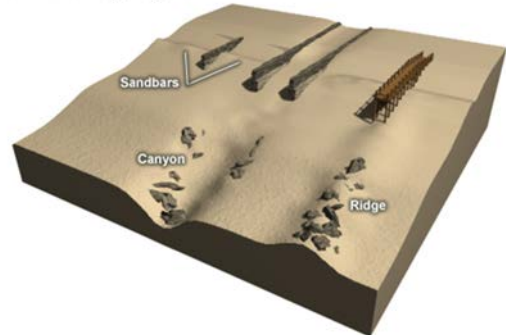
Surf Zone Bathymetry Factors



©The COMET Program

(b)

Surf Zone Bathymetry Factors



©The COMET Program

(c)

Figure 5. The Nearshore Environment

a) The different zones nearshore: Shoaling, breaker, surf and swash. b) Man-made bathymetric structures: Groins, jetties and piers. c) Natural bathymetric features: Sandbars, canyons and ridges. Adapted from [10] The University Corporation for Atmospheric Research. (2004). The Comet Program. (2004). Rip Currents: Nearshore Fundamentals. [Online]. Available: http://www.cityoforangebeach.com/pages/know_your_beach/ripcurrents/near_shore_formation/print.htm#21.

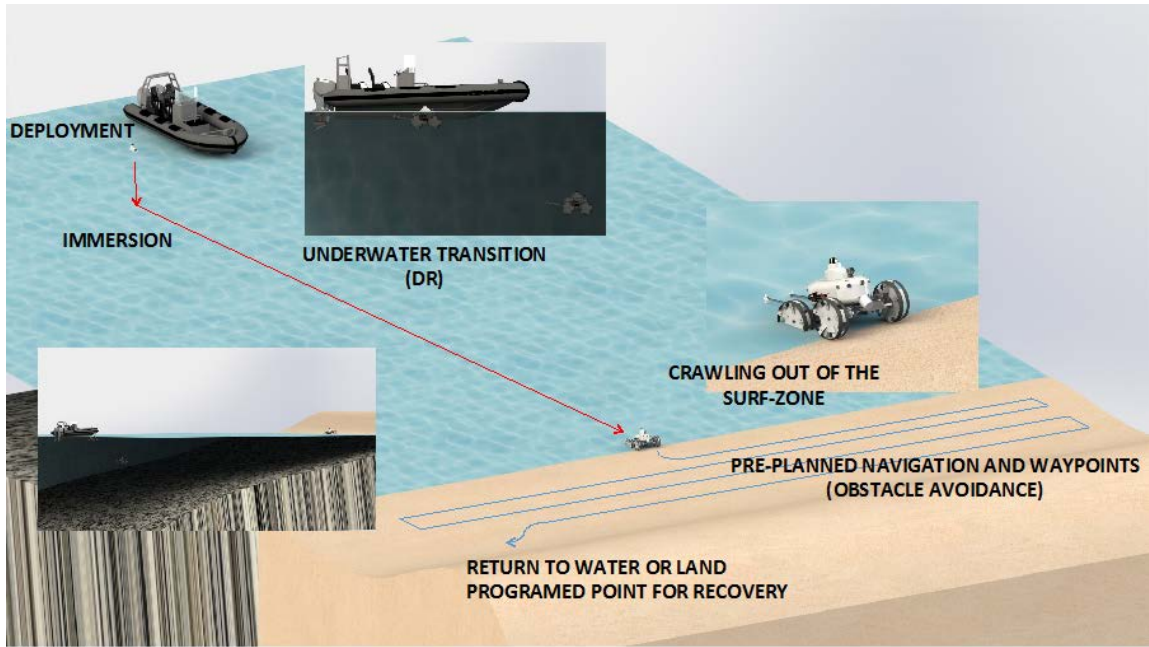
This area is operationally complex, especially when it comes to the use of robots with advanced sensors and capabilities to replace man and animals in the battlefield. The goal is to be able to conduct operational missions in the surf zone with less risk to human lives. As an example, the C-talon [8] provides a limited solution primarily because it is tethered and constrains the operator distance from the area of operation. This constitutes a capability gap [11].

To address the capability gap [11], a higher Level of Autonomy (LOA) is proposed with mid Human Robot Interaction (HRI) after deployment without the use of tether for power or fiber optics for communication.

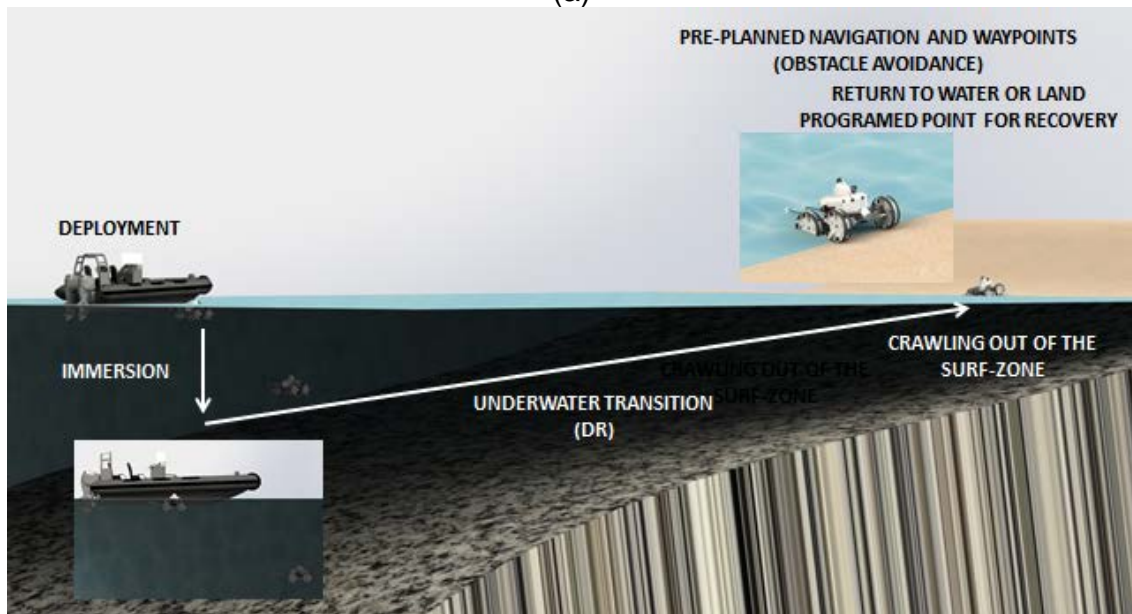
The proposed platform, referred to as the Mobile Surf-zone Amphibious Robot (*MOSARt*), is an autonomous amphibious robot that is able to successfully transition from maritime to the ground environment in the surf zone and perform assigned missions on a beachhead. Initial deployment by forces at sea from a RHIB, small boat or by forces on ground is envisioned. The maritime transition has various modes: semi-submersible, submersible between 1 to 2 meter depth and crawler.

For ground transition, the robot acts as a crawler. The mode of transition depends on the type of bottom, the amount of debris and the level of coyness required for the specific operation.

In the surf zone, the robot uses its sensor suite to perform the assigned missions. Potential field algorithms are proposed as methods to achieve preplanned points and avoid obstacles. Once the primary mission is performed, the robot returns to the initial deployment point for recovery, as depicted in Figure 6.



(a)



(b)

Figure 6. *MOSARt* CONOPS. (a) A broad view of the CONOPS, (b) An underwater view of the CONOPS.

1. Constraints

Limitations, shown in Table 1, are imposed as part of this research for testing and future improvement in accordance with our proposed mission. The

platform is expected to perform above the threshold of limitations set in this section, and these serve as a starting point to assess its performance.

Table 1. CONOPS Constraints

Maritime Transition		Ground Transition	
Sea State	2 (0.1 to 0.5 m waves)	Sea State	2 (0.1 to 0.5 m waves)
Currents	Marine or river below 1 knot	Weather	Day/ night operation
Operational depth	1-2.5 m	GPS Coverage	Not guaranteed
Bottom types	Sandy with occasional rocks	Beach type	2 (Perpendicular wave approach, angle of incidence 1° - 10° with respect the normal to the coastline)

The objective of this research work is to design, assemble and implement an autonomous surf-zone robot for waterborne operations. This research is done in parallel with Oscar Garcia's thesis [12], which focuses on the autonomy, electronic and sensors integration for the robot.

C. MOSART DESIGN CONCEPT

We conceptualize components that will enable the desired capabilities of the robot in order to comply with the CONOPS; the design concept is shown in Figure 7.

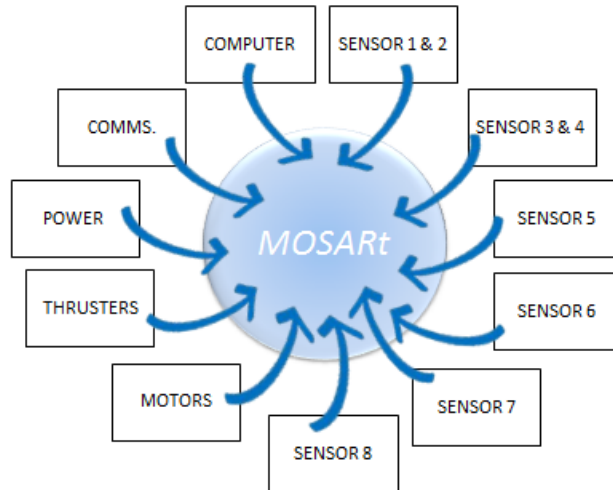


Figure 7. MOSARt Concept

The conceptual parts can be explained as follows:

- Sensor 1 and 2: Forward and aft 180 degrees environment awareness
- Sensor 3 and 4: Velocity on ground and water
- Sensor 5: Depth
- Sensor 6: Potholes detection
- Sensor 7: Attitude and environment detection (land or water)
- Sensor 8: Position
- Motors: Mobility on land
- Thrusters: Mobility on water
- Power: Batteries provide energy for all components; no external tether or connection is required
- Communications: Internal (wired) and external (wireless) communications
- Computer: Provides processing power and integrates sensors, actuators and communications

THIS PAGE INTENTIONALLY LEFT BLANK

II. THEORY AND MAIN COMPONENTS SELECTION

A. CONSIDERATIONS FOR MARITIME MOBILITY

Temperature affects parts and electronics; water chemistry affects seals, cables, produces oxidation that degrades operation of mechanical parts, specific gravity affects the buoyancy and general performance of the robot. In this section the more relevant parameters for an efficient robot design are considered [13].

Key water environment parameters are considered for the operational robot design. These include; salinity, pressure, compressibility, conductivity, temperature, density, depth, viscosity, turbidity, specific gravity among others. Only the more critical ones are addressed as part of this research:

1. Pressure (kPa)

Ocean pressure increases linearly and is referenced to atmospheric pressure at sea-level. For every 10 meters of depth, the pressure increases by one atmosphere, see Figure 8. For this project, pressure is used to provide data or determine the depth of the robot [12].

The vehicle's structure must withstand high pressures without deformation. Additionally, air-filled compartments must withstand pressures at 2.5 meters of depth [12]. Therefore, IP67/IP68 component sealing standards for cables and connectors are required.

Distance		Pressure		
Feet	Meters	ATM	PSI	kPa
18,000	5486	0.5	7.34	50.6
0	0	1	14.7	101.3
-33	-10	2	29.4	202.6
-66	-20	3	44.07	303.9

Figure 8. Pressure in Atmospheres from Various Levels

Pressure in atmospheres (ATM), pound per square inches (PSI) and kilopascals (kPa) for different depths, (feet and meters), for comparison and reference. Adapted from [13] R. D. Christ and R. L. Wernli, *The ROV Manual, A User Guide for Remotely Operated Vehicles*. Oxford, England, Butterworth-Heinemann, 2013.

a. Waterproof Cylinder for Internal Electronics

The CONOPS established an operational depth no greater than 2.5 meters. However, to account for possible malfunctions and future operations at higher depths, a waterproof cylinder for electronics rated for depths up to 45.72 meters was selected (see Figure 9 and Table 2). For additional specifications please refer to [14].

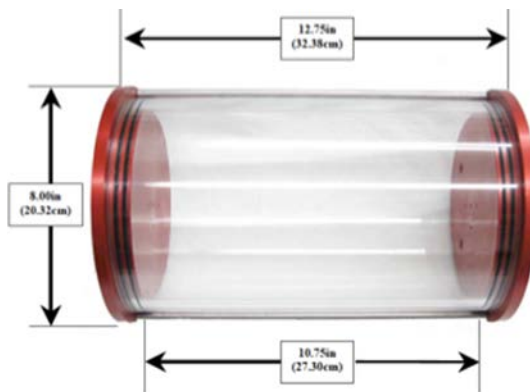


Figure 9. Waterproof Vessel by CrustCrawler

Source: [14] A. Dirks. (2015, June 15). Waterproof Vessel - Technical Guide. [Online]. Available: <http://crustcrawler.com/products/Waterproof%20Enclosure/>.

Table 2. CrustCrawler Waterproof Vessel Specifications

Weight	5.12 kg
Endcap material	Precision machined 6061-T6 aluminum. Red anodize, scratch resistant, hard finish
Cylinder material	Optically clear acrylic
Cylinder dimensions	Length (30.48cm) x OD (17.78cm) x ID (16.51) Depth rating: 45.72 m Overall length: 32.28 cm
Hull penetrators	Sea-Con MicroWetcon Bulkhead Penetrator (7/16 - 20 thread) with 20in. (30.48cm) female connector with Delrin locking sleeve. Each wire can handle up to 14 amps of current All bulkhead penetrators are 8-wire /18 gauge

Source: [14] A. Dirks. (2015, June 15). Waterproof Vessel - Technical Guide. [Online]. Available: <http://crustcrawler.com/products/Waterproof%20Enclosure/>.

Connection to internal electronics, inside the cylinder, required COTS waterproof connectors of 24, 12, 4 and 3 pins, as seen in Figure 10.



Figure 10. Aviation Waterproof Connectors

24, 12, 4 and 3 pin connectors for the waterproof cylinder, these expand the installed capacity of the cylinder to manage all the electronics that are part of the internal electronics.

To include the connectors in the design, the waterproof cylinder end caps are modified using CNC milling as shown in Figure 11.

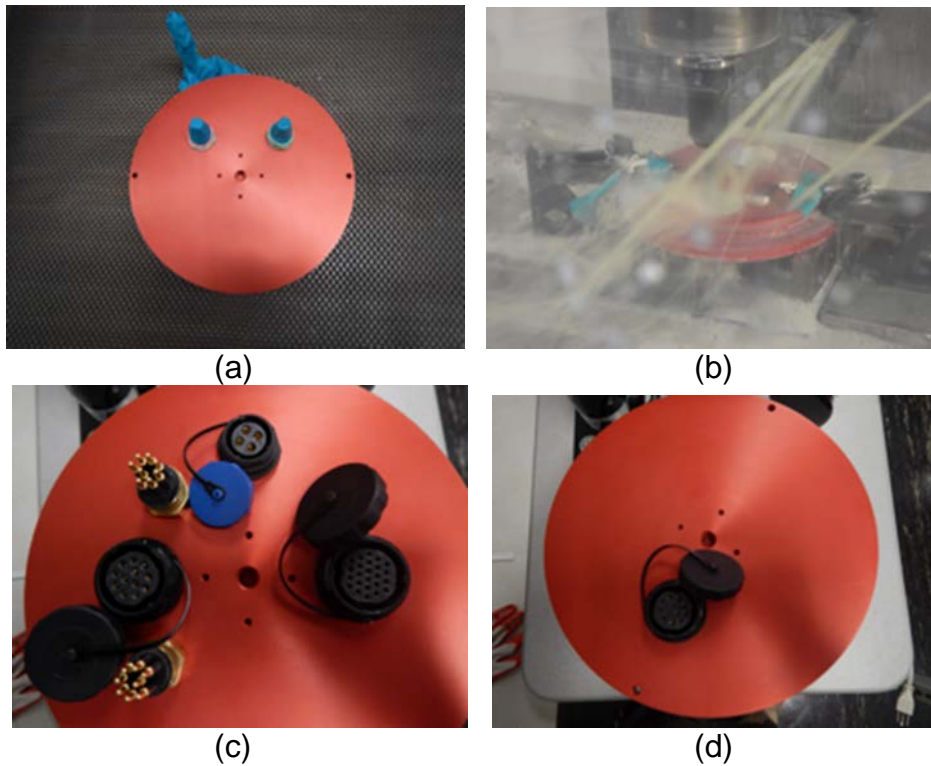


Figure 11. Connectors Added on Waterproof Cylinder End Caps

(a) Bow end cap before CNC milling process with two 8-pin connectors as purchased, (b) Bow end cap during CNC milling process, (c) Bow end cap after CNC milling with additional connectors (24, 12 and 4 pins) plus two 8-pin connectors, total 56 pins to the bow, (d) Stern end cap after CNC milling with additional connector (12 pins).

The internal electronics were built, tested and integrated as part of [12], and incorporated in the design. Care was taken to produce a structure that allowed for the correct fit of all electronic devices housed in the waterproof cylinder.

The internal electronics included the electronics stack, two controllers, two 12V fans to prevent overheating, and a GPS in addition to various cables and connectors.

2. Water Tank Test

The seals for connector modifications to the cylinder were successfully tested in a water tank at a depth of 1.2 meters for 1 hour and 30 minutes. This suggests that the modification did not affect the overall performance of the cylinder for our minimum operational depth, as depicted in Figure 12.

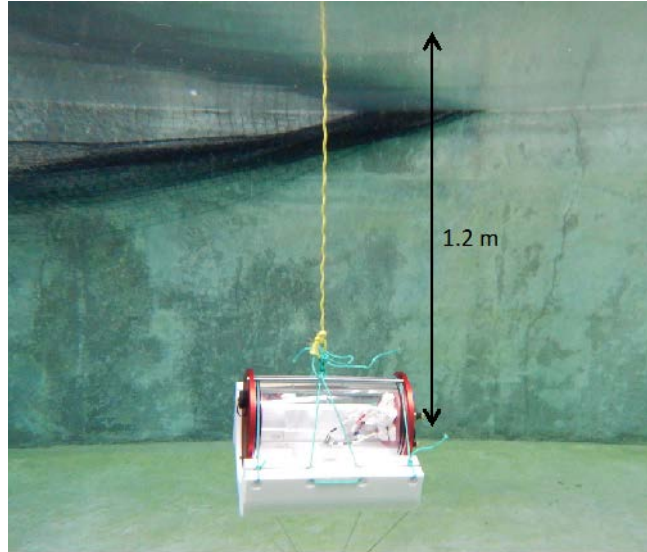


Figure 12. Waterproof vessel test

a. *Materials Selection*

The materials for the platform were selected to meet the minimum platform functionality requirements. Because *MOSARt* is both amphibious and terrestrial, the detail for the design was complex and modular. Consequently, FDM materials, PC and ABSplus-P430, were selected to meet these requirements. Both are production grade thermoplastics from Stratasys, the majority of the parts for *MOSARt* were produced in these materials.

FDM processes are optimized for design modeling with Solidworks CAD (in our particular case). We were able to fast prototype and transition to production for proofs of concept. Aluminum 6061-T6 was selected for the skid

(chassis). These three materials provide adequate structural strength for parts tested at greater depths than the CONOPS established.

Selected material properties related to pressure and density are shown in Table 3. For more detailed information, see Appendix A.

Table 3. Selected Materials

Section	Material	Characteristics
Water section	Stratasys-PC (polycarbonate)	Ultimate tensile strength (XZ): 42 MPa Specific gravity: 1.2
	Stratasys- ABSplus-P430	Ultimate tensile strength (XZ): 33 MPa Specific gravity: 1.04
Land section	Aluminum 6061- T6	Ultimate tensile strength: 310 MPa Specific gravity: 2.7

Properties of materials selected related to pressure and density. Source: [15, 16] PC (polycarbonate), production-grade thermoplastic for FORTUS 3D production systems (Spec sheet). (2015). Stratasys. [Online]. Available: <http://www.stratasys.com/materials/fdm/pc>. ABSplus-P430, production-grade thermoplastic for DESIGN series 3D printers (Spec sheet). (2015). Stratasys. [Online]. Available: <http://www.stratasys.com/materials/fdm/absplus>.

3. Hopkinson Bar and Instron Tests

These tests were performed on FDM solid and sparse samples as part of a lab assignment by Garcia and Palacios, (Appendix A). The principal results are contrasted with a Kevlar sample of similar dimensions (length 1 cm, diameter 1 cm).

Figure 13 shows the final results of these tests and a picture of the final condition of the samples after the Instron test. The J parameter is calculated according to equation 2.1.

$$J = \frac{Y_d}{\rho_o} \quad (2.1)$$

In this equation Y_d is the yield strength and ρ_o is the density of the material.

Kevlar Dynamic Yield [MPa]:	101.51
Kevlar Quasistatic Yield [MPa]:	105.70
Solid 3D Material Dynamic Yield [MPa]:	107.49
Solid 3D Material Quasistatic Yield [MPa]:	58.61
Sparce 3D Material Dynamic Yield [MPa]:	71.12
Sparce 3D Material Quasistatic Yield [MPa]:	45.29
Kevlar Young's modulus E (INSTRON) [GPa]:	3.5
Solid 3D Material Young's modulus E (INSTRON) [GPa]:	2.5
Sparce 3D Material Young's modulus E (INSTRON) [GPa]:	2.2
J Kevlar [k Nm/kg]:	85.91
J solid 3D [k Nm/kg]:	95.16
J sparce 3D [k Nm/kg]:	68.01



Figure 13. Hopkinson Bar and Instron Tests Results

Principal results of the tests and final condition of the samples after Instron test, from left to right (Kevlar, solid FDM and sparse FDM).

Kevlar is a high tensile strength synthetic fiber that is widely used in the industry to reinforce products and in the production of helmets and vests for personal protection. By comparing the FDM samples to a known material we conclude that solid and sparse FDM parts have enough strength for the intended application. A J parameter close to the one of Kevlar gives support to the latter conclusion. For further information in the results of this experiment see Appendix A.

4. Absorption Test

An absorption test is performed on the FDM parts using two samples, see Figure 14. Both measured one cubic inch; one was printed in sparse (sample T1) and the other in solid (sample T2). Deposition structure using FDM when observed under a super zoom camera showed FDM thermoformed tooling porosity in the printed parts, see Table 4.

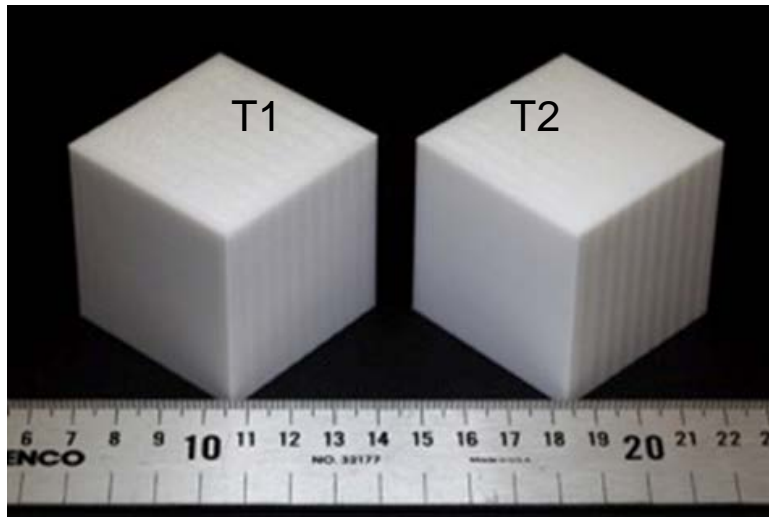


Figure 14. Sparse and Solid FDM Samples T1 and T2 for Test

Table 4. FDM Samples Deposition Structure and Absorption Test Results

	<p>Dry: 145g Soak in fresh water (24hrs): 147g Drying (24 hrs.): 146g Drying (48 hrs.): 146g</p> <p>Solid PC print: Sinks in tap water, absorbs tap water. Approx. 1% weight gain in 24 hrs.</p>
<p>20 x 20 mm–Solid deposition structure–T2</p>	
	<p>Dry: 52g Soak in fresh water (24hrs): 58g Drying (24 hrs.): 57g Drying (48 hrs.): 53g</p> <p>Sparse PC print: Floats in tap water, absorbs tap water. Approx. 11% weight gain in 24 hrs.</p>
<p>20 x 20 mm–Sparse deposition structure–T1</p>	

Samples were submerged in a bucket of fresh water for 24 hours at a depth of 40 centimeters. Water was absorbed by both samples. Drying at room temperature showed water remained in the interior of the samples after 48 hours. It was determined that these parts needed to be sealed and waterproofed. Further tests were performed to provide an inexpensive way to seal parts.

(1) Parts Sealing Test

Two new samples, one sparse (sample T3) and one solid (sample T4), similar to the ones in Figure 14, are used to test coating methods for 3D printed parts. According to Stratasys, the producer of these materials, “the porosity of FDM parts presents an obstacle when used in functional prototypes for direct digital manufacturing applications that require the sealing of gases and liquids.” Various sealing methods have been validated for FDM parts in [17]:

1. Smoothing station
2. Epoxy coating
3. Epoxy infiltration
4. Dipping
5. Painting and filling

Since some parts require a precise fit due to equipment requirements, the first three methods are not feasible. Dipping uses solvents, but the dimensional accuracy is difficult to control and the solvent melting action is quick and aggressive [17].

Therefore, the painting and filling technique was used. Samples were coated separately with a liquid repellent treatment (Rust-Oleum Never Wet–multisurface) and then tested in the same manner as the absorption test. Results are shown in Table 5.

Table 5. Cubes T3 and T4 Absorption Test Results with Coating

Part / type of FDM	Coating	Conditions/Results
1 inch cube / PC solid–T4	Rust-Oleum Never Wet	Dry before coating: 146 g Dry after coating: 149 g Soak in fresh water (2 hours 30 minutes): 149 g Solid print: Sinks in tap water, no water absorption
1 inch cube / PC sparse–T3	Rust-Oleum Never Wet	Dry before coating: 52 g Dry after coating: 55 g Soak in fresh water (2 hours 30 minutes): 95 g Sparse print: Floats in tap water, absorbs tap water. Approx. 72% weight gain in 24 hrs.

Initial tests with the liquid repellent showed that it could be used on solid FDM parts. Additional tests were performed by combining two coatings: a black rubber coating (Plasti-Dip) and a liquid repellent treatment (Rust-Oleum Never Wet–multisurface). An FDM sparse part T5 was coated as depicted in Figure 15. The objective of this test was to verify whether or not additional coats could seal a sparse printed FDM component.



Figure 15. Coating Process on FDM Part T5

(a) FDM part with two layers of black rubber coating (first coating), (b) FDM part with liquid repelling treatment (second coating).

The part absorbed the rubber coating and created an even surface for application of the liquid repellent. The part was then submerged in a water tank for 15 minutes to check the effectiveness of the seal. We noticed that bubbles were forced out of the sealed part and that it gained weight. Table 6 shows the results of this test.

Table 6. FDM Part T5 Absorption Test Results

Coating	Conditions/Results
Plasti Dip and Rust-Oleum Never Wet	Dry before coating: 2540 g Dry after coating: 2614 g Test depth: 1.37m Final weight: 3375 g Sparse print coated: Absorbs water Time submerged: 15 minutes

The FDM part absorbed 29% of its original weight, coating proved ineffective.

Another test was performed on a 34 cm x 34.7 cm x 12 cm FDM T3 part without any coating. With an initial weight of 2540 grams, it was submerged in fresh water at a depth of ten centimeters. The part filled with water in two minutes and thirty-seven seconds with a final weight of 3375 grams. Finally, a test of the Doppler cone FDM (sample T6) part was conducted, see Figure 16. Two tests were performed:

1. Drop test: Using a syringe with needle, droplets are allowed to fall into the surface of the cone from a height of approximately 10 centimeters at different planes and angles of incidence. The action of the treatment on the surface causes the droplets to take spherical shape and roll off the piece without absorption.



Figure 16. Drop Test for Doppler Cone T6

The test shows the formation of water spheroid drops on the flat surface due to the effect produced by the liquid repellent treatment.

2. Submersion test: The piece was submerged in a bucket of fresh water for 2 hours. A change in weight by 3 grams was observed. This is considered negligible for our expected time of operation.

The conclusion is that solid FDM parts coated with the liquid repellent proved effective, while coated sparse FDM parts were not. Sharp edges were problematic for the liquid repellent coating, since a specific angle of incidence

(165°) has to be present for it to work as advertised; Both tests show that the part (test sample T6), Figure 16, is not absorbing significant amounts of water, and complies with the estimated operational time for the *MOSARt*. In Figure 17, we see the assembled parts ready for tank and sea trials.

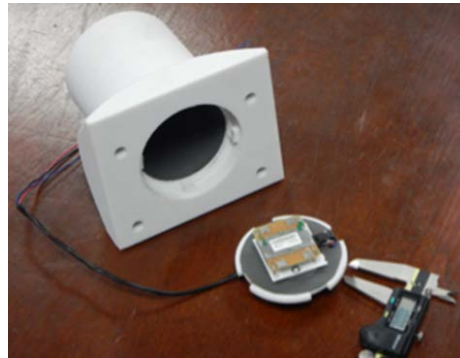


Figure 17. Doppler Cone Assembly

Doppler cone FDM part with anti-radiation material inside, and cabled Doppler sensor on end cap.

It was decided to sparse print all water section components except for the Doppler cone. It was printed solid and coated to keep water out of the cylinder during Doppler sensor operation.

Since sparse print parts absorb water we expect, during initial amphibious operations, for the Center of Mass (COM) to change. The platform will be trimmed to compensate for these changes during fill and drain transitions in the surf zone.

5. Viscosity and Drag

Viscosity measures liquid internal resistance to flow caused by objects moving in a fluid. It is a function of salinity and temperature. Because Drag is a function of density, drag will change in the transition from fresh water to salt water [13]. The density of fresh water is 1000 kg/m^3 and the density of seawater is 1035 kg/m^3 .

For quadratic drag, drag increases as the square of the velocity, see equation 2.4. Drag is also affected by the platform's shape; with a constant volume the vehicle's shape affects the drag force, and is represented by the "drag coefficient" (C_d). Figure 18 shows various shapes mapped to their respective drag coefficients [13].

Shape	Sphere	Hemisphere	Cone	Cube	Angled Cube	Long Cylinder	Short Cylinder	Streamlined Body	Streamlined Halfbody
Direction of water flow									
C_d	0.47	0.42	0.50	1.05	0.80	0.82	1.15	0.04	0.09

Figure 18. Drag Coefficients for Various Shapes

C_d for basic shapes serve as an initial approach to hull design. Adapted from [13] R. D. Christ and R. L. Wernli, *The ROV Manual, A User Guide for Remotely Operated Vehicles*. Oxford, England, Butterworth-Heinemann, 2013, p. 75

With the use of shape comparison from Figure 18, we estimate the drag coefficient for *MOSARt* by mapping the front cross-sectional area ($A=2771.27 \text{ cm}^2$) of the vehicle with the cross sectional area of the short cylinder ($A=5887.97 - C_d$ of 1.15). A linear correlation between the two shapes gives an estimated C_d of 0.54; see Figure 19.

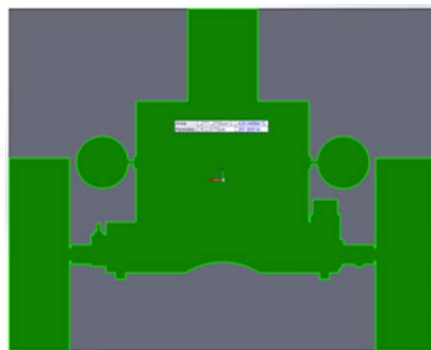


Figure 19. Basic Shape and Actual Front Cross-Sectional Area of the Robot

The basic short cylinder cross-section ($C_d=1.15$) is shown in grey color. In green color is the actual front cross-sectional area of the vehicle ($C_d=0.54$) obtained by linear calculations.

There are two types of drag according to Butcher and Rydill [18]:

a. Skin Friction Drag

Skin Friction Drag occurs between the skin of the surface in contact with the water and the water itself. The flow of water moving tangent to the surface contributes to the resistance. In general this drag is related to the surface area and the flow velocities over the skin. It is important for the design to have minimum sharp discontinuities: these cause negative pressure gradients and increase drag as the flow separates from the vehicle's hull [13].

The Reynolds number (Re), equation 2.2, determines the vehicle's flow characteristics which are related to drag, V is the flow velocity (m/s), l is the characteristic length of the body (m), commonly calculated as the hydraulic diameter d_h (m) using equation 2.3; A is the area section of the duct (m^2), and p is the wetted perimeter (m). ν is the kinematic viscosity ($1.04 \times 10^{-6} m^2/s$ —for seawater and $1.005 \times 10^{-6} m^2/s$ —for fresh water).

$$Re = \frac{Vl}{\nu} \quad (2.2)$$

$$l = d_h = \frac{4A}{p} \quad (2.3)$$

There are three basic types of flow around a body: laminar ($Re < 2300$), transient (approaches critical $2300 < Re < 4000$ where the flow changes from laminar to turbulent) and turbulent ($Re > 4000$). Figure 20 shows a skin surface detail on an ideal vehicle.

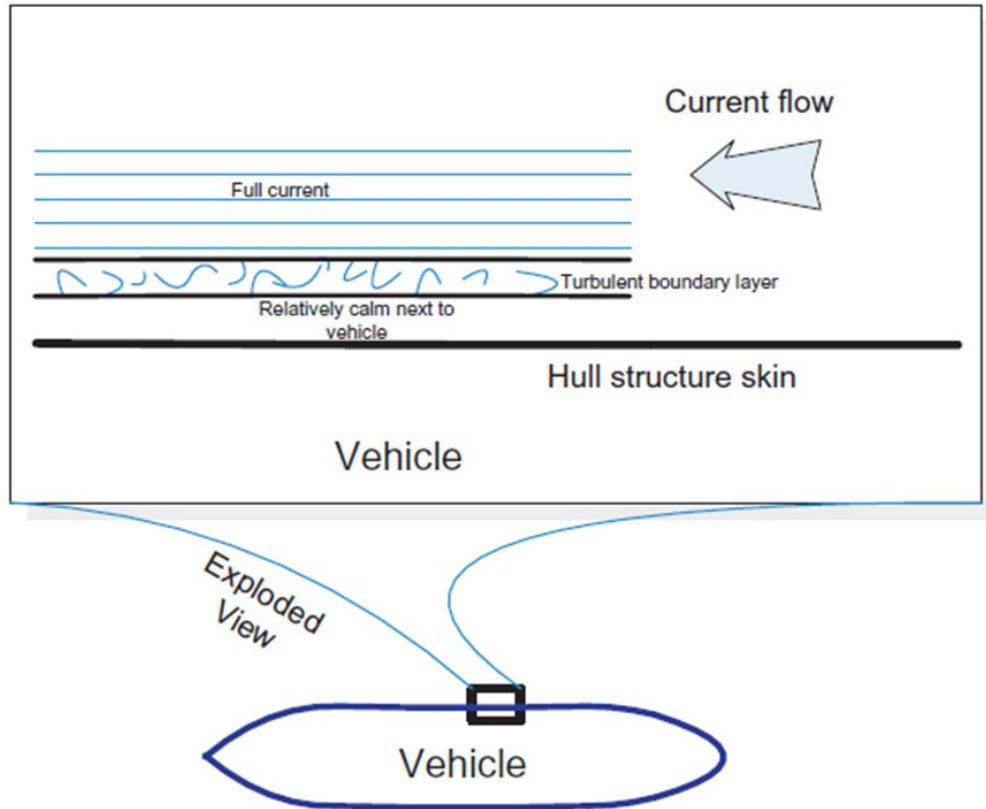
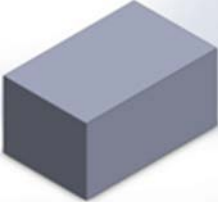
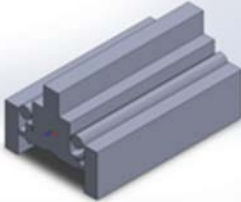


Figure 20. Ideal Form with Skin Surface Detail

In this ideal form the flow closer to the skin is relatively calm, a turbulent boundary layer is created over it allowing a smooth flow of the shape through the fluid. Source: [13] R. D. Christ and R. L. Wernli, *The ROV Manual, A User Guide for Remotely Operated Vehicles*. Oxford, England, Butterworth-Heinemann, 2013, p.80.

Reynolds numbers for the platform are calculated using two approximations: a 3D rectangle that completely encloses the platform and a volume with a shape similar to the front cross-sectional area of the platform with the tail extended, see Table 7.

Table 7. Volumes for Reynolds Number Estimation

Volume approximation		
Description L x W x H	Rectangle (1.350 m x 0.856 m x 0.686 m)	Front cross-sectional area x 1.350 m
Volume [m³]	0.794	0.374
$l = d_h$ [m]	0.762	0.0541
Re	373673 (turbulent)	26529 (turbulent)

The volume of the vehicle is approximated with the shapes observed; the volume is reduced dramatically as the front cross-sectional area is used for the calculations, all volumes, cross sections and perimeters are estimated using Solidworks.

b. Form Drag

As water moves outward it makes room for the robot's body and drag is created. It is a function of the platform cross-sectional area and shape. Typical drag curves are shown in Figure 21.

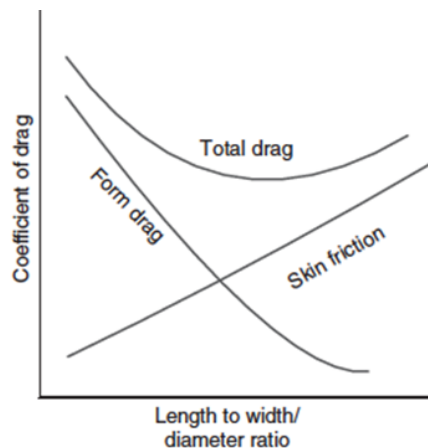


Figure 21. Drag Curves

Typical skin, form and total drag curves for a vehicle. Source: [13] R. D. Christ and R. L. Wernli, *The ROV Manual, A User Guide for Remotely Operated Vehicles*. Oxford, England, Butterworth-Heinemann, 2013, p. 79.

Net thrust to net drag ratio is an important metric. A positive ratio indicates that thrust exceeds the net drag; a negative ratio will require another thruster or a change in design to allow the use of the selected thrusters. To calculate the net thrust, vehicle's drag (D_v) must be calculated.

$$D_v = \frac{1}{2} \sigma A V^2 C_d \quad (2.4)$$

Using equation 2.4 vehicle drag is calculated for different vehicle velocities. In the vehicle drag equation σ as in equation 2.5, is the density of seawater over the gravitational acceleration (1035 kg/m³ and 9.8 m/s² respectively), A is the characteristic area, V is the velocity in (m/s) and C_d is the drag coefficient;.

Another way to calculate the drag is by using the volume of the vehicle to the 2/3 power as shown in equation 2.6 from [13]. In this equation the characteristic area is substituted by the volume (L^3), all other factors remain the same.

Power calculations are performed using equations 2.7 for (P_{REQ}) required power and 2.8 for (P_T) total power. The denominator value of 76 in equations 2.7 and 2.8 is a conversion factor to get the units of power in horsepower (hp). The quantity 6.8 (kg) in equation 2.8 is the amount of thrust provided by the projected thrusters. The multiplicative factor 0.8 included in equation 2.8 accounts for an 80% use with respect to total available thrust. The vendor recommends avoiding running the thrusters at maximum power for long periods of time or permanent damage to the thruster could occur.

$$\sigma = \rho / g \quad (2.5)$$

$$D_v = \sigma (L^3)^{2/3} V^2 C_d \quad (2.6)$$

$$P_{REQ} = \frac{D_v V}{76} \quad (2.7)$$

$$P_T = \frac{6.8 \times V}{76} \times 0.8 \quad (2.8)$$

The difference between the net thrust (T_N) and net drag (D_N) is called excess thrust (T_E) and is calculated using equation 2.9. The acceleration (a) that the thruster provides to the vehicle is calculated according to equation 2.10 where m is the mass of the vehicle.

$$T_E = T_N - D_N \quad (2.9)$$

$$a = (T_N - D_N) / m \quad (2.10)$$

6. Thruster Selection and Configuration

The 400HFS-L Hi-flow Thruster (Figure 22) is fabricated by CrustCrawler and was selected because it provides the required thrust for the vehicle as shown in Table 8.



(a)



(b)

Figure 22. CrustCrawler Inc. 400HFS-L Hi-flow Thruster and ESC

(a) Programmable brushless thruster with principal dimensions; three of this type (two lateral, one vertical) are selected for the platform while on water operation, (b) ESC controller. Source: [19] 400HFS-L Hi-Flow Thruster - Data Sheet. (2015). CrustCrawler. [Online]. Available: <http://crustcrawler.com/products/uov2/index.php>.

Each thruster is controlled by an Electronic Speed Controller (ESC) that uses Pulse Width Modulation (PWM). For thruster specifications, please see Appendix A. Figure 23 provides thrust vs. current ratings as given by CrustCrawler.

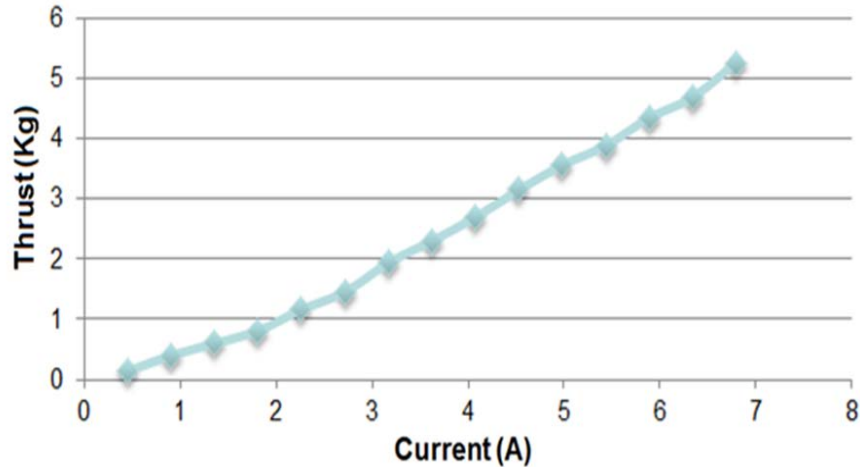


Figure 23. Thrust (kg) vs. Current (A) Rating at 24V (130W max)

Adapted from [19] 400HFS-L Hi-Flow Thruster - Data Sheet. (2015). CrustCrawler. [Online]. Available: <http://crustcrawler.com/products/urov2/index.php>.

Various thruster configurations were studied in an effort to determine appropriate means of propulsion; some are shown in Figure 24.

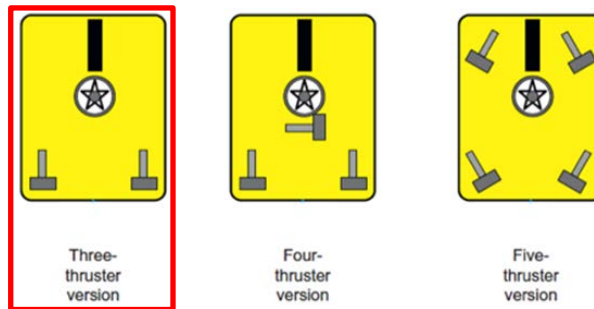


Figure 24. Various Thruster Configurations for ROVs

Three-thruster configuration allows fore/aft and yaw movement. Fourth thruster adds lateral movement. Five-thruster configurations allow any horizontal direction and with various vertical thrusters also pitch and roll. Adapted from [13] R. D. Christ and R. L. Wernli, *The ROV Manual, A User Guide for Remotely Operated Vehicles*. Oxford, England, Butterworth-Heinemann, 2013, p.124.

The dependence of the stability of the platform on geometry and thruster location is shown qualitatively in Figure 25.

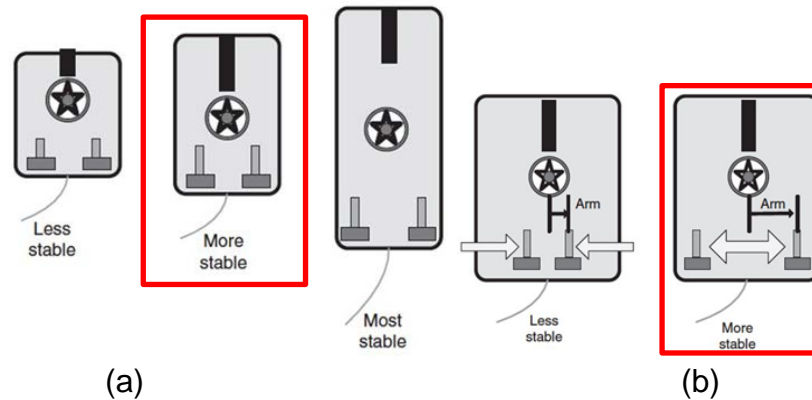


Figure 25. Effects of Vehicle Geometry and Thruster Location on Stability

(a) Vehicle geometry and stability, (b) Thruster placement and stability. Adapted from [20] R. D. Christ and R. L. Wernli, *The ROV Manual: A User Guide for Observation-Class Remotely Operated Vehicles*. Amsterdam, Holland, Butterworth-Heinemann, 2007.p. 26

The three-thruster configuration, in red on Figure 24, was sufficient to support our CONOPS. It minimizes the degrees of freedom (DOF) to surge, heave, pitch and yaw. The single vertical thruster is used to move vertically (heave) and induce platform rotation (yaw) and assists in bearing control while in water. The two lateral thrusters provide translation (surge) and rotation (yaw) as depicted in Figure 26.

With a drag coefficient $C_d=0.54$, front cross-sectional area $A=0.2771\text{ m}^2$, vehicles' volume $L^3=0.067\text{m}^3$, sea water density $\rho=1035\text{ kg/m}^3$, gravitational constant $g=9.8\text{ m/s}^2$, vehicle drag is calculated for different vehicle velocities as shown in Table 8.

Power was calculated using equations 2.6 and 2.7 and listed in Table 8. Entering arguments included a thrust of 6.80 kg and scale factor of 0.8, this restricts thruster power at a safe 80%. The vendor recommends running the thrusters at full power only for a few seconds.

Excess thrust was calculated via equation 2.9. Theoretically the robot can move at a speed of 1 knot in the water. The acceleration that the thruster can provide to the vehicle is then 0.0427 m/s^2 , according to equation 2.10.

Table 8. Vehicle Performance Parameters for Different Velocities

V [m/s]	D_V [kg] using A	D_V [kg] using L^3	P_{REQ} [HP]	P_T [HP]	$T_N - D_N$
0.51	2.0552	1.2235	0.0138	0.0365	0.0227
1.02	8.2208	4.8940	0.1103	0.0730	-0.0373
1.53	18.4968	11.0114	0.3724	0.1095	-0.2629
2.04	32.8833	19.5759	0.8827	0.1460	-0.7366
2.55	51.3801	30.5873	1.7239	0.1825	-1.5414

Velocities in m/s corresponding to 1–5 knots, vehicle drag (D_V) in kilograms, power required (P_{REQ}) and power provided by the thruster (P_T) in horsepower; net thrust and net drag difference ($T_N - D$) in horsepower. Vehicle's drag calculated using the robot's volume is no further used in the calculations and is performed only for comparison. The prototype is able to move in the water at an approximate speed of 0.51–0.77 m/s (1-1.5 knots) according to these calculations.

7. Buoyancy and Stability

Typically, an underwater vehicle moves with 6 degrees of freedom (DOF): three translations and three rotations, as shown in Figure 26 and Figure 27. Translation and rotation are controlled via actuators [13]. According to this, our platform has 3 DOF (surge, heave and yaw). Roll and pitch require trimming with ballast prior to operation.

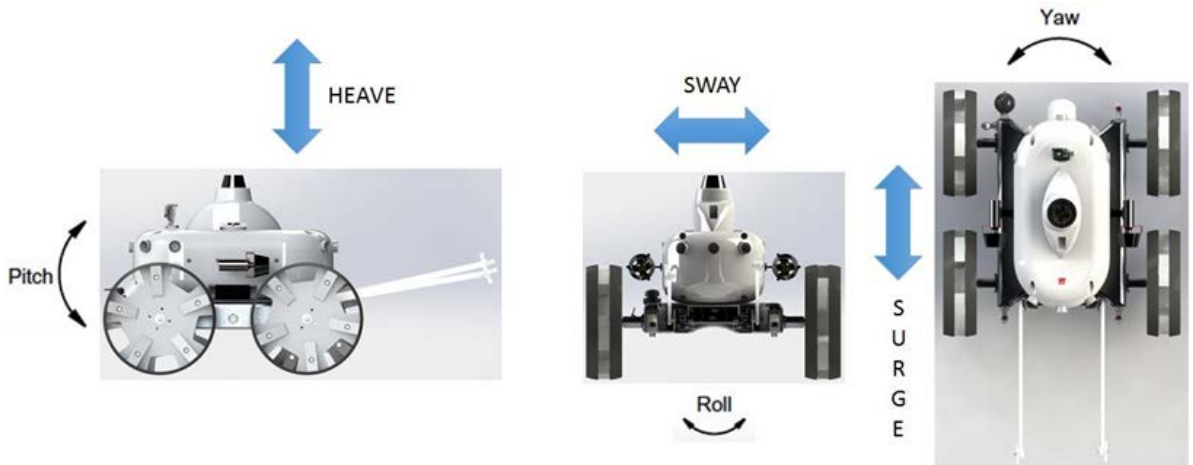


Figure 26. Degrees of Freedom (DOF)

6 DOF are depicted, not all are part of the *MOSARt* design, these are restricted to the number and configuration of the actuators selected. 3 DOF are designed for the *MOSARt* (surge, heave and yaw). Pitch and roll are trimmed by ballast prior to operation, and sway is not considered, it would require a fourth thruster.

a. Hydrostatic Equilibrium

Archimedes' principle states that a force equal to the weight of the displaced fluid buoys up a body partially or totally immersed in a fluid. All weight forces are centered in a point in the body called center of gravity (CG). The resultant forces that counteract the downward pull of gravity through the CG are located in the center of buoyancy (CB). For completely submerged, neutrally buoyant vehicles the distance between CB and CG are considered for horizontal stability. Metacentric height becomes relevant for a semi-submersible mode of operation [13].

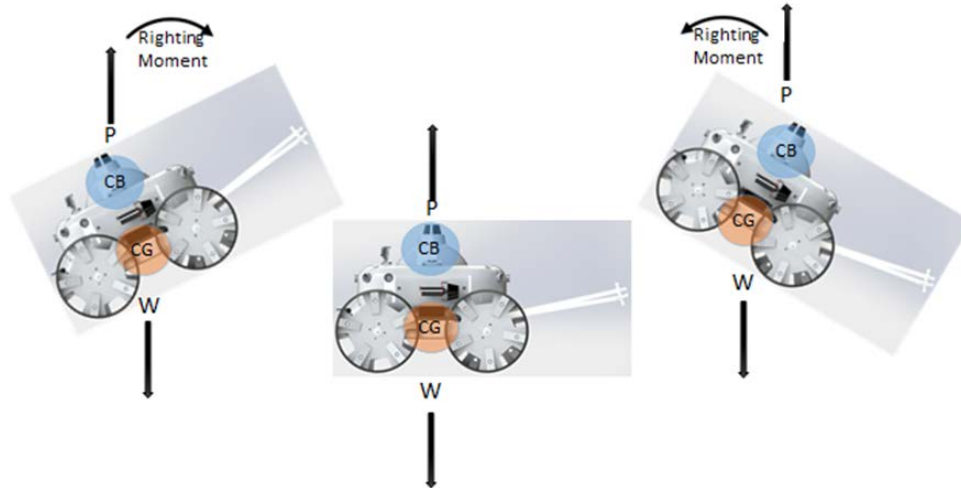


Figure 27. Vehicle's Longitudinal Righting Moment

Righting moment is shown in the figure. This is the ideal case for an underwater vehicle, as part of the research the correct location of the CB and CG are addressed in the design. Platform is to be trimmed prior to operation to assure static equilibrium.

For stability the vehicle must have a high CB and a low center of gravity CG, this allows a righting moment, see Figure 27 and Figure 28. If the distance between CB and CG called BG, becomes smaller, the righting moment decreases logarithmically until stability is lost [13].

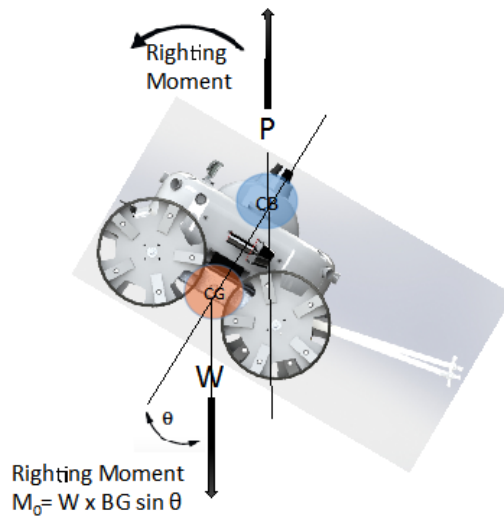


Figure 28. Longitudinal Righting Moment Detail

b. Transverse Stability

Lateral stability is governed by the position of CG and CB in the vehicle. Horizontal displacements of the CB relative to the CG in the vehicle's reference frame will produce righting moments [13], as shown in Figure 29.

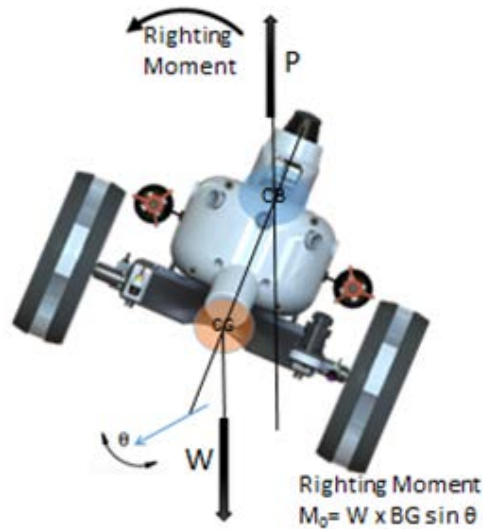


Figure 29. Lateral Righting Moment

Horizontal displacements, caused by the different components of the vehicle make the CB and CG lose co-linearity as the robot inclines and are separated by a distance d that is a function of the angle of inclination. CB and CG remain the same and equal to the vehicle's weight, but their moment is $(W \times d)$ and is also function of the roll angle (θ). Trimming is the alignment of the CB and CG; this is a key step to have proper stability for water operation (Figure 30).

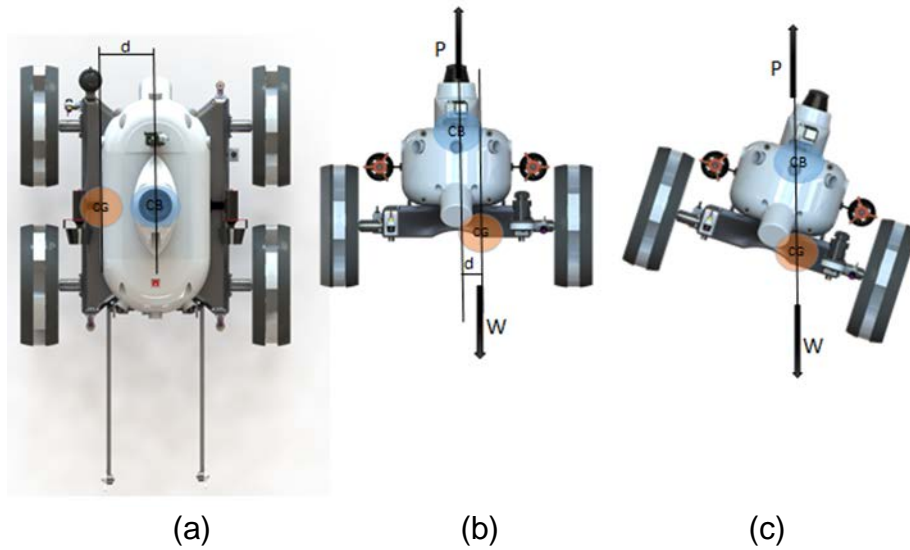


Figure 30. Change in Lateral Stability

Figure 30 shows how lateral stability changes if the vehicle is not correctly trimmed to align CG and CB. (a) Top view of CG and CB loss of co-linearity, (b) Front view of CG and CB loss of co-linearity, (c) CG and CB realigned with vehicle now heeling to port.

Two types of moments are then specified: the righting moment (force rotating the vehicle about CG goes in opposite direction to the inclination) and the heeling moment (force goes in the same direction to the inclination) [13].

c. Water Density and Buoyancy

Desired buoyancy, depends on the selected mode of mobility in water: semi-submersible (positively buoyant), submersible (neutrally buoyant) or crawler (negatively buoyant), in Figure 31. This is achieved by attaching a buoyancy device to the structure or adding ballast if required. In either case the platform is trimmed prior to operation.

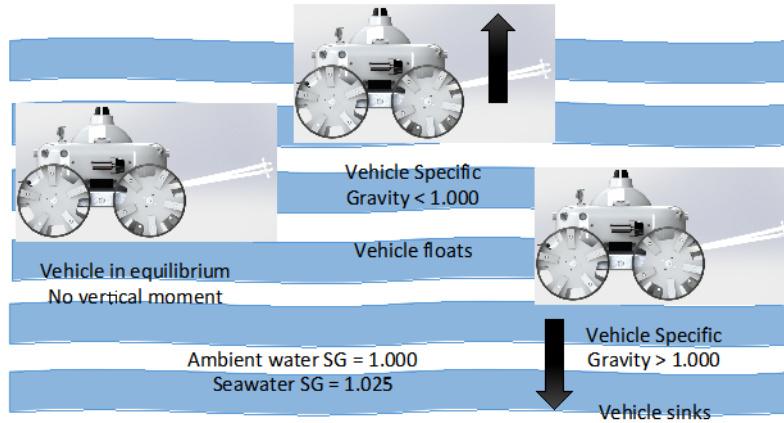


Figure 31. Specific gravity (SG) and vehicle buoyancy

Sparse FDM parts are positively buoyant even after they are filled with water. Solid FDM parts are negatively buoyant before and after they are filled with water. Solid FDM parts like the Doppler cone, aluminum parts like the skid and partially the 5WGen(1.5), sensor, cables, electrical and mechanical components will affect the equilibrium and stability of the vehicle. Their placement impacts the operational trim of the vehicle.

B. CONSIDERATIONS FOR LAND MOBILITY

The selection of land drivetrain components is linked to the size of the platform and the location of the principal components. Motors, chains, ball bearings and sprockets are the choice for the land drivetrain. These components are made of stainless steel to avoid corrosion and to withstand the harsh conditions of the surf zone.

1. Land Motors

MOSARt uses two Maxon 406166 motors. These motors have a high power planetary gear head that is:

- 32 mm in diameter
- Rated at 4–8 Nm torque load.
- Provides 90 watts of power with graphite brushes

For specifications on the motor and gear head, see Appendix A. The motors had to be waterproofed to protect them from the wet surf-zone environment. Three motors were waterproofed and tested. The results are shown in Table 9.

Table 9. Waterproofing Methods for Land Motors

Motor	Coatings / protection applied	Comments	Test result
Maxon motor	Scheme A: Rubber coating / wax / FDM jacket	Only shaft exposed	Passed
Maxon motor	Scheme A: Rubber coating / wax / FDM jacket	Gearbox and shaft exposed	Passed
Maxon motor	Scheme B: Rubber coating, electric tape, liquid electric tape	Liquid electric tape on contacts only	Passed

Different schemes for waterproofing are applied for testing on three similar electric motors.

Motors were prepared according to the protection scheme in Table 9, and then connected and tested. The tests included:

- A bucket test: Immersion in 40 centimeters of water for three days.
- A water tank test: Motors were immersed in a water tank at approximately 1.5 meters depth and run for 3 hours.

Tests were successful for the protection of both, mechanical and electrical parts. Care was taken with to protect the shafts for prolonged immersion periods. Grease or marine silicone was applied to prevent water intrusion into the mechanical components of the gearbox. The following step is to test waterproofing on the actual motors to be used in the *MOSARt*. Scheme A, in Table 9, is applied to each motor and a bucket test is performed, Figure 32.

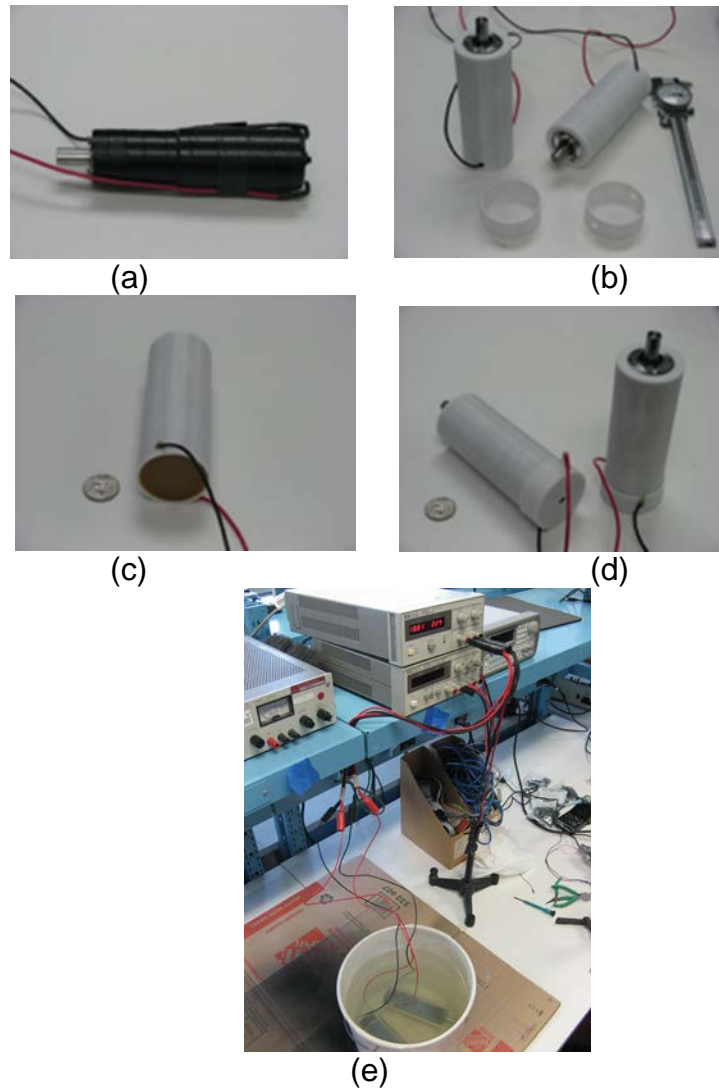


Figure 32. Land Motor Waterproofing Scheme and Test

(a) Motor is covered with rubber coating and electric tape, (b) Motor is fitted into FDM jacket, (c) Melted wax is poured into FDM jacket till motor is covered, (d) Cables are passed through end caps. (e) Bucket test

After running the motors for an hour, a current and rpm fluctuation of the motors required us to stop the test. The motors were hot to the touch and wax had melted wax inside the motor jacket (Figure 33).



Figure 33. Effects of Motor Heat on Wax Waterproofing

Motors lost their centered position as the wax started to melt, connections were broken and proper operation not guaranteed any longer.

Wax was rejected as a waterproofing technique. High temperature potting compound was subsequently used to waterproof the land motors. This is a more complex method; a special piece was produced in FDM to allow the encoder shaft that is located in the back of the motor to rotate freely after the motor is potted and thus guaranteeing the operation of the motors, see Figure 34. Epoxy curing times were approximately 24 hours.



Figure 34. Motor Encoder Shaft Cap

Encoder shaft covered with a specially design FDM solid piece to allow proper rotation after potting.

2. Chain Drives

The chain drive was selected as means to transmit power to parallel shafts. Chain maintenance requires proper alignment and lubrication. A regular wash in kerosene and dip in oil is also recommended [21].

3. Pitch and Speed Ratio

Pitch and speed ratio are expressed by equation 2.11, where n_2 is the output speed, n_1 is the input speed, both measured in revolutions per minute; N_2 and N_1 are the number of teeth of the output and input sprockets , respectively.

$$\frac{n_2}{n_1} = \frac{N_1}{N_2} \quad (2.11)$$

Using an odd number of teeth for the driving sprocket (between 17 and 25) is recommended. The output sprocket is commonly limited to 120 teeth. Using equation 2.11 the speed ratio is calculated for a driving sprocket of 13 teeth and an output sprocket of 45 teeth at 0.28.

4. Center Distance and Chain Length

The pitch radii, r_1 and r_2 of the sprockets is calculated via equation 2.12 when the speed ratio is less than 3. Equation 2.13 is used when the ratio is greater than 3 [21].

$$c = 2(r_1 + r_2) \quad (2.12)$$

$$c = 2(r_2 - r_1) \quad (2.13)$$

Once an initial center distance c is calculated the chain length can be estimated using equation 2.14 and the new center is recalculated by equation 2.15 [21].

$$L = 2c + \pi(r_1 + r_2) + \frac{1}{c}(r_2 - r_1) \quad (2.14)$$

$$c = \frac{1}{4} \left[b + \sqrt{b^2 - 8(r_2 - r_1)^2} \right] \quad (2.15)$$

where

$$b = L - \pi(r_2 + r_1) \quad (2.16)$$

Using equations 2.12–2.16, Table 10 shows the results obtained for $r_1 = 2.65\text{cm}$ and $r_2 = 9.10\text{cm}$.

Table 10. Center Distance and Chain Length Calculations

c [cm]	L [cm]	b [cm]	c2 [cm]
23.52	84.24	47.30	22.74

5. Chain Pitch, Chain Velocity and Platform Velocity

The pitch radius on a sprocket with N teeth is defined by equation 2.17 in which p , the chain pitch, is the length of a single link from center pin to center pin [21].

$$r = \frac{Np}{2\pi} \quad (2.17)$$

The number of feet coming off the sprocket per unit time is called chain velocity and is defined by equation 2.18. The number 2361.6 is a conversion factor to get the results in meters per second.

$$V = \frac{Npn}{2361.6} \quad (2.18)$$

The chain velocity V is calculated for the drive (V_{s1} - 13 teeth) and driven (V_{s2} - 45 teeth) sprocket and then an estimation of the velocity of the platform (V_p) is obtained and shown in Table 11 by using equation 2.19, where RPM_{s2} are the rpm of the driven sprocket attached to the Whег and r_w is the radius of the Whег. The number 6000 is a factor to get the result in meters per second.

$$V_p = \frac{RPM_{s2} \times 2\pi r_w}{6000} \quad (2.19)$$

Calculations are made using the following parameters (Appendix A):

- Maxon motor (273752) nominal speed: 6500 rpm
- Maxon motor planetary gearhead GP 32 HP (326661): 23:1 reduction.
- Speed ratio N_2 / N_1 : 3.46

Table 11. Vehicle Speed Estimation on Land

RPM output on motor	Chain velocity V_{s1}	RPM on driven sprocket	Chain velocity V_{s2}	Estimated V_p (m/s)
282.6	0.38	81.64	0.38	1.55

6. Power Capacity of Roller Chains

In accordance with the American Chain Association (ACA), the design power capacity is given by equation 2.20, where H_r is the horsepower rating that is found in ACA tables, K_1 is the service factor, given in Table 12 and K_2 is the multiple-strand factor, given by Table 13 from [21].

$$H_d = H_r K_1 K_2 \quad (2.20)$$

Table 12. Service Factors (K_1) for Single Strand Roller Chains

Type of driven load	Type of Input Power		
	LC engine hydraulic drive	Electric motor or turbine	LC engine mechanical drive
Smooth	1.0	1.0	1.2
Moderate shock	1.2	1.3	1.4
Heavy shock	1.4	1.5	1.7

Source: [21] A. Ugural, "Chapter 13: Belts, chains, clutches, and brakes," in *Mechanical Design: An Integrated Approach*, McGraw-Hill, New York, NY, 2004. pp. 507–558.

Table 13. Multiple-strand factors (K_2) for roller chains

Number of strands	Multiple-strand factor
2	1.7
3	2.5
4	3.3

Source: [21] A. Ugural, "Chapter 13: Belts, chains, clutches, and brakes," in *Mechanical Design: An Integrated Approach*, McGraw-Hill, New York, NY, 2004. pp. 507–558.

The required chain lubricants for the rated horsepower capacity are [21]:

- Type A: Manual or drip lubrication, oil applied periodically with brush or spout can.
- Type B: Bath or disk lubrication, oil level is maintained in the casing at predetermined height.
- Type C: Oil stream lubrication, oil supplied by circulating pump inside chain loop or lower span.

As given by equation 2.20, with $H_r = 0.77$, $K_1 = 1.5$, $K_2 = 1$, the designed power capacity is calculated to be $H_d = 1.155\text{hp}$.

Based on our calculated requirements, the chain (Figure 35), sprockets (Figure 36) and ball bearings (Figure 37) were selected as follows:

Chain:

- A high strength, resistant to chemical attacks and highly resistant to corrosion chain made of Stainless Steel 304-grade.
- Chain size: #25SS
- Tensile Strength: 304 kg



Figure 35. Hitachi #25SS Roller Chain–3.048m (10 ft)

Sprockets:

- The drive sprocket has 13 teeth and the driven sprocket has 45 teeth as shown in Figure 36 and Appendix A. The drive ratio of the sprockets selected is 3.46.
- Material: Stainless steel 303.
- Centre distance: The distance between centers is 25.25 cm, ideal is 22.74 cm but limitations are imposed by space required for other components.
- Chain pitch: #25 (0.25”–0.635 cm)
- Drive ratio (sprocket reduction ratio): 3.46

For more specifications on selected sprockets please see Appendix A.

7.

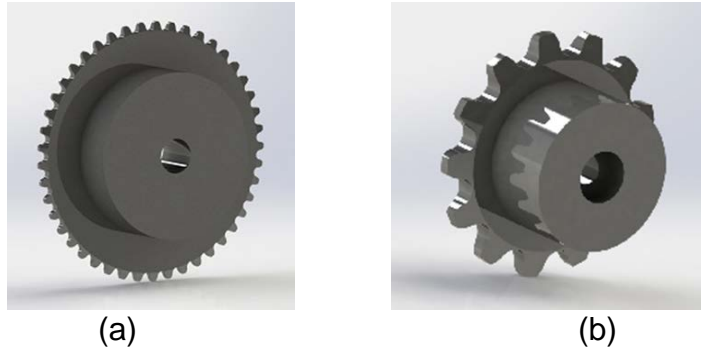


Figure 36. *MOSARt* sprockets

(a) Rendered version of 45 teeth sprocket, (b) Rendered version of 13 teeth sprocket. Source: [22, 23] 45 teeth sprocket specification (SS 304). (2015). SDP-SI. [Online]. Available: <http://sdp-si.com/eStore/Catalog/Group/585>; 13 teeth sprocket specification (SS 304). (2015). SDP-SI. [Online]. Available: <http://sdp-si.com/eStore/Catalog/Group/585>.

Ball bearings:

- Flanged double sealed ball bearing for a shaft diameter of 1.27 cm (0.5") with a dynamic load capacity of 140.6 kg.



Figure 37. Flanged Double Sealed Ball Bearing (Rendered Version)

7. 5WGen Whег Modification

Bell's Whег design [5], (5WGen), was scaled up 1.5 times to match the size of the *MOSARt*. This allowed for:

- Clearance of small fixed obstacles on land (5 to 15 cm height)
- Protection of thrusters, structure and sensors
- Obstacle climbing capability for obstacles up to 17 cm in height

The size of the modified 5WGen was limited in diameter (36.42 cm) to allow proper transmission for sonic sensors without interference or masking by the Whieg structure.

An additional feature included a rubber track on either side of the main body of the Whieg (Figure 38). This reduces impact while operating on hard surfaces as cement, concrete or hardened sand, but allows full action of the legs for climbing and the cross members as detailed in [5] for weight distribution on beach surfaces.

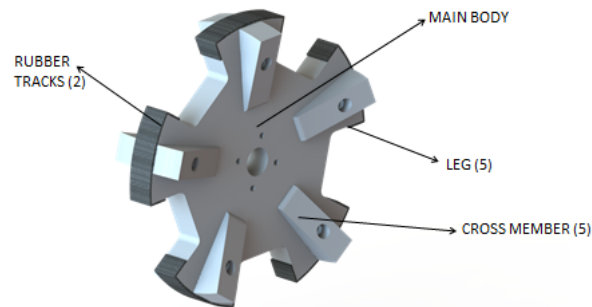


Figure 38. 5WGen(1.5)–(Rendered Version)

04 5WGen(1.5) will be used as part of the design. Each one consists of one main body with 5 legs, 5 cross members that are attached to the main bodies by stainless steel screws; and two rubber tracks.

Calculated theoretical parameters are resumed in Table 14.

Table 14. *MOSARt* Calculated Parameters

Drag coefficient (C_d)	0.54
Reynolds number (Re)	26529 (turbulent)
Front cross sectional area (A)	0.277 m ²
Hydraulic diameter (d_h)	0.0541 m
Calculated velocity (water)	1-1.5 knots
Calculated velocity (land–flat surface)	1.55 m/s
Design power capacity (H_d)	1.15 hp
Degrees of Freedom (DOF)	Surge, heave and yaw

III. DESIGN

The challenges of the maritime environment drive the design of the robot; the CONOPS was used to inform the high-level requirements and map them to systems or components that enable a specific capability.

A. DESIGN THEORY

The design of a robot with waterborne capabilities takes into account among others [20]:

1. Power Sources

There are various ways to power robots: off-board, on-board or hybrid. Off-board or surface powered is commonly related to a tether in order to provide the required power. On-board or vehicle-powered are the type of platforms that have the capacity to carry their means for operation and propulsion, hybrid use on-board power and are charged with an off-board power cord. For our prototype the on-board method was selected.

Two different sets of batteries are selected taking into account the estimated 1–2 hours of continuous operation: for the power bus (two high power polymer Li-Ion Module 22.2V 10Ah) and for the internal electronics (one high power polymer Li-Ion module 11.1V 5Ah). Both types of batteries come with a built in circuit that protects the batteries from draining while the vehicle is in operation.

2. Autonomy Levels for Unmanned Systems (ALFUS)

According to the National Institute of Standards and Technology (NIST), various terms are important to provide metrics for autonomy from [24]:

- Level of Autonomy (LOA)
- Human Independence (HI)
- Mission Complexity (MC)

- Environmental Complexity (EC)

Modes of Unmanned Systems (UMS) from [24]:

- Fully autonomous: Accomplish mission without human intervention.
- Semi-autonomous: Human and/or UMS plan and perform the mission; requires HRI.
- Teleoperation: Human operator receives feedback form sensors to operate the robot using any type of linked communications.
- Remote control: Operator controls without feedback from sensors.

The MOSARt is proposed as a semi-autonomous system.

3. Communications

Different methods are used for communications depending on the environment and distance: hard-wire, acoustic, optical or radio frequency (RF). The type of information that is exchanged using these linkages is outlined is in Table 15.

Table 15. Information Types and Linkages

Information Type	Description	Linkage
Telemetry	Data or video	Tether, RF, optical, acoustic or others
Tele-presence	Sensor feedback	
Control	Upload/download of operational instructions	
Records	Upload/download mission record and files	

Communication to and from the robot is accomplished by the use of one or a combination of linkages. The type of information and link required varies according to the environment the robot is operating in, and the level of autonomy. Adapted from [13]: R. D. Christ and R. L. Wernli, *The ROV Manual, A User Guide for Remotely Operated Vehicles*. Oxford, England, Butterworth-Heinemann, 2013, p. 63.

Both autonomy and communications are addressed as part of Garcia's thesis [12] and are considered in the design. Additionally, the electronics, sensors and other components are considered and included in the design for integration and construction of the robot.

4. Photo/Video Transmission

For after action review, a mounting for a GoPro Hero 3 camera is implemented.

B. MOSART DESIGN

An ideal robot would have the following characteristics according to [20]:

- No physical linkage (cables, fiber optics, tethers, etc).
- Unlimited power available.
- Very small.
- A very high data capability for sensors.
- Capable of withstanding all environments and transition between them.
- Adaptable to different operational conditions.

That would be an ideal design, but we are constrained mainly by the CONOPS and other factors that affect the design process; therefore there is a trade-off that takes into account aspects as cost, size, actuators, manipulators and operational requirements [20].

Parts are sketched and modeled using Solidworks. Once the parts are modeled, material properties are added to get a more accurate model of the vehicle in regards to weight, centers of gravity and moments of inertia, among other parameters that can be used during the design process.

The design process starts with the decision to combine two modes of propulsion, thrusters (propellers) for maritime mobility and whlegs (wheels and legs) with motors, sprockets, chains and ball bearings for land mobility. This

decision merges an untethered ROV for water mobility with a skid with whegs for land mobility.

The selected waterproof cylinder imposed design restrictions on our platform. This was addressed early in the design. Various configurations were initially planned using Solidworks as shown in Figure 39.

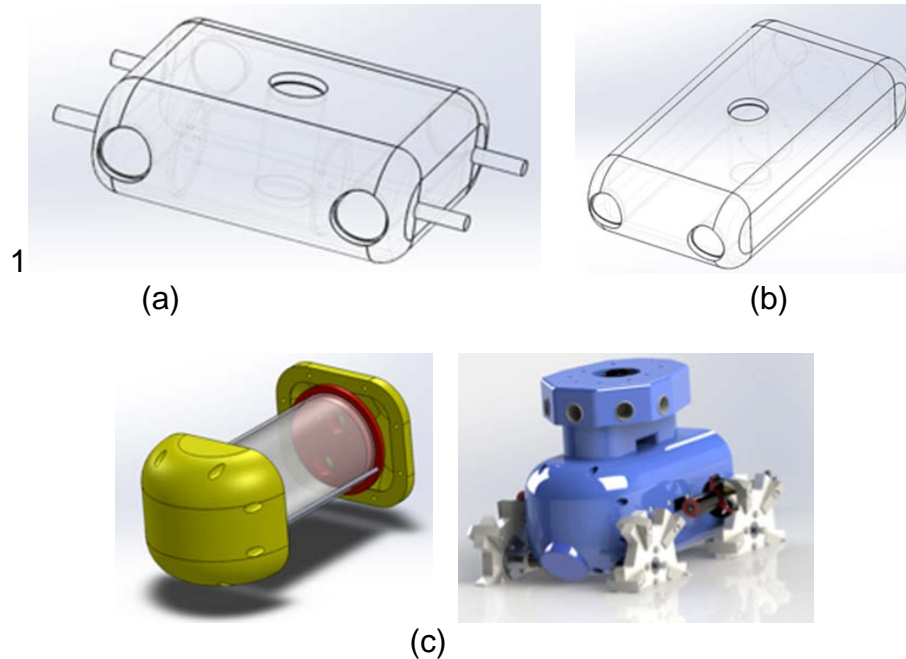


Figure 39. Initial Design Approaches

(a) Length 57.2 cm, width 68 cm, height 25 cm. waterproof cylinder located to horizontally and parallel to the front plane of the design, (b) Length 103.7 cm, width 52 cm, height 25 cm waterproof cylinder located to the stern and parallel to the right plane of the design; The location of the waterproof cylinder keeping normal ROV-type configurations for the water section is problematic; the size of the platform is too big for the desired size. Additionally, these designs contemplate the location of the thrusters “onboard” the water section, with the implementation of through holes to direct the water flow, (c) Length 48.79 cm, width 28 cm, height 24 cm. Rendered version. In this later approach the cylinder is fitted in a smaller water section, one vertical thruster and two laterals are envisioned. Sonic sensors are located over the sail and 4WGen are used in the design.

Figure 40 shows a rendered version of the final design. It is modular because it allows for future structural modifications and the addition of sensors for new missions.

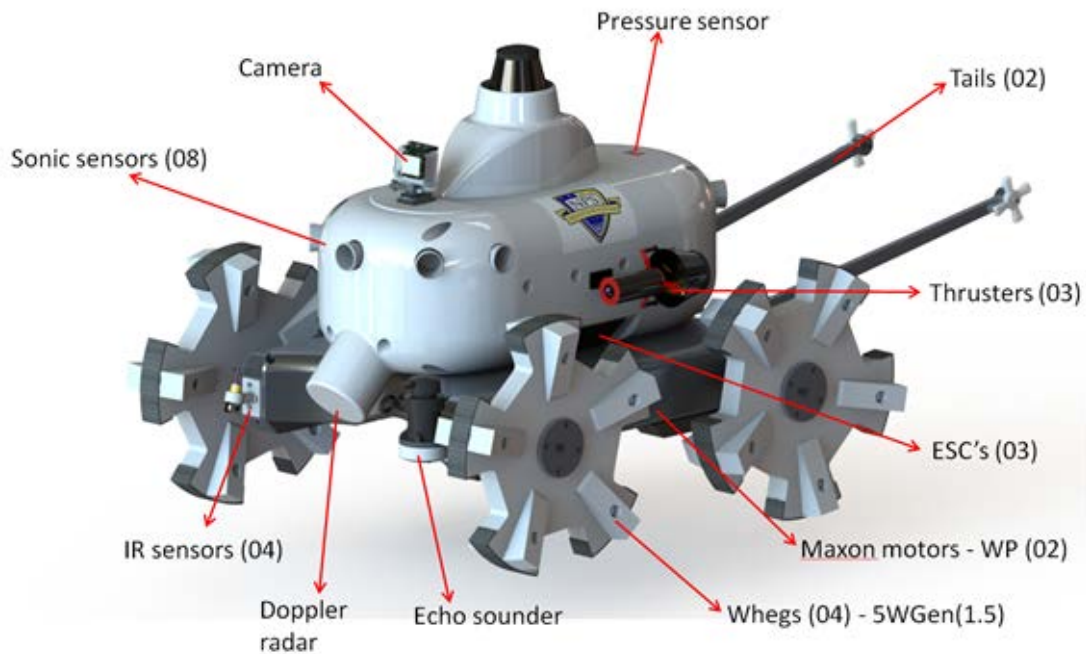


Figure 40. *MOSARt* - Final Design (Rendered Version)

In this final design the cylinder is fitted in a smaller water section, one vertical thruster and two laterals are located. Sonic sensors are now part of the main water structure and 5WGen are used in the design to provide protection to the structure.

The principal characteristics of the platform are listed in Table 16 and Figure 41 shows the principal axes of the vehicle. These are extracted from the Solidworks design. They are an approximation of the principal parameters that will determine the behavior of the vehicle in the water.

Table 16. *MOSARt* General Properties

Property	Value	
Mass [kg]	64.620	
LOA (length overall) tail extended [cm]	136.70	
Main body dimensions [cm] (L x W x H)	88.27 x 76 x 67.53	
Volume [m ³]	0.066	
Surface area [m ²]	10.506	
Center of mass [m]	X= -0.297 Y= 0.158 Z= 0.080	
Principles axes of inertia [kg m ²]-Taken at the center of mass	I _x = (-0.011, -0.013, 1.000) I _y = (1.000, -0.009, 0.011) I _z = (0.009, 1.000, 0.013)	P _x = 1.059 P _y = 1.307 P _z = 2.160
Moments of inertia [kg m ²]-Taken at the center of mass and aligned with the output coordinate system	L _{xx} = 1.307 L _{yy} = -0.008 L _{zz} = -0.003	L _{xy} = -0.008 L _{yy} = 2.160 L _{zy} = -0.014
Materials	Land	Water
	Aluminum 6061-T6	FDM: ABSplus and PC

Values obtained from Solidworks for the built in model of the *MOSARt*. The platform components and parts are attached to the structure using nylon or stainless steel bolts when appropriately. Addition of fastening elements as screws and potting compound in will affect the location of the moments of inertia.

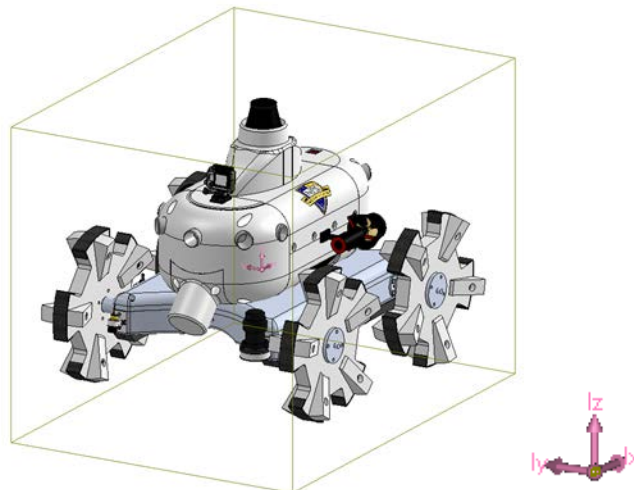


Figure 41. *MOSARt*'s Principal Axes

To a better understand the vehicle's design we divide it in two basic sections, water and land. Each section independently addresses the crucial aspects, respectively. The dimensions and sketches for each part are listed in Appendix B.

1. Water Section

This section consists of 6 structural FDM parts; these are attached together using nylon screws (Figure 42).

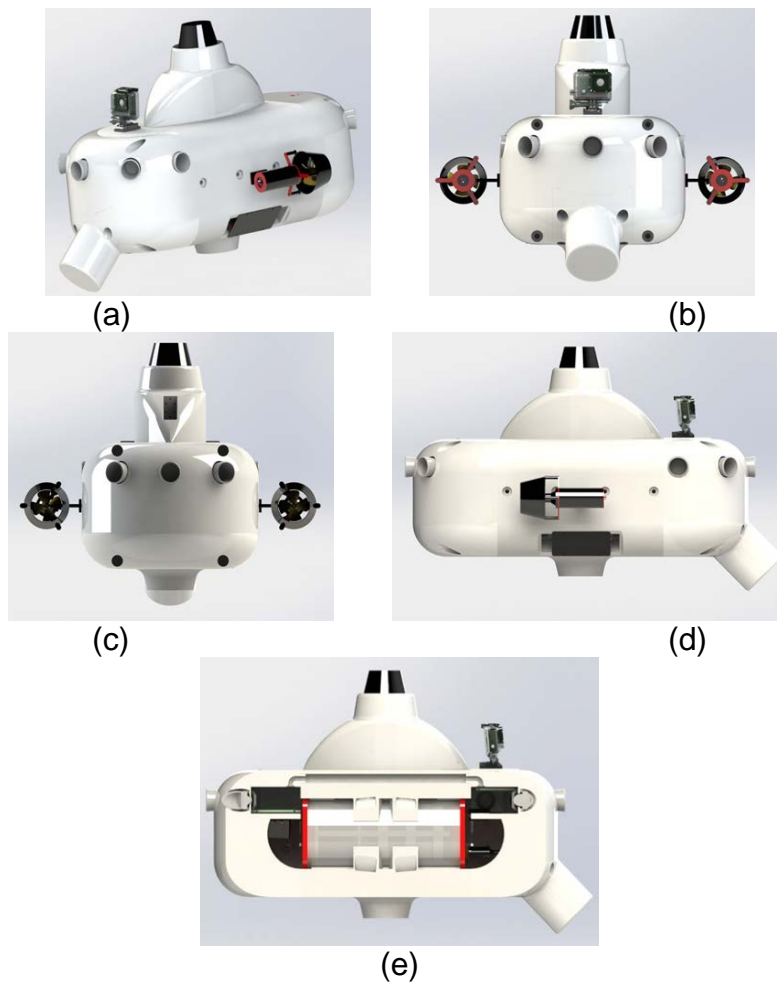


Figure 42. Water Section (Rendered Version)

Platform's rendered versions: (a) isometric view, (b) Bow view, (c) Stern view, (d) Starboard view. (e) Internal cut view.

FDM parts are printed on-campus using two different FDM printers from Stratasys, a FORTUS 400mc for PC parts and an uPrintSE for ABS parts. The water section is composed of:

Structural FDM parts:

- Bow end cap
- Stern end cap
- Middle section bottom/upper
- Doppler cone
- Sail

Sensors, actuators and waterproof cylinder:

- 3 Thrusters (400HFS-L Hi-flow)
- 8 acoustic sensors (Maxsonar XL-WR)
- 3 ESC (Phoenix EDGE HV60–potted)
- 1 Doppler radar
- 1 Pressure sensor
- 1 Camera (GoPro HERO3 with waterproof mount)
- Waterproof cylinder assembly (includes cylinder internal electronics and connectors)
- Bow electronics
- Stern electronics

a. Bow End Cap

The shape for the end cap is a hemisphere split in two and separated by a flat section of the same shape ($C_d=0.42$). This shape gives to the bow a low drag coefficient but is affected by the extrusion cuts made to fit the sonic sensors. Screws are used to fasten this piece to the middle section. Nylon screws attach the Doppler cone and the camera is attached via an FDM mounting piece (Figure 43).



Figure 43. Bow End Cap (Rendered Version)

The back view, Figure 44, shows the internal structure. This is a hemisphere extruded cut with a flat division to separate the cabling area and the bow electronics compartment; this includes a through hole on the division to allow the connector coming out of the cylinder to fit. The top area has slots to fit the bow electronics-mounting piece.

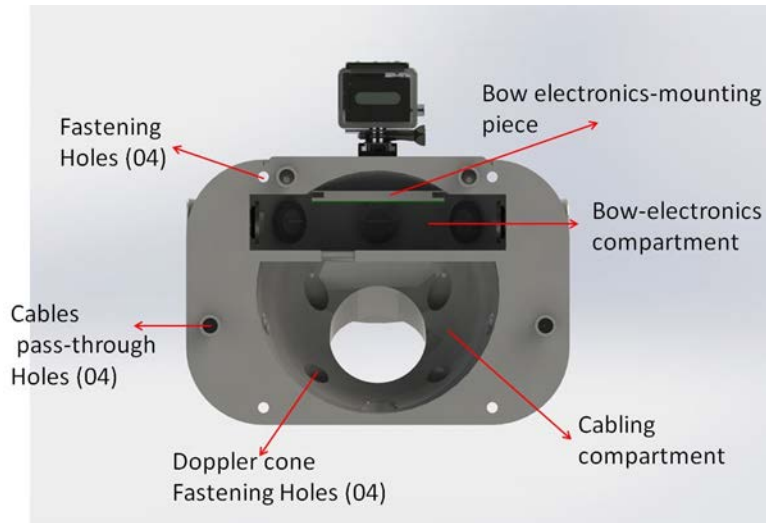


Figure 44. Bow End Cap—Back view (Rendered Version)

The bow end cap holds five sonic sensors in an electronics compartment and. This is accomplished by creating mounting surfaces with angles of 36 degrees with respect to the longitudinal center-line of the piece, for proper area coverage by the array (Figure 45).

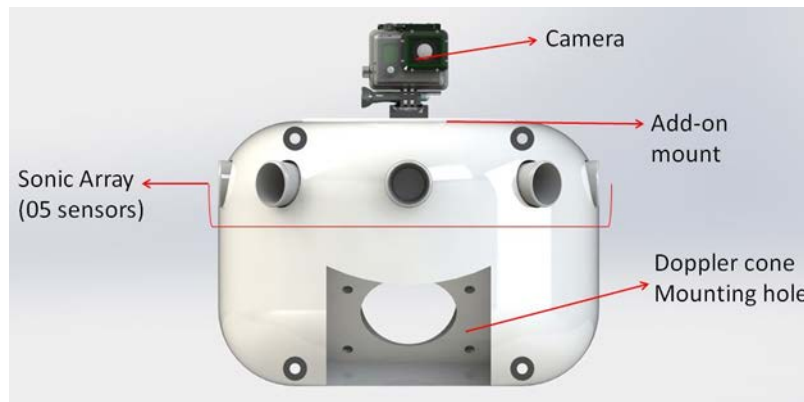


Figure 45. Bow End Cap—Front view (Rendered Version)

The add-on mount positions the camera. By reprinting the piece with different fittings, other sensors or actuators could be attached (Figure 46).

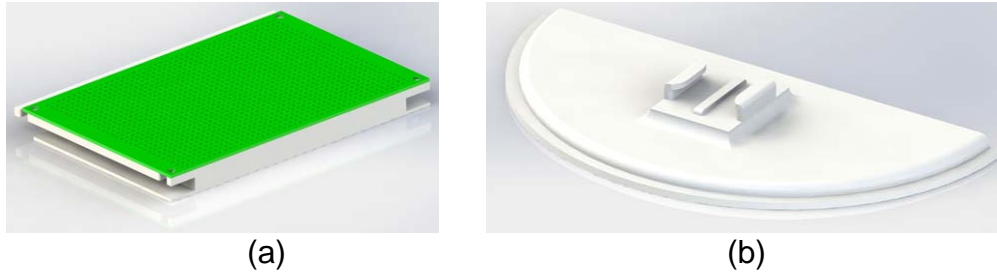


Figure 46. Bow End Cap Components (Rendered Version). (a) Bow electronics-mounting piece, (b) Bow add-on mount piece.

b. Stern End Cap

The stern end cap is mirror structure to the bow end cap. It fits three, instead of five sonic sensors, and has a through hole on the top to locate the pressure sensor. Additionally, the stern end cap holds one of the ESC's (Figure 47).

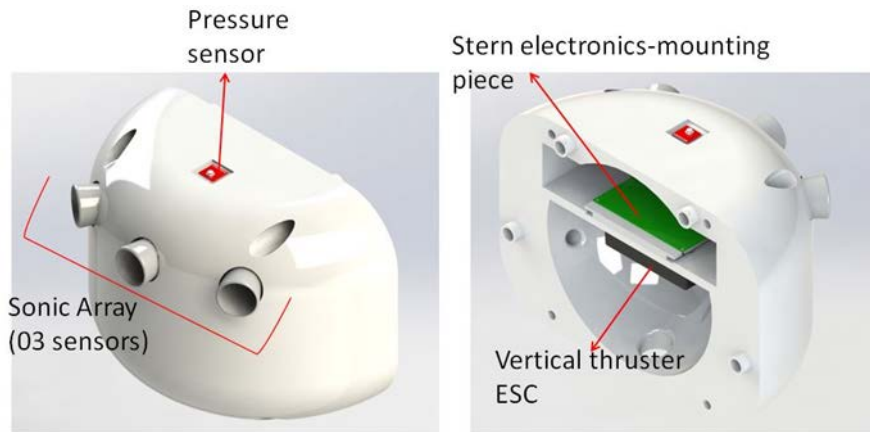


Figure 47. Stern End Cap Main Features and Components (Rendered Version)

c. Middle Section Bottom/Top

The middle section (Figure 48) consists of two pieces that combine to make up the water section's principal body. It holds the waterproof cylinder with internal electronics and connectors. It gives support to the three thrusters for water mobility and provides structural strength to the entire water assembly.

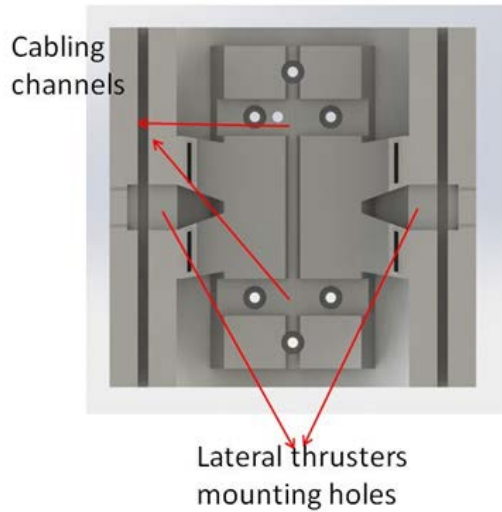


Figure 48. Middle Section Features and Components (Rendered Version)

The two pieces are structurally identical with modifications to make them fit together properly.

The location of the center vertical thruster made the three thruster configuration challenging. The problem was to locate the vertical thruster in such a way so that it would provide vertical capability centerline. To accomplish this, a set of four channels that surround the waterproof cylinder is implemented.

The four channels surround the waterproof cylinder and end on the top piece in a circular inlet/outlet hole matching the sail design holding the thruster in position vertically. At the bottom, there is an outlet/inlet circular extruded cut which extends vertically down, similar to a Kort nozzle to direct the water flow (Figure 49 and Figure 50).

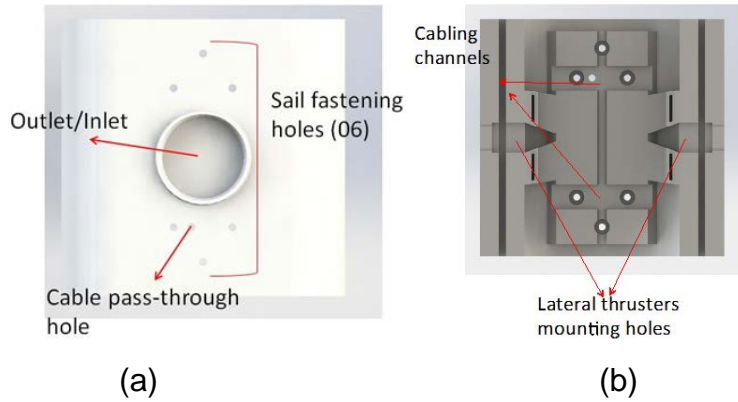


Figure 49. Top Middle Section Features (Rendered Version). (a) Top view, (b) Bottom view.

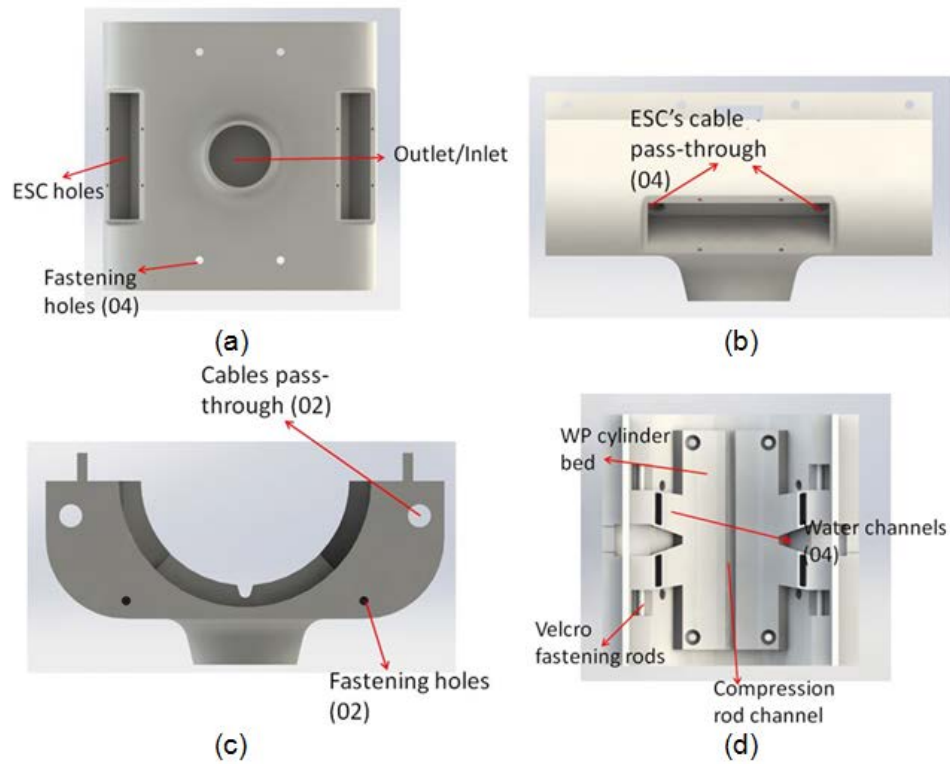


Figure 50. Bottom Middle Section Features (Rendered Version)

(a) Bottom view, (b) Lateral view, (c) Front view, (d) Top view. The four channels surround the waterproof cylinder, each channel is 0.9 cm x 4.23 cm. Water is directed down/up by the thruster upper inlet/outlet and redirected around the mid-section to the bottom inlet/outlet. Openings on top and bottom of the middle section operate depending on the thruster propeller turning direction (clockwise/counter-clockwise).

The middle section incorporates:

- A bed on each bottom/top part to accommodate the waterproof cylinder and channels to fit its compression rods.
- Fasten structures to secure the cylinder with Velcro once in position.
- Outside apertures on each side to hold the lateral thrusters ESC's on the bottom part.
- Holes for cables from the vertical ESC and thruster on the top part.
- Pass cables coming from the bow and stern go longitudinally in the structure (4 through holes—2 cm diameter), to allow internal cabling without adding friction by having cables crossing on the outside of the structure.

d. *Electronics Rack*

The rack is located inside the waterproof cylinder in the robot's middle section and holds all internal electronics (Figure 51):

- 1 computer
- 5 processors
- 2 controllers
- GPS
- 1 Battery (11.1V 5Ah) for electronics
- Cooling fans

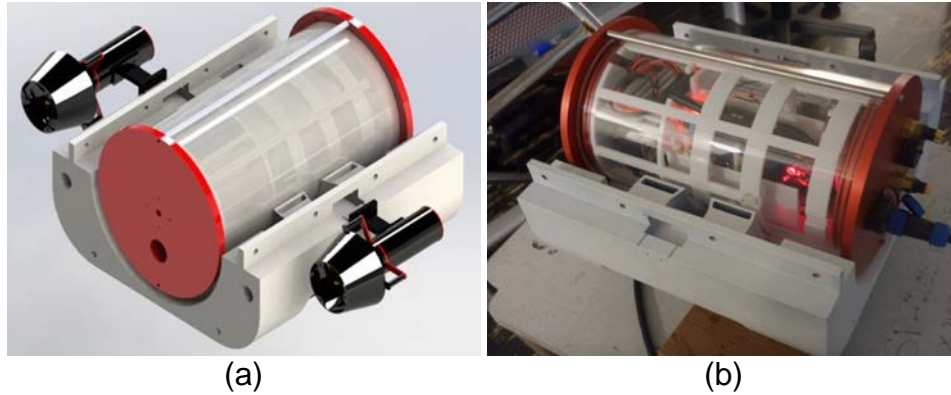


Figure 51. Designed Interior Electronics Rack

(a) Electronics rack location on the robot (Rendered Version), (b) Implemented electronics rack.

The internal electronics rack is a puzzle-like piece with a few nylon bolts to hold components to the structure. The rest of the structure attaches to itself giving strong structural support while keeping all components easily accessible and configurable. It is designed to fit precisely into the waterproof cylinder having enough room for cables and connectors making it a custom-made piece for this robot and its specific requirements.

The rack, depicted in Figure 52 is formed by: three vertical square structural beams, five vertical square support beams, two circular structural divisions top/bottom, two support vertical divisions, one internal electronics stack mount and three rings (one structural, two support).

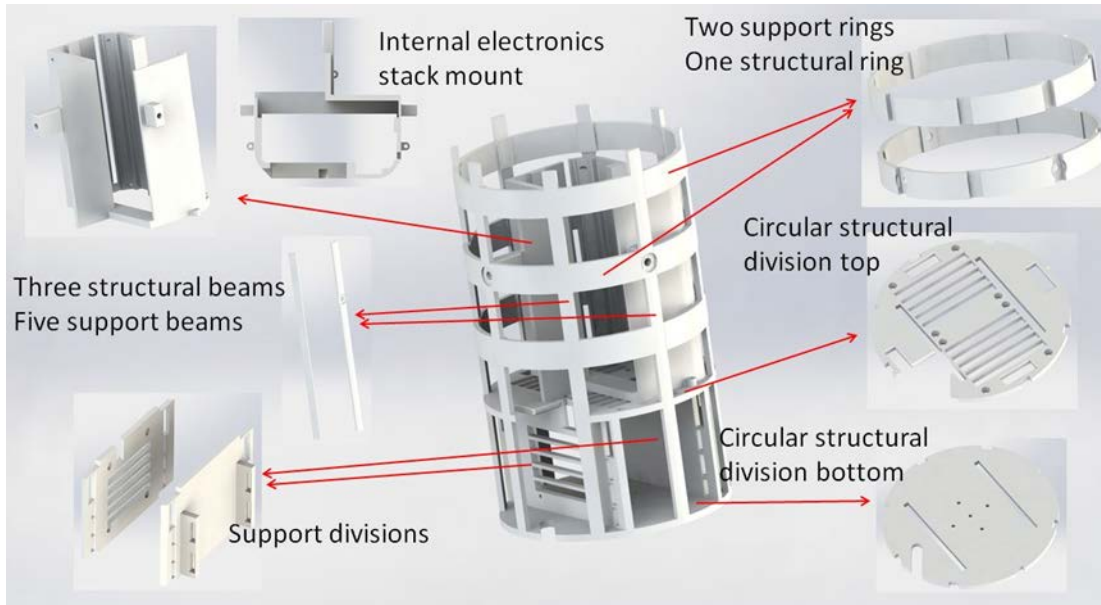


Figure 52. Electronics Rack with all Features (Rendered Version)

e. Doppler Cone

The cone is a coated solid print FDM component located in the bow end cap (Figure 53).



Figure 53. Doppler Cone Design Evolution (Rendered Version)

To the right is the final version of the Doppler, separated from the bow end cap. To the left is the first design where it was part of the bow end cap.

As part of the cone, a cap that supports the Doppler was designed, this slides in the cone cylinder and is secured by the structure as shown in Figure 53 and Figure 54.

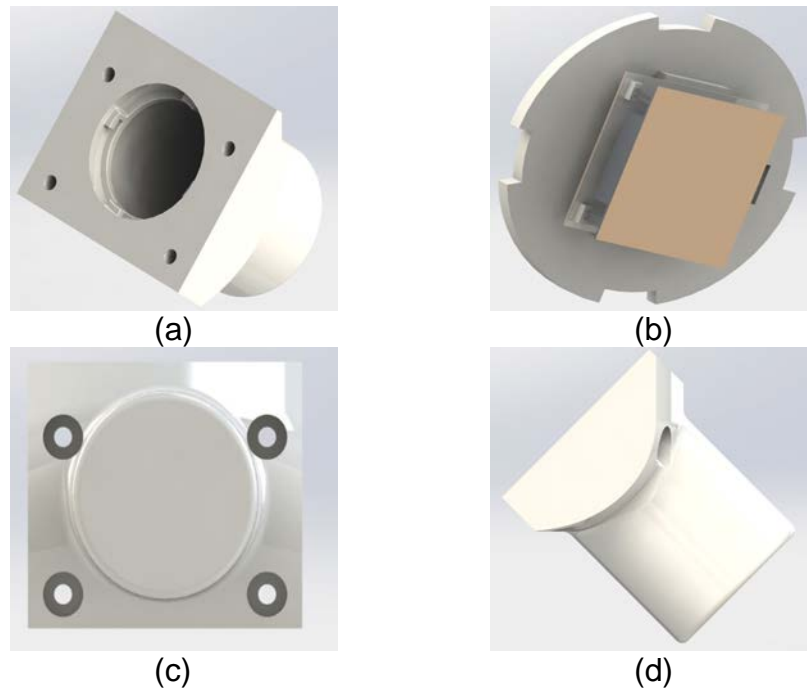


Figure 54. Doppler Cone Sensor and Features (Rendered Version)

(a) Isometric view showing the fastening holes, and cap locking features, (b) Cap supporting the Doppler sensor, (c) Front view, (d) Lateral view.

f. Sail

The main purpose of the sail was to hold the vertical thruster and direct the flow of thruster water. The part has a tear drop-shape to minimize drag. It has holes to fasten it to the middle section and has a cable pass-through for electric connections to the vertical thruster (Figure 55).

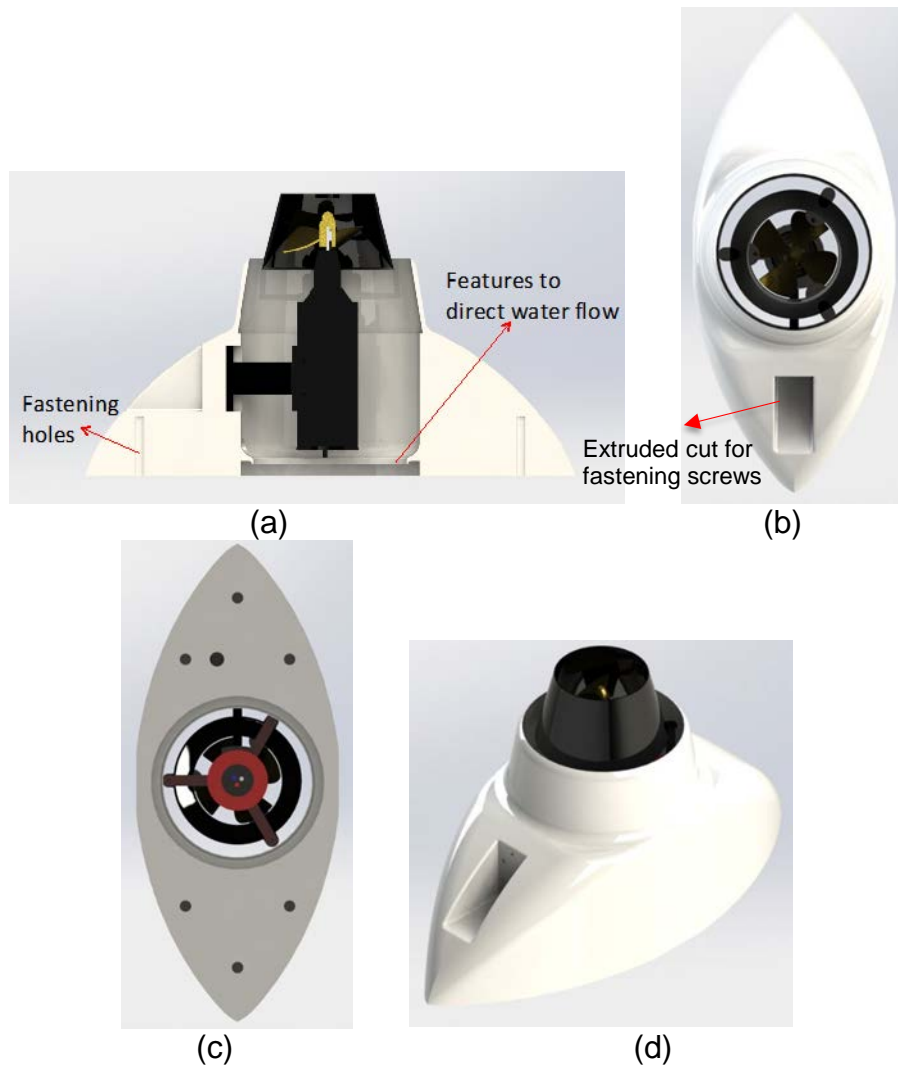


Figure 55. Sail Features (Rendered Version)

(a) Cross sectional cut to show fastening holes and internal features of the part, (b) Top view of the sail showing the extruded cut made for fastening screws to the vertical thruster, (c) Bottom view showing fastening holes and cable pass-through hole, (d) Isometric view.

2. Land Section

This section, shown in Figure 56, is structurally made of two aluminum pieces (skid top and bottom) that are joined together by stainless steel screws. Together they form a skid that provides support for the entire robot on land. It fits the drivetrain; electric components, tail and the water section are attached to it.

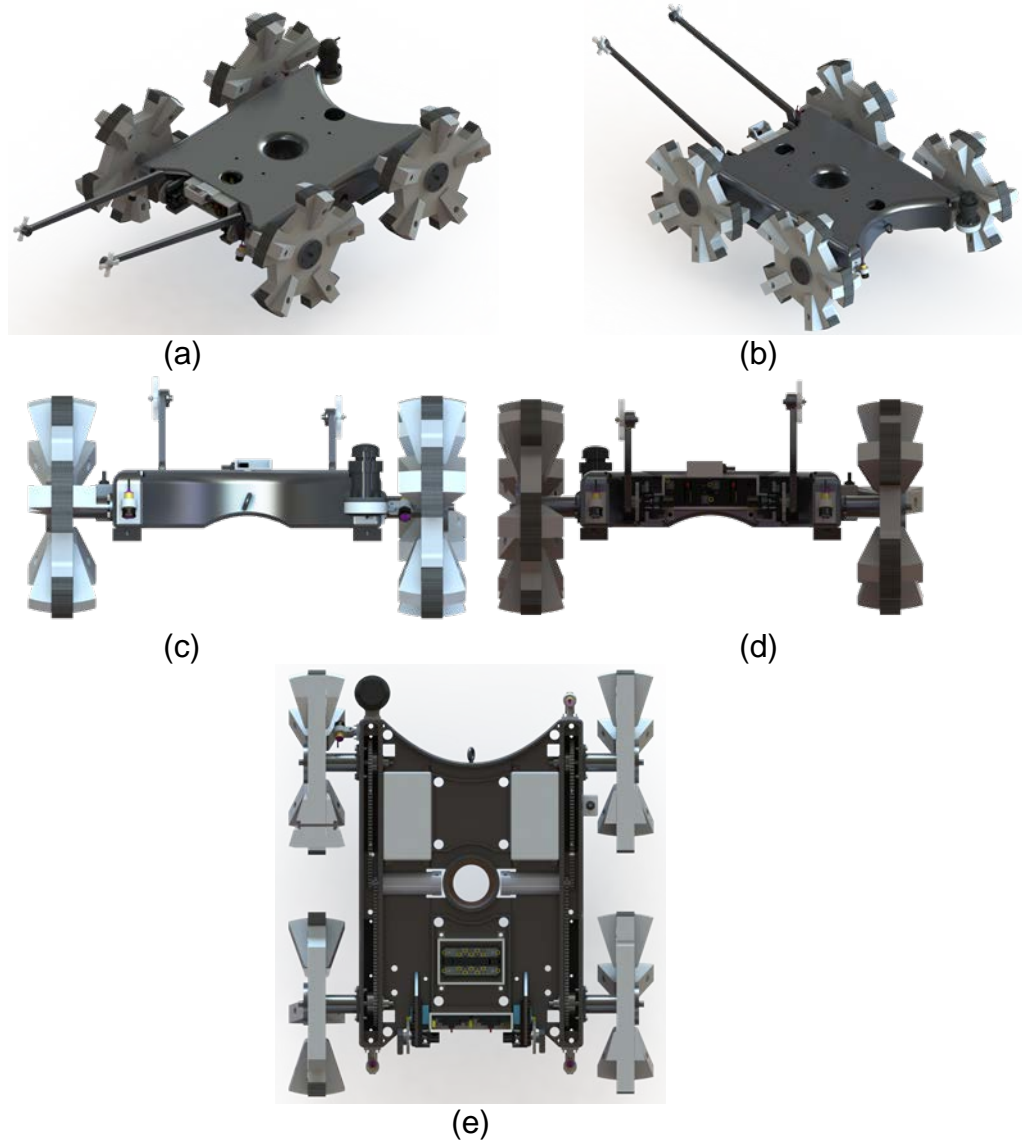


Figure 56. Land Section (Rendered Version)

(a) Isometric view from the stern, (b) Isometric view from the bow, (c) Front view, (d) Stern view. (e) Top cross section.

The land section is composed as shown in Figure 57:

FDM parts:

- 4 Whegs–5WGen(1.5)
- 2 Battery holders
- 1 Switch box holder

- 1 Circuit breaker and switch box holder
- 1 Electric bus bar box holder
- 2 Land motor jackets for waterproofing
- 4 IR sensor mounts
- 1 echo sounder mount
- 2 whegs for tails

Aluminum 6061-T6 parts:

- Bottom skid
- Top skid
- 4 shafts
- 4 shaft supports
- 4 whegs base
- 2 tail support pieces for tail servo mounts
- 2 tails
- 1 safe line eye bolt

Sensors, actuators, electrical and mechanical components:

- 4 IR sensors
- 1 echo sounder
- 2 land motors–potted
- 2 tail servo mounts
- 2 electric circuit breakers
- 2 electric switches
- 1 electric bus bar
- 4 chains SS
- 4–13 teeth sprockets SS

- 4–45 teeth sprockets SS
- 8 flanged double sealed ball bearings
- 4 shaft collars SS

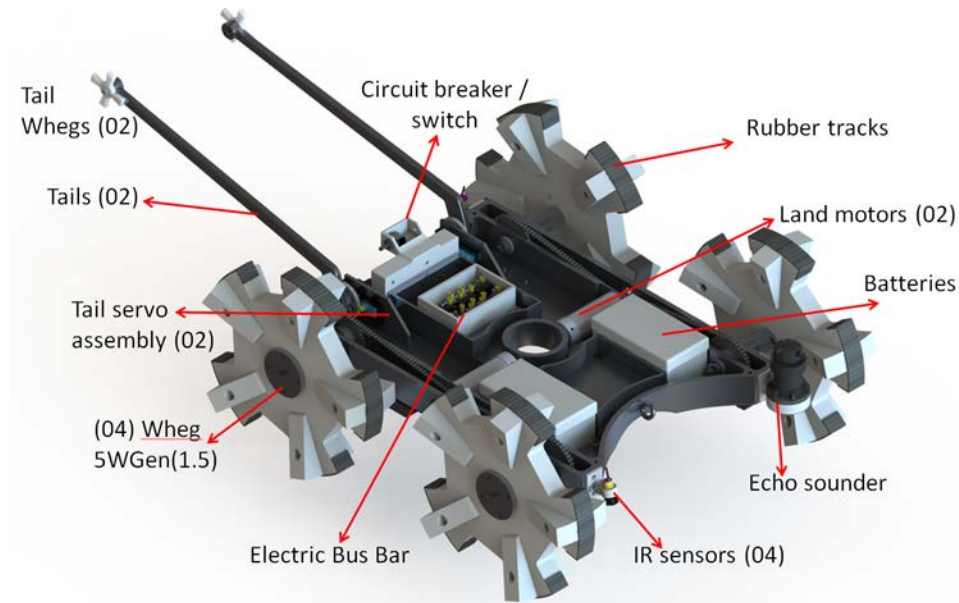
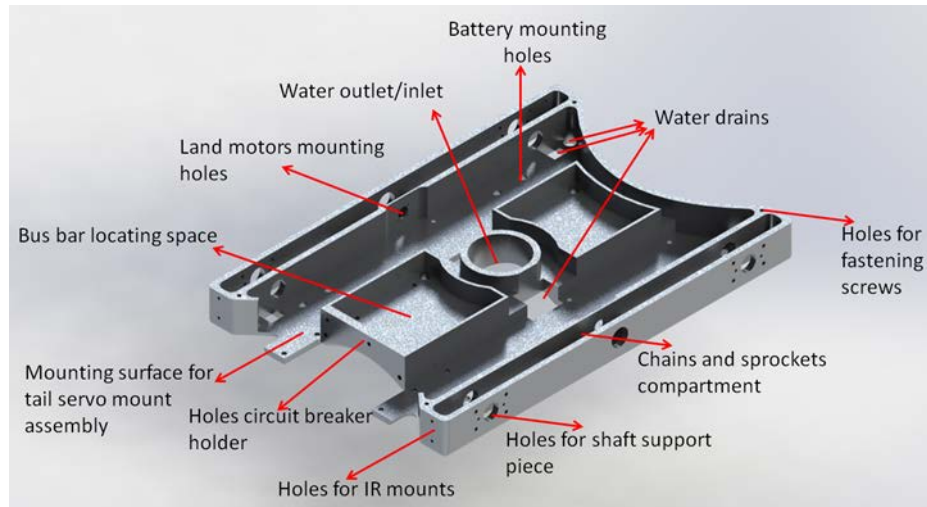


Figure 57. Land Section Sensors and Actuators (Rendered Version). The Top Skid is Not Present in Order to Visualize the Interior of the Land Section.

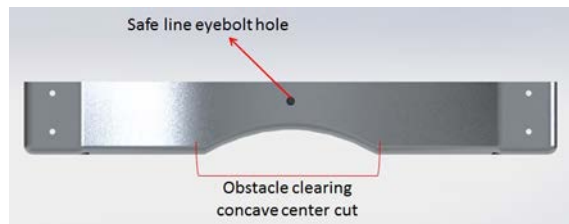
a. Bottom Land Skid

The bottom skid shown in Figure 58 is a complex part. It holds all the main external components for the robot including batteries, electrical connections, IR and echo sounder sensors, among others. It has an open transom to allow water to drain in the transitions to land from water.

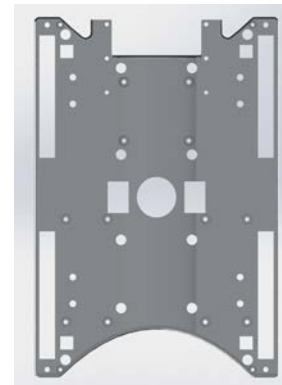
It is a CNC milled piece of aluminum 6061-T6. The skid provides the vehicle with a sturdy structure to withstand the harsh conditions of the surf zone without damaging the platform or its principal components.



(a)



(b)



(c)

Figure 58. Bottom Skid (Rendered Version)

(a) Bottom skid with main features, (b) additional features on bottom skid, front view, (c) bottom view shows more clearly all drain and fastening holes.

The power bus is also located in this part to provide electric power to all actuators as depicted in Figure 59. The two 22.2V batteries are connected in parallel and power is distributed to the different components via bus bar where a protection circuit breaker is installed which serves also as an on/off switch for the main electric power of the vehicle

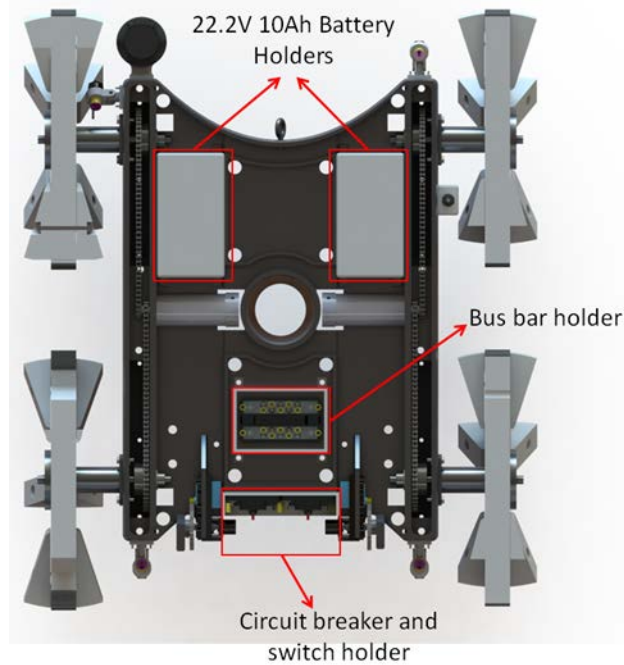
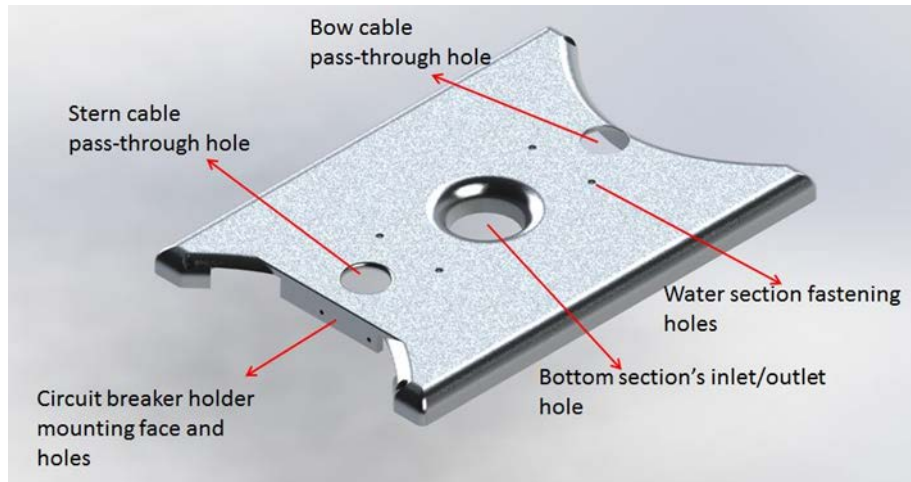


Figure 59. Power Bus Main Components

b. Upper Land Skid

The upper skid is shown in Figure 60. It integrates the water and land sections by supporting the former with four nylon screws and attaches to the latter with SS screws. It provides space for cables and the junction boxes required to make the robot functional.

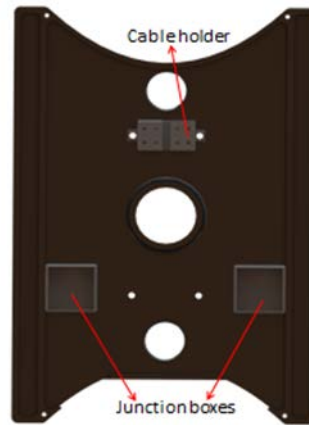
Two cable pass-through holes (6 cm diameter) allow for proper electric and electronic connections. In the center of the piece there is an inlet/outlet through hole for the middle and bottom sections.



(a)



(b)



(c)

Figure 60. Upper Skid

(a) Isometric view showing main features, (b) top view, (c) Bottom view with cable holder and junction boxes.

c. Drive Train

The drive train provides the crawler capabilities on land and in the water. The components are detailed in Figure 61.

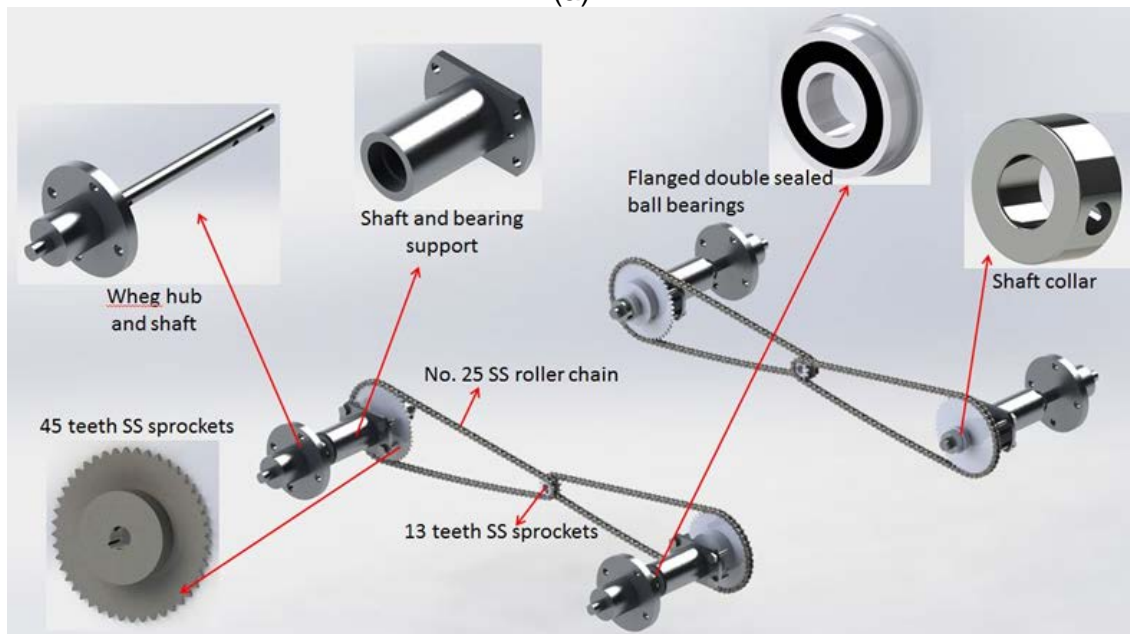
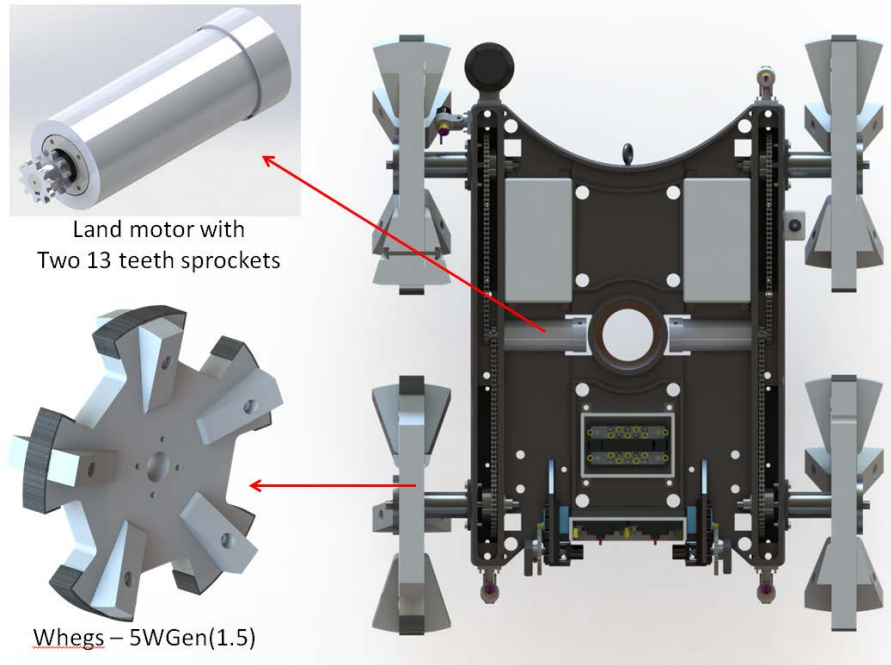


Figure 61. Drive Train with Components (Rendered Version)

(a) Top view with components, (b) Drive train detailed with components.

Four milled PVC pieces provide the chain with protection from debris (Figure 62).

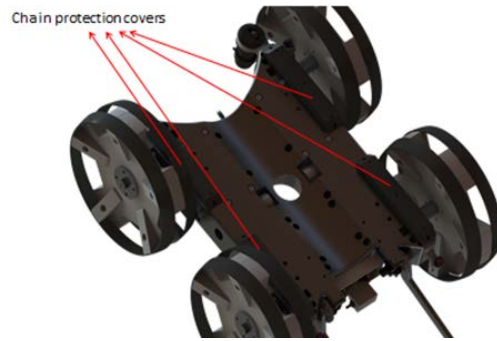


Figure 62. Chain Protection Covers

d. Tail Assembly

For climb assist over various obstacles, two tail assemblies are used in the design.

The assembly shown in Figure 63 was used by Halle in [1], with the following modifications:

- Incorporates a waterproof (WP) 180 degrees servo, with a gear ratio that provides 20 degrees of rotation to the tail. The tail is scaled up and redesigned to meet the robot's size.
- The mini Whег was scaled up. The “one way” check bearing was kept and the potentiometer previously used to get data on tail position was not implemented, it was replaced by a simpler code based on robot's attitude using an inertial measurement unit (IMU) as part of [12].



Figure 63. Tail Assembly with Components (Rendered Version)

e. Component Holders and Mounts

Electrical components for the platform are organized with holders and mounts as depicted in Figure 64. The holders for switches, batteries, circuit breakers, junction boxes and bus bar were potted to waterproof the components.

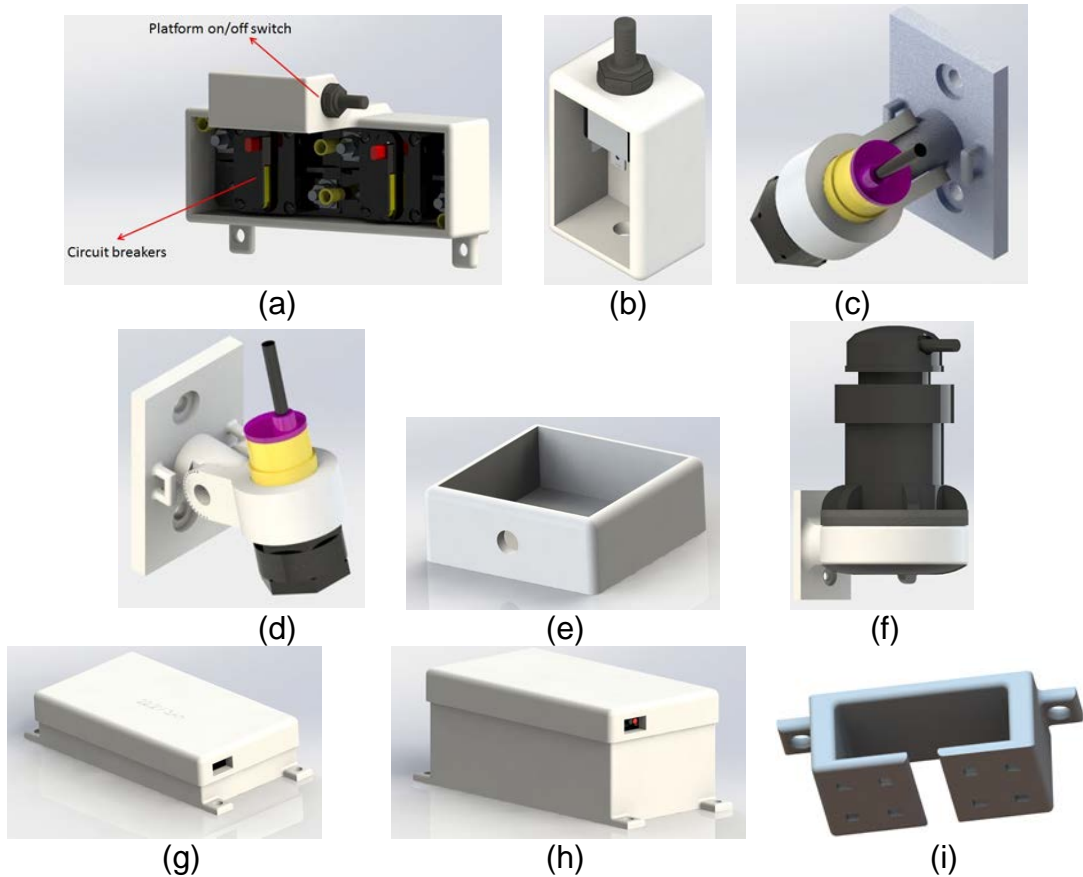


Figure 64. Component Holders and Mounts (Rendered Version)

(a) Circuit breaker and main switch holder, (b) Thruster on/off switch holder, (c) 45° IR sensor mount, (d) IR sensor mounts. (e) Junction boxes (02). (f) Echo sounder mount. (g) 22.V 3Ah battery holder. (h) 22.V 10Ah battery holder. (i) Cable holding piece.

THIS PAGE INTENTIONALLY LEFT BLANK

IV. CONSTRUCTION AND INTEGRATION

A. PARTS PRODUCTION

1. FDM Parts

FDM parts are printed on campus using Solidworks as CAD for modeling and a FORTUS 400mc for PC parts or an uPrintSE for ABS parts.

Once sketched and modeled in Solidworks parts are checked dimensionally for accuracy and saved in a stereo lithography (*.STL) file. They are then sent to print using FDM technology. This process allows a short transition time between concept and prototyping for proof of concept and test. The general process for FDM parts production is depicted in Figure 65.

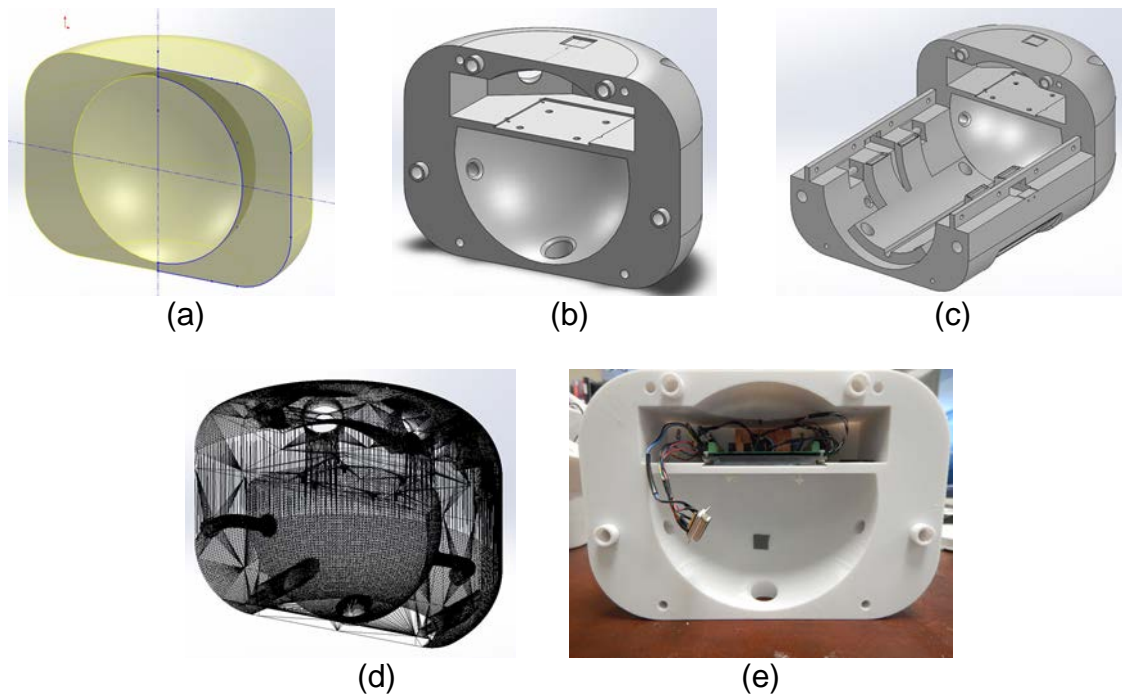


Figure 65. FDM Process for Stern End Cap

(a) Sketch and 3D generation in Solidworks, (b) modeled part with material properties for measurement check, (c) 3D model assembly fitting check, (d) front view of part after printed in sparse PC material.

Main electronics were modeled in Solidworks to assure a proper fit in the design. For this to occur, the specifications are verified for the layer thickness capability of each printer (uPrintSE = 0.254mm and FORTUS40mc = 0.127mm). The minimum clearances are required to ensure tight fits between modeled parts.

2. CNC Milled Parts

Aluminum parts were CNC milled from bulk aluminum plates (Table 17), in the physics department workshop. Solidworks and Mastercam were used to create the HAAS - Vertical Machining Center tool paths for milling the parts as shown in Figure 66.

Table 17. Bulk Aluminum Material

Part	Dimensions (L x W x H) [cm]
Bottom land skid	73.66 x 48.26 x 3.8
Upper land skid	73.66 x 48.26 x 6.35

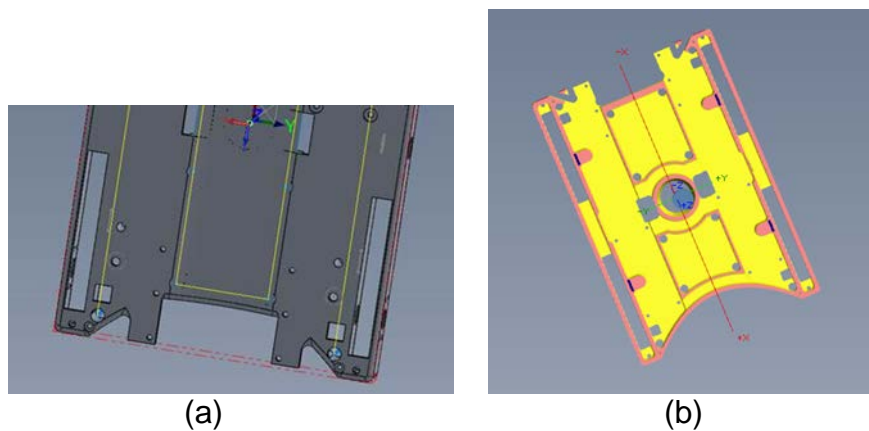


Figure 66. Tool Path Generation and Milling Simulation

(a) Tool paths generated using Mastercam for Solidworks, (b) Simulation with all tool paths and tools in Mastercam for Solidworks.

Test parts were milled in High Density Urethane (HDU) foam to validate tool paths before the aluminum was machined. Figure 67 illustrates the process.

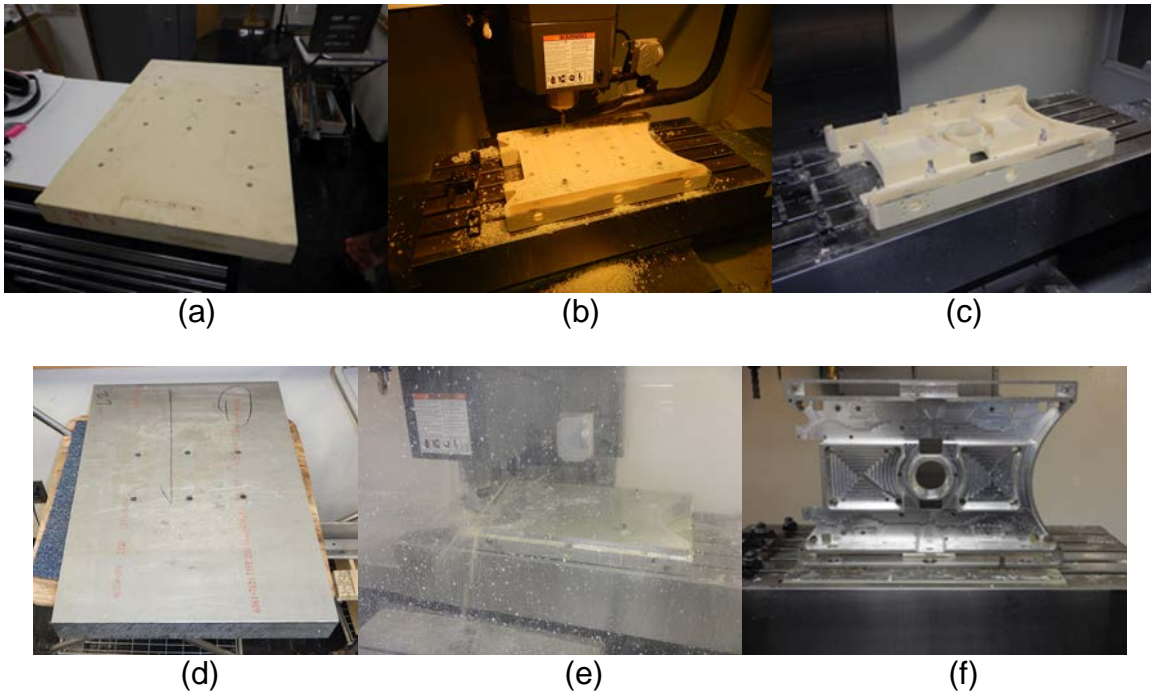


Figure 67. CNC Milling Process for Bottom Skid

(a) Bulk HDU foam with reference holes, (b) HDU milled on a vertical machining center, (c) HDU foam for bottom skid showing all features for fitting and accuracy tests, (d) bulk aluminum 6061-T6 with reference holes, (e) aluminum milled on a vertical machining center, (f) Aluminum CNC milled bottom skid with all features.

The HDU foam piece was then used to check form fit for mechanical, electrical and electronic components (Figure 68).

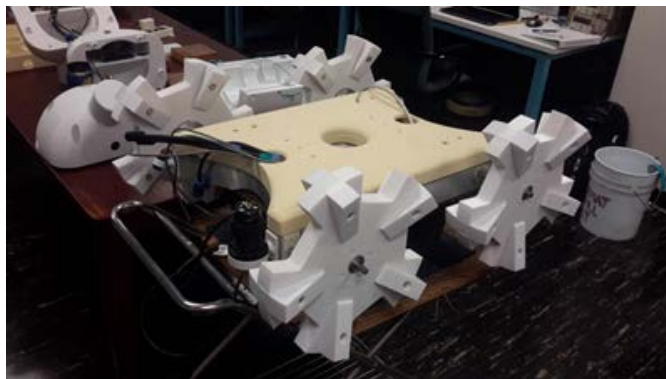


Figure 68. Top and Bottom Land Skid Fitting Test

B. INTEGRATION

1. Drive Train

The shaft and bearing supports were fixed to the bottom skid structure by pins and screws. Four shafts are cut from 1.27 cm diameter aluminum rods to proper length (24 cm). The rods are then passed through the shaft and bearing supports and end in the Whieg hubs; Figure 69 depicts individual parts and the assembly.

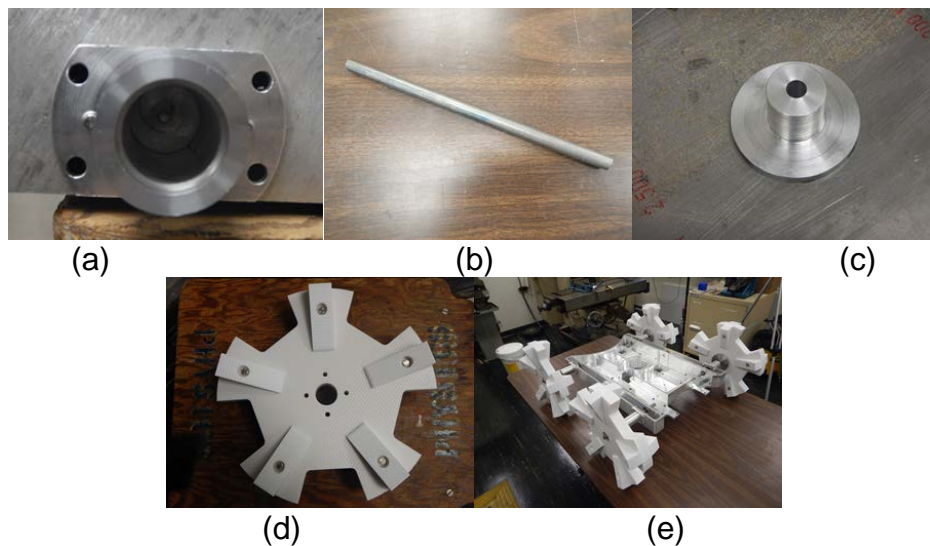


Figure 69. Drive Train Without Chain—Parts and Assembly

(a) Shaft and bearing support pinned to bottom skid, (b) Shaft, (c) Whieg hub, (d) AXV Lab 5WGen Whieg. (e) Parts assembled.

The sprockets hub and bore diameters were adjusted to match. This included a keyway to fit two 13 tooth counter faced sprockets on the motor shafts. The 45 tooth sprocket hubs were reduced in diameter and pinned to the shafts. Ball bearings were face mounted to the bottom skid structure and fixed by shaft collars. Finally, number 25 SS roller chains were cut to size and assembled, see Figure 70.

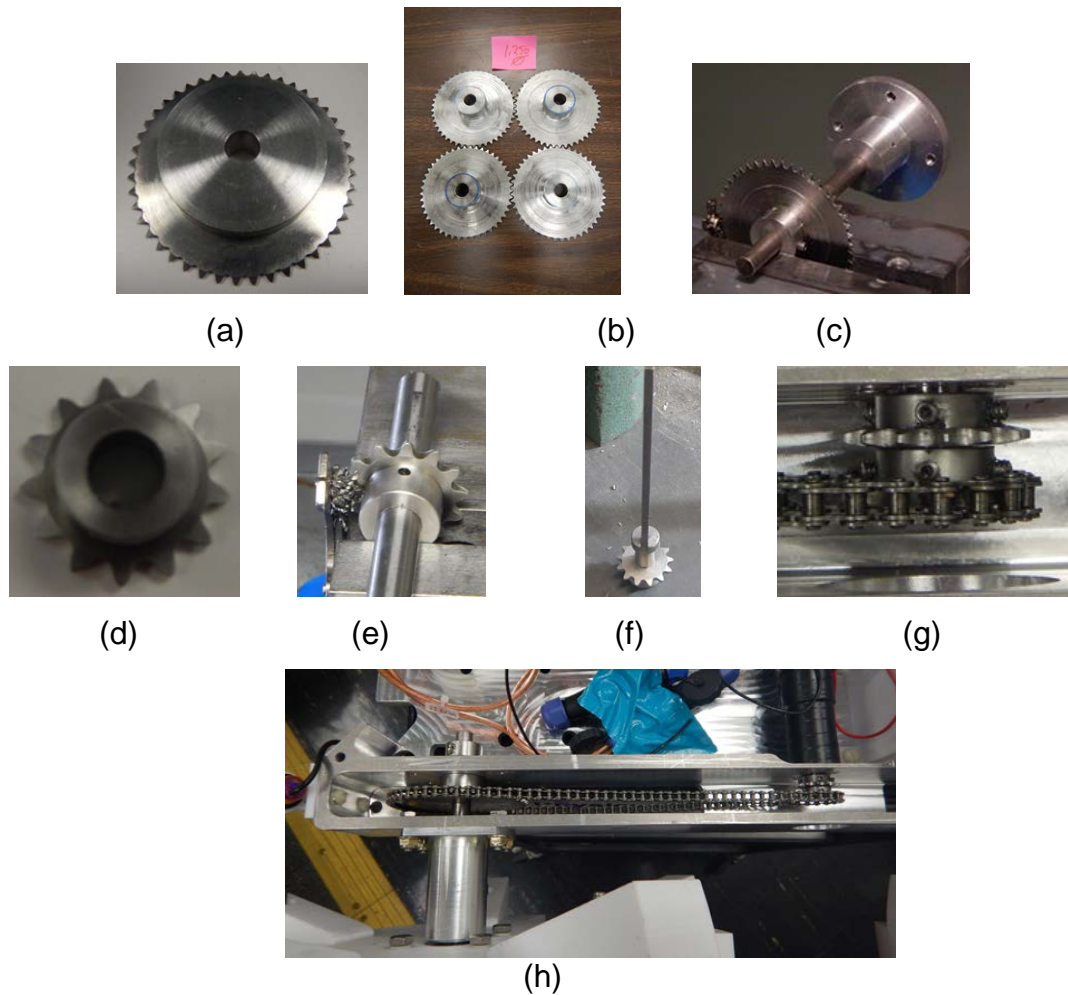


Figure 70. Sprockets Machining to Fit Design

(a) 45 teeth sprockets, (b) 45 teeth sprockets with reduced hub for weight reduction, (c) Pinning holes on 45 teeth sprockets, (d) 13 teeth sprockets. (e) Cut on 13 teeth sprocket hub and pinning holes. (f) Machined keyway to fit on motor shaft. (g) 13 teeth sprockets pinned to motor shaft. (h) Final assembly with sprockets and chain.

Parallel integration of the land and water sections was required. The sections were mechanically linked together by screws; electrically and electronically the sections were connected using cables. Figure 71 shows lab tests performed to calibrate the response of the platform to the signals sent by controllers.

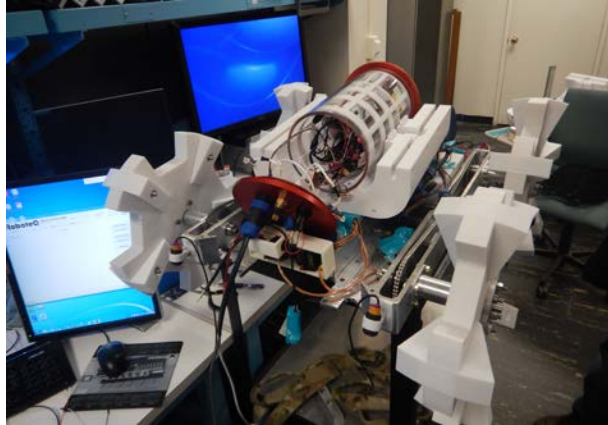


Figure 71. Drivetrain Integration Lab Test

2. Sensors, Electronics and Electric Components

Sensors electronics testing and characterization was completed by Garcia in [12], Figure 72 depicts the characterization process for the sonic sensors.

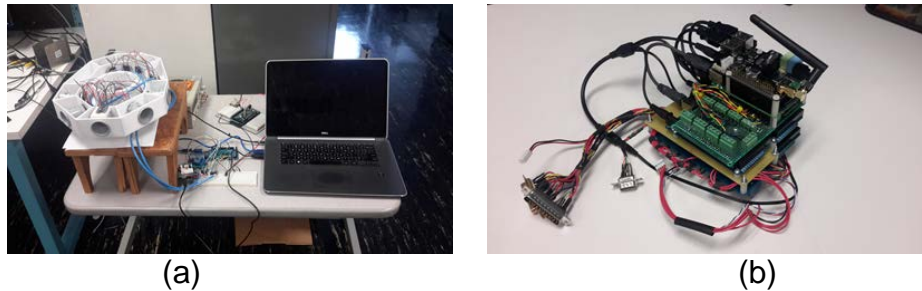


Figure 72. Sensors and Electronics Testing and Characterization

(a) Maxsonar sensors characterization is performed as part of Garcia's thesis, (b) Internal electronics building and testing. Source: [12] O. Garcia, "Sensors and algorithms for an unmanned surf zone robot," unpublished.

Integration included bench tests for all sensors and electronics. This included waterproof techniques for key components. Cables routes and connectors were also determined in this process, see Figure 73.

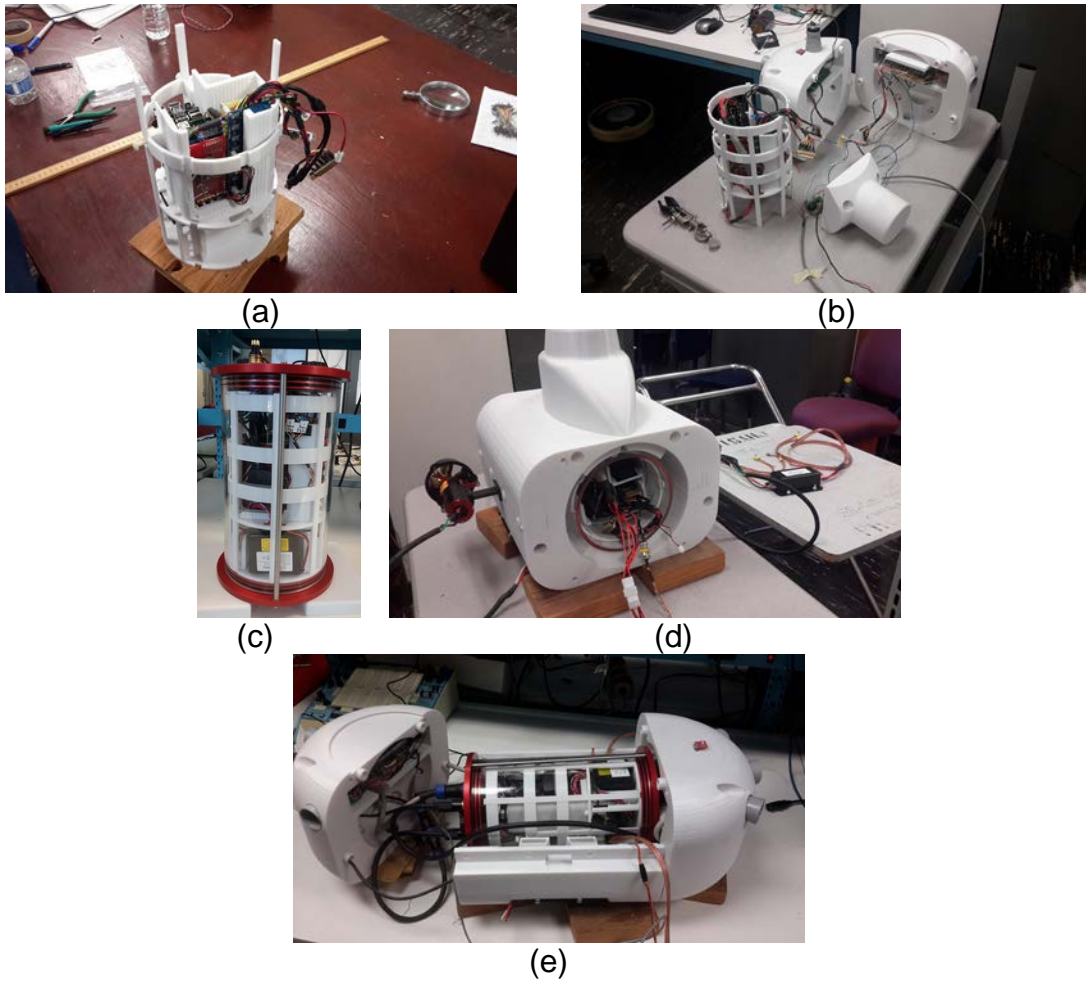


Figure 73. Integration Process for Internal Electronics and Sensors

(a) Internal electronics assembled in the electronics rack, (b) Internal electronics lab test with Maxsonar sensors, Doppler and bow and aft electronics, (c) Electronics rack in the WP cylinder, (d) Electronics rack in the waterproof cylinder and middle section. (e) Internal electronics connection and sensors test. Source: [12] O. Garcia, "Sensors and algorithms for an unmanned surf zone robot," unpublished.

Figure 74 shows a schematic of the electronic components, communication protocols and relations to allow functionality for the *MOSARt*.

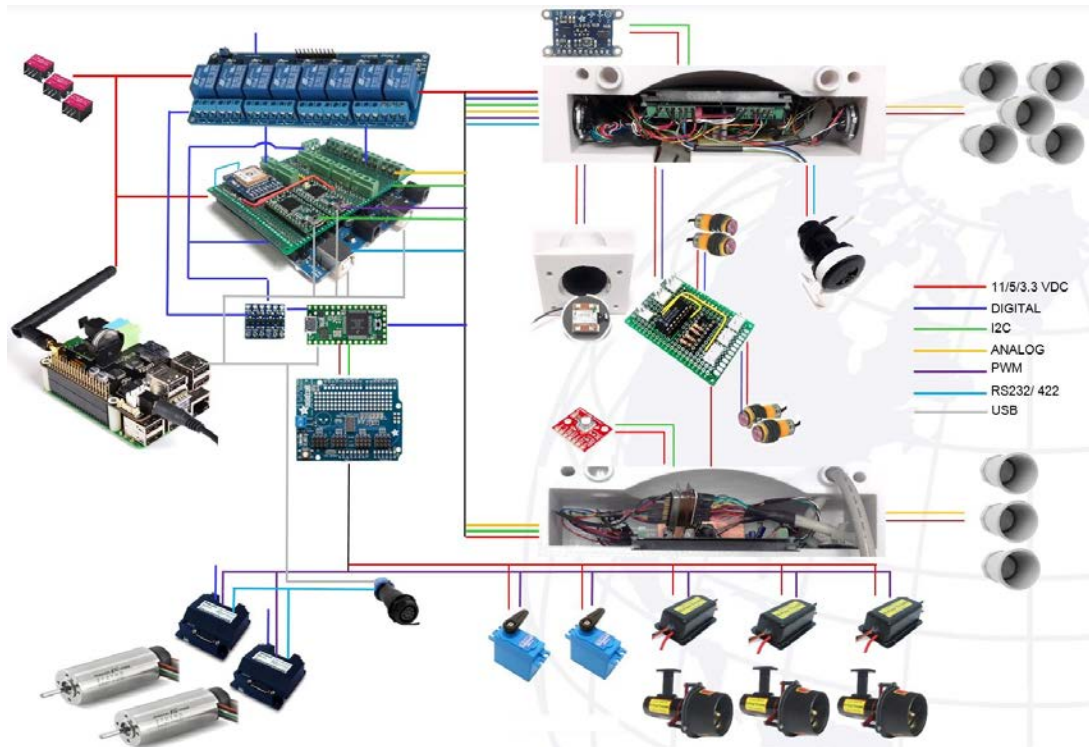


Figure 74. Electronic Components Schematic

Source: [12] O. Garcia, "Sensors and algorithms for an unmanned surf zone robot," unpublished.

3. Waterproofing

For amphibious operations, the actuators, electronics and electric connections were properly waterproofed.

The technique was to pot the device or connector with potting compound as seen in Figure 75. The process involved initial lab and field trials to assure that components operate as expected before and after potting. Electronics and electric components were potted in situ. Cables and connectors were waterproofed using FDM printed molds.

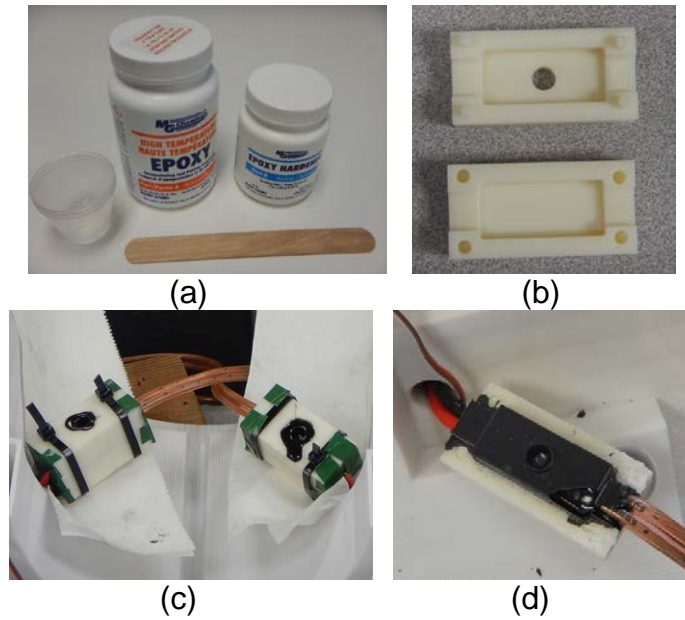


Figure 75. Cable Connection Potting Process

(a) Potting used. High temperature potting compound, (b) FDM potting molds, (c) Potting application and cure period, (d) Final connection potted and WP.

Further waterproof tests will be required prior to future amphibious water operations. The sections and connections include:

- Bow and aft electronics compartments.
- Doppler sensor support cap.
- Thruster connections to ESC.
- Bus bar holder.
- Junction boxes.
- Switch boxes.
- Circuit breaker holder.
- All cable connections.
- All waterproof connectors (on cable side only).

Figure 76 shows the platform in its final integration stage, all components, sensors and actuators are integrated with exception of the tail assembly.

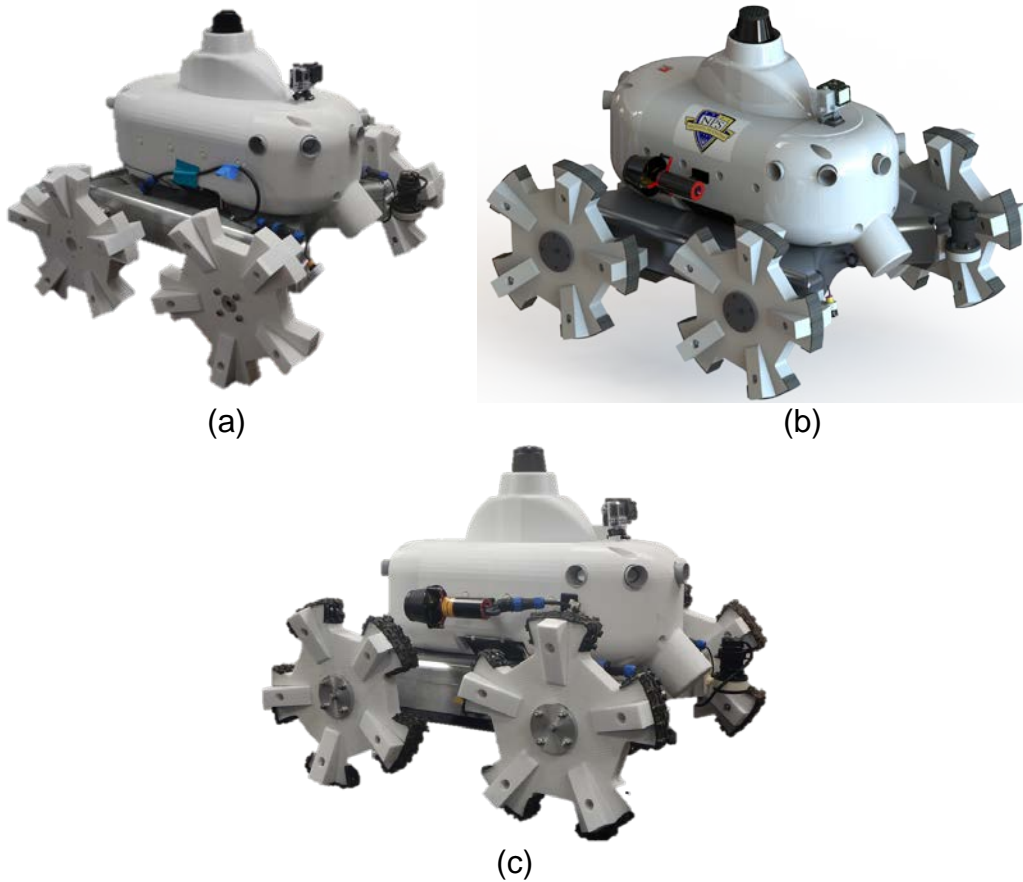


Figure 76. *MOSARt* in Final Integration Stage

(a) Real *MOSARt* assembled in advanced integration stage, (b) Rendered version of the *MOSARt*, (c) *MOSARt* assembled and integrated.

For the construction and integration of *MOSARt* some important milestones were reached as shown in Table 18.

Table 18. *MOSARt* Milestones

	Total
Platform Design time (CAD hours)	3600 hours (Approximately 5 months)
Electronics design and integration	4320 hours (Approximately 6 months)
FDM material (PC)	19 canisters (17731.23 cubic inches)
FDM material (PC support)	3 canisters (250.48 cubic inches)
Fabrication time	728.26 hours (30.3 days)
FDM material (ABS)	2 ½ canisters (140 cubic inches)
FDM material (ABS support)	½ canister (28 cubic inches)
Fabrication time	80 hours (3.3 days)
Aluminum 6061-T6	Two plates (73.66cm x 48.26cm x 3.8cm and 73.66cm x 48.26cm x 6.35cm)
Workshop time	400 hours (Approximately 16 days)

Modularity is an important feature of the design; this allows modifications and future research to be developed, in a modified version of *MOSARt* that could fit a different suite of sensors and actuators.

During initial lab tests the platform performed inside the parameters described in Table 14. These results when mapped in the CONOPS show that the minimum performance parameters (velocity and operational depth) of the platform in water and land are expected to agree as part of land and sea tests.

Lab tests successfully demonstrated that the integration of the platform was correctly performed.

THIS PAGE INTENTIONALLY LEFT BLANK

V. CONCLUSION

The goal of this project was to design and implement a prototype surf-zone robot for waterborne operations. To do so we studied the physics and then outlined and implemented the techniques required to perform various activities and tasks to design a platform to support the given concept of operations. We are confident that these results indicate that the platform, as designed, will successfully operate under the current CONOPS restrictions.

A. PHYSICS

1. Physics Motivated and Drove the Design

Conditions of the operational environment were studied to generate a proper CONOPS. The design took into account the operational environment and key parameters including pressure, water density, drag and stability, among others. The resultant surf-zone design met the expectations with regard to these objectives.

2. Pre-production Models

Physics related parameters including inertia, gravity and friction were used in the CAD environment as part of collision and dynamic tests to assess the compatibility of pieces prior to production.

3. Material and Component Selection

Physics related calculations and experiments were used for material and component selection. These calculations helped estimate operational performance parameters for water and land operations.

B. TECHNIQUE

1. CAD Modeling

The CONOPS requirements influenced the sketch models for bodies and assemblies produced in Solidworks. Every part was tested for form fit and this process included the material properties of each component prior to production. These properties included: component type, weight, color, volume and density.

2. Component Production

FDM and CNC milling technologies were used for fast prototyping. This allowed the team to move from concept to design and production in a timely and cost-effective manner.

3. Strength Tests

Material strength properties of the materials used in MOSARt were tested for suitability in surf-zone conditions.

C. EFFICIENT DESIGN

1. Space Efficiency

The modeling process helped maximize the use of space in the design process. Every part, cable and connection was modeled to test the form fit of the platform prior to production.

2. Modularity

The platform was designed to be modular. The ability to add and remove future components and sensors was a consideration in the design. It was determined that the fore and aft end caps will need to be modified in future versions to better support this objective.

3. Amphibious and Terrestrial Capabilities

MOSARt was successfully designed to operate in water and on land. The ability to transition from water to land has not been tested in the field. Our models indicate a good probability of success.

4. Water Protection

A primary design objective was to protect key electronic components from water damage by intrusion. The waterproof cylinder for electronics successfully served this purpose. Components external to the cylinder were potted for protection. These have been tank tested but not dynamically tested in an actual operational environment.

D. FUTURE WORK AND RECOMMENDATIONS

To validate the project in an operational environment the following tasks must be completed:

- Conduct water tank tests
- Conduct surf-zone tests
- Integrate the tail assembly to assist climbing capabilities
- Pot all external electronic components
- Extensively validate platform performance characteristics for land and sea operations via Solidworks simulations

This research advances the work previously completed by the AXV group and provides a durable platform for future research.

The continuation of this work is important to guarantee improved capabilities for the fleet in the fields of unmanned vehicles and robotics. The project, in concert with the research conducted by Garcia in [12], provides a special set of capabilities to naval forces for future operations in the surf zone.

THIS PAGE INTENTIONALLY LEFT BLANK

APPENDIX A. COMPONENTS SPECIFICATIONS

A. THRUSTERS

Table 19. Thruster Specifications

Motor Specifications	
Motor type	High efficiency brushless
Weight	185 g
Max Power	400 W (130W max for the thruster)
Gear Ratio	4.28:1
Shaft Diameter	5.0 mm
Maximum Case Temperature	100°C
Operating Voltage	12–50 V
Operates in forward and reverse thrust	
Connector Specifications	
Depth Rating	91.44 m / 3 wire
Thruster and Propeller Specifications	
Thruster housing / end caps	T-6 Aluminum
Thruster Seal (motor)	Flexible, polyurethane encapsulating compound
Thruster seal (shaft seal)	Fluoroloy Lip Seal followed by encapsulating grease gallery
Thruster weight (in air)	0.453 kg
Thruster weight (in water)	255 g
Thruster length	15.87 cm
Finish	Black / red Type II Hard Anodized Finish
Propeller size	60 mm–4 blade
Propeller material	Solid Brass
Propeller adapter	Machined aluminum / anodized type II black
Kort nozzle adaptor material	0.090 Aluminum
Kort nozzle adaptor offset	120 degrees
Thrust rating: (6.79kg) (approx.. 130 W max)	
12 V	3.62 kg of thrust max
24 V	6.79 kg of thrust max
50 V	6.79 kg of thrust max

Adapted from [19] 400HFS-L Hi-Flow Thruster - Data Sheet. (2015). CrustCrawler. [Online]. Available: <http://crustcrawler.com/products/urov2/index.php>.

THIS PAGE INTENTIONALLY LEFT BLANK

B. MATERIALS

1. ABSplus-P430 (Production Grade Thermoplastic)

MECHANICAL PROPERTIES	TEST METHOD	ENGLISH		METRIC	
		XZ AXIS		XZ AXIS	
Tensile Strength, Ultimate (Type 1, 0.125", 0.2"/min)	ASTM D638	4,700 psi		33 MPa	
Tensile Strength, Yield (Type 1, 0.125", 0.2"/min)	ASTM D638	4,550 psi		31 MPa	
Tensile Modulus (Type 1, 0.125", 0.2"/min)	ASTM D638	320,000 psi		2,200 MPa	
Tensile Elongation at Break (Type 1, 0.125", 0.2"/min)	ASTM D638	6%		6%	
Tensile Elongation at Yield (Type 1, 0.125", 0.2"/min)	ASTM D638	2%		2%	
IZOD Impact, notched (Method A, 23°C)	ASTM D256	2.0 ft-lb/in		106 J/m	

MECHANICAL PROPERTIES	TEST METHOD	ENGLISH		METRIC	
		XZ AXIS	ZX AXIS	XZ AXIS	ZX AXIS
Flexural Strength (Method 1, 0.05"/min)	ASTM D790	8,450 psi	5,050 psi	58 MPa	35 MPa
Flexural Modulus (Method 1, 0.05"/min)	ASTM D790	300,000 psi	240,000 psi	2,100 MPa	1,650 MPa
Flexural Strain at Break (Method 1, 0.05"/min)	ASTM D790	4%	4%	2%	2%

THERMAL PROPERTIES ²	TEST METHOD	ENGLISH	METRIC
Heat Deflection (HDT) @ 66 psi	ASTM D648	204°F	96°C
Heat Deflection (HDT) @ 264 psi	ASTM D648	180°F	82°C
Glass Transition Temperature (T _g)	DSC (SSYS)	226°F	108°C
Melting Point	-----	Not Applicable ³	Not Applicable ³
Coefficient of Thermal Expansion	ASTM E831	4.90x10 ⁻⁶ in/in/°F	8.82x10 ⁻⁶ mm/mm/°C

ELECTRICAL PROPERTIES ⁴	TEST METHOD	VALUE RANGE
Volume Resistivity	ASTM D257	2.6x10 ¹⁵ - 5.0x10 ¹⁶ ohm-cm
Dielectric Constant	ASTM D150-98	2.3 - 2.85
Dissipation Factor	ASTM D150-98	0.0046 - 0.0053
Dielectric Strength	ASTM D149-09, Method A, XZ Orientation	130 V/mil
Dielectric Strength	ASTM D149-09, Method A, ZX Orientation	290 V/mil

OTHER ²	TEST METHOD	VALUE
Specific Gravity	ASTM D792	1.04
Flame Classification	UL94	HB (0.09", 2.50mm)
UL File Number	-----	E345258
Rockwell Hardness	ASTM D785	109.5

Figure 77. ABSplus-P430 Properties

Adapted from [16]: ABSplus-P430, production-grade thermoplastic for DESIGN series 3D printers (Spec sheet). (2015). Stratasys. [Online]. Available: <http://www.stratasys.com/materials/fdm/absplus>.

2. PC-Polycarbonate (Production Grade Thermoplastic)

MECHANICAL PROPERTIES ¹	TEST METHOD	ENGLISH		METRIC	
		XZ AXIS	ZX AXIS	XZ AXIS	ZX AXIS
Tensile Strength, Yield (Type 1, 0.125", 0.2"/min)	ASTM D638	5,800 psi	4,300 psi	40 MPa	30 MPa
Tensile Strength, Ultimate (Type 1, 0.125", 0.2"/min)	ASTM D638	8,300 psi	6,100 psi	57 MPa	42 MPa
Tensile Modulus (Type 1, 0.125", 0.2"/min)	ASTM D638	282,000 psi	284,000 psi	1,944 MPa	1,958 MPa
Tensile Elongation at Break (Type 1, 0.125", 0.2"/min)	ASTM D638	4.8%	2.5%	4.8%	2.5%
Tensile Elongation at Yield (Type 1, 0.125", 0.2"/min)	ASTM D638	2.2%	2%	2.2%	2%
Flexural Strength (Method 1, 0.05"/min)	ASTM D790	13,000 psi	9,900 psi	89 MPa	68 MPa
Flexural Modulus (Method 1, 0.05"/min)	ASTM D790	291,000 psi	261,000 psi	2,006 MPa	1,800 MPa
Flexural Strain at Break (Method 1, 0.05"/min)	ASTM D790	No break	4%	No break	4%
IZOD Impact, notched (Method A, 23°C)	ASTM D256	1.4 ft-lb/in	0.5 ft-lb/in	73 J/m	28 J/m
IZOD Impact, un-notched (Method A, 23°C)	ASTM D256	16.4 ft-lb/in	3.5 ft-lb/in	877 J/m	187 J/m
Compressive Strength, Yield (Method 1, 0.05"/min)	ASTM D695	10,000 psi	9,200 psi	69 MPa	64 MPa
Compressive Strength, Ultimate (Method 1, 0.05"/min)	ASTM D695	28,000 psi	9,400 psi	193 MPa	65 MPa
Compressive Modulus (Method 1, 0.05"/min)	ASTM D695	1,100,000 psi	227,000 psi	7,564 MPa	1,565 MPa

THERMAL PROPERTIES ²	TEST METHOD	ENGLISH	METRIC
Heat Deflection (HDT) @ 66 psi	ASTM D648	260°F	138°C
Heat Deflection (HDT) @ 264 psi	ASTM D648	261°F	127°C
Vicat Softening	ASTM D1525	282°F	139°C
Glass Transition (T _g)	DMA (SSYS)	322°F	161°C
Melting Point	-----	Not Applicable ³	Not Applicable ³

ELECTRICAL PROPERTIES ⁴	TEST METHOD	VALUE RANGE
Volume Resistivity	ASTM D257	6.0x10 ¹³ - 2.0x10 ¹⁴ ohm-cm
Dielectric Constant	ASTM D150-98	2.8 - 3.0
Dissipation Factor	ASTM D150-98	.0005 - .0006
Dielectric Strength	ASTM D149-09, Method A	80 - 360 V/mil

OTHER ²	TEST METHOD	VALUE
Specific Gravity	ASTM D792	1.2
Flame Classification	UL94	HB
Coefficient of Thermal Expansion	ASTM E831	3.8x10 ⁻⁶ in/in/°F
Rockwell Hardness	ASTM D785	R115
UL File Number	-----	E345258

Figure 78. PC - Polycarbonate Properties

Adapted from [15]: PC (polycarbonate), production-grade thermoplastic for FORTUS 3D production systems (Spec sheet). (2015). Stratasys. [Online]. Available: <http://www.stratasys.com/materials/fdm/pc>.

3. PH4857 Lab 1 by Garcia and Palacios

11/30/2015

PH4857 – LABORATORY #1

Oscar García
Ronal Palacios

1. SAMPLE PREPARATION

Three types of materials were selected for the test:

1. Kevlar-filled nylon.
2. Solid printed 3D material.
3. Sparse printed 3D material.

The samples were machined to accomplish Hopkinson Bar and Instron tests. The details are presented on Table 1. Before and after cells refers to measurements made prior and afterwards the executed test. Densities were calculated using the measured data.

TABLE N°1 SAMPLES DIMENSIONS

KEVLAR SAMPLES													
#		LENGTH (μm)				MED LENGTH	DIAMETER (μm)			MED DIAM	MASS (g)	VOL (cm3)	Rho (kg/m3)
1	BEFORE	12717	12761	12787	12662	12732	12778	12772	12765	12772			
	AFTER	12719	12632	12661	1272	9821	12811	12810	18805	14809			
2	BEFORE	12538	12547	12594	12549	12557	12778	12778	12781	12779	1.9031	1.61	1181.7
3	BEFORE	26087	26061	26046	26073	26067	12779	12778	12780	12779			
4	BEFORE	26428	26276	26298	26497	26375	12780	12777	12778	12778	3.9987	3.38	1182.2

3D SOLID SAMPLES													
#		LENGTH (μm)				MED LENGTH	DIAMETER (μm)			MED DIAM	MASS (g)	VOL (cm3)	Rho (kg/m3)
1	BEFORE	20247	20195	20218	20218	20220	8863	8862	8875	8867	1.4103	1.25	1129.6
2	BEFORE	20299	20236	20219	20231	20246	8931	8906	8894	8910			
5	BEFORE	10270	10368	10275	10306	10305	8863	8858	8835	8852			
	AFTER	10260	10238	10241	10246	10246	8961	8981	8873	8938			
6	BEFORE	10362	10377	10318	10323	10345	8860	8860	8862	8861			

3D SPARCE SAMPLES													
#		LENGTH (μm)				MED LENGTH	DIAMETER (μm)			MED DIAM	MASS (g)	VOL (cm3)	Rho (kg/m3)
1	BEFORE	20252	20197	20189	20245	20221	8925	8903	8892	8907	1.3175	1.26	1045.8
2	BEFORE	20216	20168	20256	20223	20216	8947	8923	8953	8941			
3	BEFORE	10342	10317	10303	10302	10316	8972	8938	9024	8978			
	AFTER	10424	10246	10250	10252	10293	9031	9008	8863	8967			
4	BEFORE	10282	10318	10349	10268	10304	8969	8951	8939	8953			

Table 2 shows factory data available for each sample.

TABLE N°2 SAMPLES FACTORY DATA

FACTORY DATA				
MATERIAL	lb/in ³	kg/m ³	kg/cm ³	QUASISTATIC YIELD [Pa]
KEVLAR	0.042	1162.556	0.001163	1.00E+08
3D SOLID		1190		6.77E+07
3D SPARCE				5.77E+07

2. QUASISTATIC YIELD STRESS TEST - INSTRON

Ideally, L/D = 2 samples are used on this tests, but because the 3D printed material had a tendency to bend during the compression, in both cases (solid and sparse) L/D = 1 samples were used.

Figure 1 shows a consolidated result for each material. The raw experimental curves showed in the beginning of the elastic regime curved imperfections (called toes), which corresponds to adjustments of the sample during the compression due non-perfect flatness of the sample's surface. This effects had to be filtered out by subtracting the strain value that corresponded to the end point of the toe.

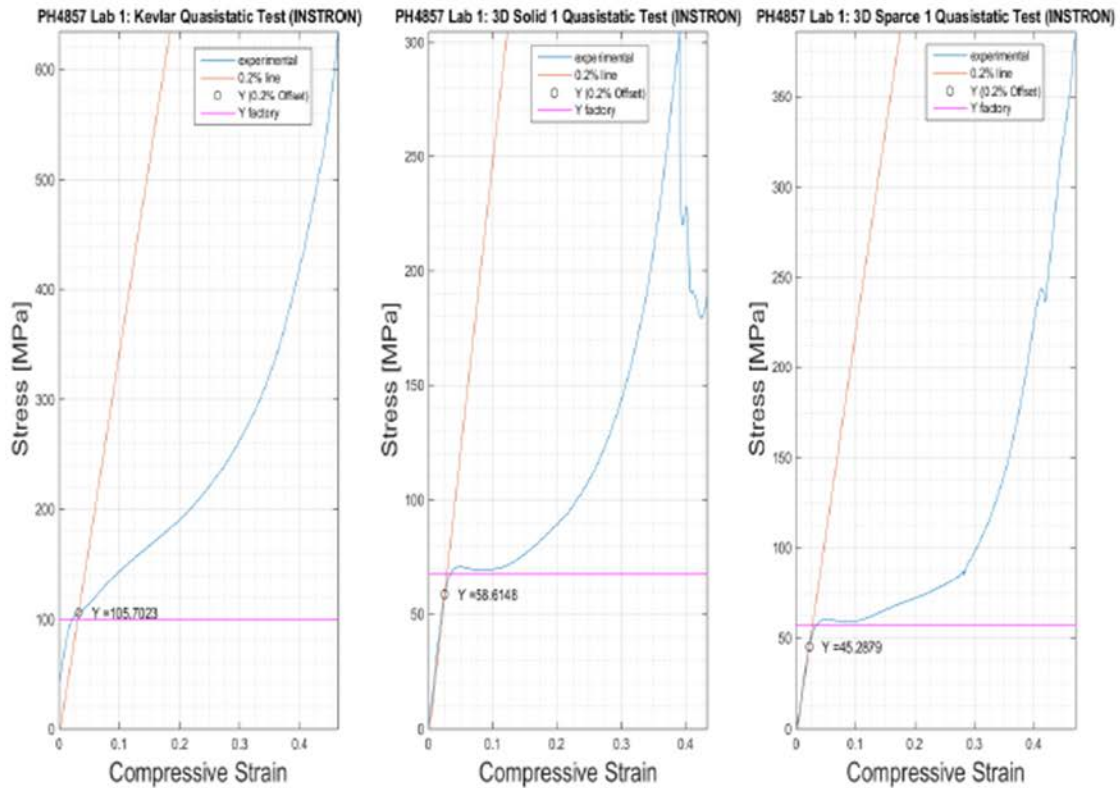


FIGURE N°1 QUASISTATIC YIELD TEST

For defining the yield strength, the 0.2% Offset method was implemented on the Matlab code. To achieve this, a segment of the elastic regime had to be manually selected, then the program calculates the linear coefficients (the slope m , which correspond to the Young's Module and the Stress axis intersection b) and finally the line is graphed with a 0.002 strain offset. The intersection is calculated by searching the minimum difference between the stress at a particular strain point for the curve and the offset line.

It can be seen that the factory yield stress coincide with the curving point of the elastic – plastic curve, whereas the 0.2% Offset yield strength lies underneath this value. The exception is for Kevlar, where the both values coincide in an acceptable range.

Both 3D printed samples shows the breaking point of these materials at the end of the stress-strain curve, being the solid 3D printed material the most obvious. This is not shown on the Kevlar sample, as this did not break during compression (see figure 2).



FIGURE N°2 SAMPLES AFTER INSTRON TEST (KEVLAR – 3D SOLID – 3D SPARCE)

3. DYNAMIC YIELD STRESS TEST – HOPKINSON BAR

Figure 3 shows the results for the dynamic yield test done in the Hopkinson Bar. The corresponding rate vs time was included to validate the data taken.

Under these conditions (soft polymers testing), the Hopkinson Bar is more useful for studying the plastic behavior under strain rate conditions. Therefore, an accurate reading of the dynamic yield is not expected. Still, the 0.02% Offset technique was implemented to calculate the dynamic yield stress.

Kevlar's dynamic yield presented a similar value that the one obtained in the Instron (quasistatic) and factory data, but, as it usually is for a dynamic yield, a higher value was expected. It must be noticed that the strain rate in this case did not reach 800 [1/s]. Both 3D printed material presented a higher value for the dynamic yield stress in comparison to their quasistatic value.

The dimensions of the samples after the Hopkinson Bar are detailed on Table 1.

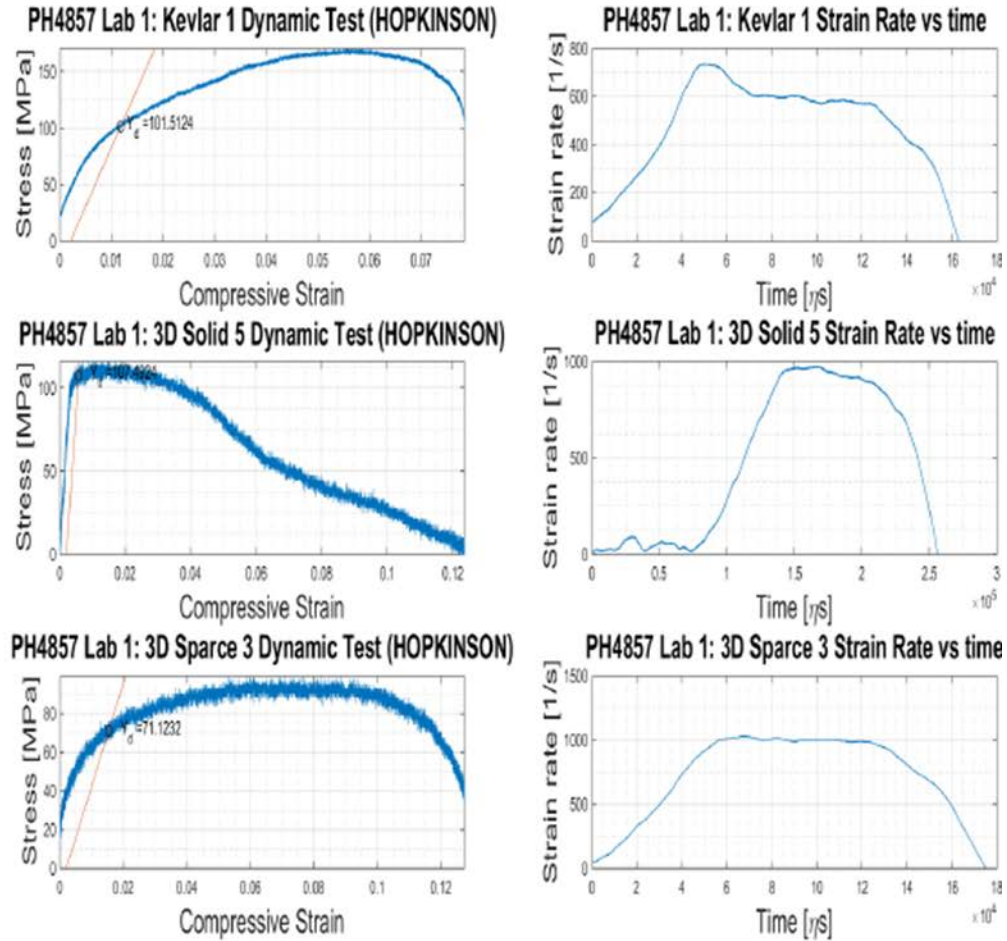


FIGURE N°3 DYNAMIC YIELD TEST

4. RESULTS

Table 3 shows the printout of the Matlab program. The Young's modulus (E) was determined by means of the slope of the linearized elastic region of the quasistatic test. Solid and sparse 3D printer material shared almost same value of E (88% similar), which validates this result, as both samples are made of the same material.

The parameter J was calculated by

$$J = \frac{Y_d}{\rho_0}$$

It can be seen, that the material that presented the best J parameter (under this test conditions) is the Solid 3D Material.

TABLE N°3 TEST RESULTS PRINTOUTS

***** RESULTS - HW#5 - *****	
Kevlar Dynamic Yield [MPa]:	101.51
Kevlar Quasistatic Yield [MPa]:	105.70
Solid 3D Material Dynamic Yield [MPa]:	107.49
Solid 3D Material Quasistatic Yield [MPa]:	58.61
Sparce 3D Material Dynamic Yield [MPa]:	71.12
Sparce 3D Material Quasistatic Yield [MPa]:	45.29
Kevlar Young's modulus E (INSTRON) [GPa]:	3.5
Solid 3D Material Young's modulus E (INSTRON) [GPa]:	2.5
Sparce 3D Material Young's modulus E (INSTRON) [GPa]:	2.2
J kevlar [k Nm/kg]:	85.91
J solid 3D [k Nm/kg]:	95.16
J sparce 3D [k Nm/kg]:	68.01

5. MATLAB CODE

```

clear all
clc
clf

rho_k = 1181.658799; % [kg/m3] calculated
rho_sol3D = 1129.614995; % [kg/m3] calculated
rho_spa3D = 1045.762549; % [kg/m3] calculated

facY_k = 100; % [MPa] factory quasistatic Yield
facY_sol3D = 67.7; % [MPa] factory quasistatic Yield
facY_spa3D = 57.7; % [MPa] factory quasistatic Yield

kevlar2 = xlsread('kevlar2.xlsx',1); % read the results from excel
solid3D1 = xlsread('kevlar2.xlsx',2); % read the results from excel
sparce3D1 = xlsread('kevlar2.xlsx',3); % read the results from excel

figure(1)
subplot(1,3,1)
i = find(kevlar2(:,1)==0.03178); % end point of "toe"
zero_e= kevlar2(i,1);
zero_s= kevlar2(i,2);

% kevlar2(:,2) = kevlar2(:,2) - zero_s;
kevlar2(:,1) = kevlar2(:,1) - zero_e;

plot(kevlar2(:,1),kevlar2(:,2))
grid on
grid minor
hold on
b=1;
for a=1:length(kevlar2(:,1))
    if (kevlar2(a,1)>0.00203 && kevlar2(a,1)<=0.01) % for selecting segment of elastic
        x1(b) = kevlar2(a,1); % values entered manually
        y1(b) = kevlar2(a,2);
    end
end

```

```

        b= b+1;
    end
end

linearCoef = polyfit(x1,y1,1);
E_gk = linearCoef(1);
elastic=@(E) linearCoef(1)*(E-(0.002+linearCoef(2)/linearCoef(1)))+linearCoef(2);
ezplot(elastic)
xlabel('Compressive Strain','FontSize', 18)
ylabel('Stress [MPa]','FontSize', 18)
title('PH4857 Lab 1: Kevlar Quasistatic Test (INSTRON)','FontSize',12)
axis([0 max(kevlar2(:,1)) 0 max(kevlar2(:,2))])

for a=1:length(kevlar2(:,1))
    d(a) = abs(kevlar2(a,2)-elastic(kevlar2(a,1)));
end
id1 = find(d == min(d)); % simple way to find intersection of the 0.2% offset

plot(kevlar2(id1,1), kevlar2(id1,2),'kO')
text(kevlar2(id1,1), kevlar2(id1,2),[' Y =',num2str(kevlar2(id1,2))], 'Color',
'k','FontSize', 10)
hline1 = reffline([0 facY_k]);
hline1.Color = 'm';
legend('experimental','0.2% line','Y (0.2% Offset)','Y factory')
hold off

% figure(2)
subplot(1,3,2)
i = find(solid3D1(:,1)==0.00601);
zero_e= solid3D1(i,1);
zero_s= solid3D1(i,2);

solid3D1(:,1) = solid3D1(:,1) - zero_e;

plot(solid3D1(:,1),solid3D1(:,2))
grid on
grid minor
hold on
b=1;
for a=1:length(solid3D1(:,1))
    if (solid3D1(a,1)>0.005 && solid3D1(a,1)<=0.02)
        x2(b) = solid3D1(a,1);
        y2(b) = solid3D1(a,2);
        b= b+1;
    end
end

linearCoef = polyfit(x2,y2,1);
E_gsol3D = linearCoef(1);
elastic=@(E) linearCoef(1)*(E-(0.002+linearCoef(2)/linearCoef(1)))+linearCoef(2);
ezplot(elastic)
xlabel('Compressive Strain','FontSize', 18)
ylabel('Stress [MPa]','FontSize', 18)
title('PH4857 Lab 1: 3D Solid 1 Quasistatic Test (INSTRON)','FontSize',12)
axis([0 max(solid3D1(:,1)) 0 max(solid3D1(:,2))])

for a=1:length(solid3D1(:,1))
    d(a) = abs(solid3D1(a,2)-elastic(solid3D1(a,1)));
end
id2 = find(d == min(d));

plot(solid3D1(id2,1), solid3D1(id2,2),'kO')

```

```

text(solid3D1(id2,1), solid3D1(id2,2), [' Y =', num2str(solid3D1(id2,2))], 'Color',
'k', 'FontSize', 10)
hline2 = reffline([0 facY_sol3D]);
hline2.Color = 'm';
legend('experimental', '0.2% line', 'Y (0.2% Offset)', 'Y factory')
hold off

% figure(3)
subplot(1,3,3)
i = find(sparce3D1(:,1)==0.0115);
zero_e= sparce3D1(i,1);
zero_s= sparce3D1(i,2);

sparce3D1(:,1) = sparce3D1(:,1) - zero_e;

plot(sparce3D1(:,1), sparce3D1(:,2))
grid on
grid minor
hold on
b=1;
for a=1:length(sparce3D1(:,1))
    if (sparce3D1(a,1)>0.005 && sparce3D1(a,1)<=0.02)
        x3(b) = sparce3D1(a,1);
        y3(b) = sparce3D1(a,2);
        b= b+1;
    end
end

linearCoef = polyfit(x3,y3,1);
E_qspa3D = linearCoef(1);
elastic=@(E) linearCoef(1)*(E-(0.002+linearCoef(2)/linearCoef(1))+linearCoef(2));
ezplot(elastic)
xlabel('Compressive Strain', 'FontSize', 18)
ylabel('Stress [MPa]', 'FontSize', 18)
title('PH4857 Lab 1: 3D Sparce 1 Quasistatic Test (INSTRON)', 'FontSize', 12)
axis([0 max(sparce3D1(:,1)) 0 max(sparce3D1(:,2))])

for a=1:length(sparce3D1(:,1))
    d(a) = abs(sparce3D1(a,2)-elastic(sparce3D1(a,1)));
end
id3 = find(d == min(d));

plot(sparce3D1(id3,1), sparce3D1(id3,2), 'kO')
text(sparce3D1(id3,1), sparce3D1(id3,2), [' Y =', num2str(sparce3D1(id3,2))],
'Color', 'k', 'FontSize', 10)
hline3 = reffline([0 facY_spa3D]);
hline3.Color = 'm';
legend('experimental', '0.2% line', 'Y (0.2% Offset)', 'Y factory')
hold off

%%

kevlarl = xlsread('shot3_sample1kevlar_50psi_PS_MT.xlsx',2); % read the results from
bar test
solid3D5 = xlsread('shot2_sample53dsolid_50psi_PS_MT.xlsx',2); % read the results fro
bar test
sparce3D3 = xlsread('shot4_sample33dsparse_50psi_PS_MT.xlsx',2); % read the results
from bar test

figure(2)
subplot(3,2,1)
plot(kevlarl(:,2), kevlarl(:,3))

```

```

grid on
grid minor
hold on
b=1;
for a=1:length(kevlarl(:,2))
    if (kevlarl(a,2)>0.000 && kevlarl(a,2)<=0.004818)
        x4(b) = kevlarl(a,2);
        y4(b) = kevlarl(a,3);
        b= b+1;
    end
end

linearCoef(1) = (y4(b-1)-y4(1))/(x4(b-1)-x4(1));
linearCoef(2)= y4(1);
% elastic = @(E) linearCoef(1)*E + linearCoef(2);

% linearCoef = polyfit(x1,y1,1);

elastic=@(E) linearCoef(1)*(E-(0.002+linearCoef(2)/linearCoef(1)))+linearCoef(2);
E_dk = linearCoef(1);
ezplot(elastic)
xlabel('Compressive Strain','FontSize', 18)
ylabel('Stress [MPa]','FontSize', 18)
title('PH4857 Lab 1: Kevlar 1 Dynamic Test (HOPKINSON)','FontSize',18)
axis([0 max(kevlarl(:,2)) 0 max(kevlarl(:,3))])

for a=1:length(kevlarl(:,2))
    d(a) = abs(kevlarl(a,3)-elastic(kevlarl(a,2)));
end
id4 = find(d == min(d));

plot(kevlarl(id4,2), kevlarl(id4,3),'kO')
text(kevlarl(id4,2), kevlarl(id4,3),[' Y_d =',num2str(kevlarl(id4,3))], 'Color',
'k','FontSize', 10)
hold off

subplot(3,2,2)
plot(kevlarl(:,4),kevlarl(:,1))
grid on
grid minor
xlabel('Time [\etas]','FontSize', 18)
ylabel('Strain rate [1/s]','FontSize', 18)
title('PH4857 Lab 1: Kevlar 1 Strain Rate vs time','FontSize',18)

% figure(5)
subplot(3,2,3)

plot(solid3D5(:,2),solid3D5(:,3))
grid on
grid minor
hold on
b=1;
for a=1:length(solid3D5(:,2))
    if (solid3D5(a,2)>0.00 && solid3D5(a,2)<=0.003225)
        x5(b) = solid3D5(a,2);
        y5(b) = solid3D5(a,3);
        b= b+1;
    end
end

linearCoef = polyfit(x5,y5,1);
E_dsol3D = linearCoef(1);

```

```

elastic=@(E) linearCoef(1)*(E-(0.002+linearCoef(2)/linearCoef(1)))+linearCoef(2);
ezplot(elastic)
xlabel('Compressive Strain','FontSize', 18)
ylabel('Stress [MPa]','FontSize', 18)
title('PH4857 Lab 1: 3D Solid 5 Dynamic Test (HOPKINSON)','FontSize',18)
axis([0 max(solid3D5(:,2)) 0 max(solid3D5(:,3))])

for a=1:length(solid3D5(:,2))
    d(a) = abs(solid3D5(a,3)-elastic(solid3D5(a,2)));
end
id5 = find(d == min(d));

plot(solid3D5(id5,2), solid3D5(id5,3),'kO')
text(solid3D5(id5,2), solid3D5(id5,3),['    Y_d =',num2str(solid3D5(id5,3))], 'Color'
    'k','FontSize', 10)
hold off

subplot(3,2,4)
plot(solid3D5(:,4),solid3D5(:,1))
grid on
grid minor
xlabel('Time [\etas]','FontSize', 18)
ylabel('Strain rate [1/s]','FontSize', 18)
title('PH4857 Lab 1: 3D Solid 5 Strain Rate vs time','FontSize',18)

% figure(6)
subplot(3,2,5)

plot(sparce3D3(:,2),sparce3D3(:,3))
grid on
grid minor
hold on
b=1;
for a=1:length(sparce3D3(:,2))
    if (sparce3D3(a,2)>=0.000 && sparce3D3(a,2)<=0.00743)
        x6(b) = sparce3D3(a,2);
        y6(b) = sparce3D3(a,3);
        b= b+1;
    end
end

linearCoef(1) = (y6(b-1)-y6(1))/(x6(b-1)-x6(1));
linearCoef(2)= y6(1);
E_dspa3D = linearCoef(1);
% elastic = @(E) linearCoef(1)*E + linearCoef(2);

% linearCoef = polyfit(x3,y3,1);
elastic=@(E) linearCoef(1)*(E-(0.002+linearCoef(2)/linearCoef(1)))+linearCoef(2);
ezplot(elastic)
xlabel('Compressive Strain','FontSize', 18)
ylabel('Stress [MPa]','FontSize', 18)
title('PH4857 Lab 1: 3D Sparce 3 Dynamic Test (HOPKINSON)','FontSize',18)
axis([0 max(sparce3D3(:,2)) 0 max(sparce3D3(:,3))])

for a=1:length(sparce3D3(:,2))
    d(a) = abs(sparce3D3(a,3)-elastic(sparce3D3(a,2)));
end
id6 = find(d == min(d));

plot(sparce3D3(id6,2), sparce3D3(id6,3),'kO')
text(sparce3D3(id6,2), sparce3D3(id6,3),['    Y_d =',num2str(sparce3D3(id6,3))],
    'Color', 'k','FontSize', 10)

```

```

hold off

subplot(3,2,6)
plot(sparce3D3(:,4),sparce3D3(:,1))
grid on
grid minor
xlabel('Time [\etas]','FontSize',18)
ylabel('Strain rate [1/s]','FontSize',18)
title('PH4857 Lab 1: 3D Sparce 3 Strain Rate vs time','FontSize',18)

%%

J_k = kevlarl(id4,3)/rho_k;
J_sol3D = solid3D5(id5,3)/rho_sol3D;
J_spa3D = sparce3D3(id6,3)/rho_spa3D;

fprintf('\n          ***** RESULTS - HW#5 - *****\n')
fprintf('Kevlar Dynamic Yield [MPa]:           %.2f\n',kevlarl(id4,3))
fprintf('Kevlar Quasistatic Yield [MPa]:         %.2f\n',kevlarl(id1,2))
fprintf('Solid 3D Material Dynamic Yield [MPa]:     %.2f\n',solid3D5(id5,3))
fprintf('Solid 3D Material Quasistatic Yield [MPa]: %.2f\n',solid3D1(id2,2))
fprintf('Sparce 3D Material Dynamic Yield [MPa]:    %.2f\n',sparce3D3(id6,3))
fprintf('Sparce 3D Material Quasistatic Yield [MPa]: %.2f\n\n',sparce3D1(id3,2))

% fprintf('Kevlar Young''s modulus E (HOPKINSON) [GPa]:           %.1f\n',E_dk/1000)
fprintf('Kevlar Young''s modulus E (INSTRON) [GPa]:           %.1f\n',E_qk/1000)
% fprintf('Solid 3D Material Young''s modulus E (HOPKINSON) [GPa]:           %.1f\n',E_dsol3D/1000)
fprintf('Solid 3D Material Young''s modulus E (INSTRON) [GPa]:           %.1f\n',E_qsol3D/1000)
% fprintf('Sparce 3D Material Young''s modulus E (HOPKINSON) [GPa]:           %.1f\n',E_dspa3D/1000)
fprintf('Sparce 3D Material Young''s modulus E (INSTRON) [GPa]:           %.1f\n\n',E_qspa3D/1000)

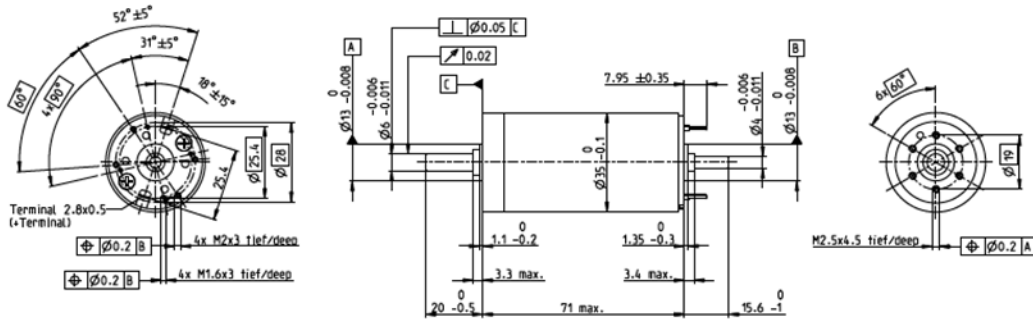
fprintf('J kevlar [k Nm/kg]:           %.2f\n',J_k*1000)
fprintf('J solid 3D [k Nm/kg]:         %.2f\n',J_sol3D*1000)
fprintf('J sparce 3D [k Nm/kg]:       %.2f\n',J_spa3D*1000)

```

C. LAND MOTORS

RE 35 $\varnothing 35$ mm, Graphite Brushes, 90 Watt

maxon DC motor



M 1:2

- Stock program
- Standard program
- Special program (on request)

Part Numbers

according to dimensional drawing
shaft length 15.6 shortened to 4 mm

273752	323890	273753	273754	273755	273756	273757	273758	273759	273760	273761	273762	273763
285785	323891	285786	285787	285788	285789	285790	285791	285792	285793	285794	285795	285796

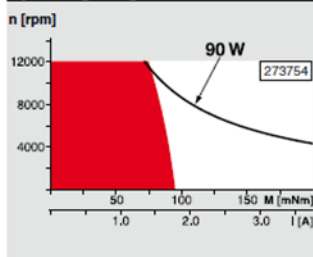
Motor Data

Values at nominal voltage																		
1	Nominal voltage	V	15	24	30	42	48	48	48	48	48	48	48	48	48	48	48	48
2	No load speed	rpm	7190	7740	7270	7560	7300	6670	5980	4760	3820	3140	2580	2110	1630			
3	No load current	mA	247	169	124	92.9	77.5	68.8	59.8	44.8	34.2	27.2	21.6	17.2	13			
4	Nominal speed	rpm	6500	7000	6490	6820	6530	5890	5180	3940	2990	2290	1720	1230	736			
5	Nominal torque (max. continuous torque)	mNm	73.1	101	97.2	101	99.4	101	101	104	106	106	106	105	105			
6	Nominal current (max. continuous current)	A	4	3.62	2.62	2.02	1.67	1.55	1.39	1.14	0.928	0.761	0.626	0.507	0.393			
7	Stall torque	mNm	929	1200	973	1080	980	890	776	620	498	398	322	255	196			
8	Starting current	A	47.8	41.1	25	20.7	15.8	13.1	10.2	6.5	4.2	2.76	1.84	1.19	0.708			
9	Max. efficiency	%	83	86	85	86	86	85	85	84	82	81	79	77	74			
Characteristics																		
10	Terminal resistance	Ω	0.314	0.583	1.2	2.03	3.05	3.67	4.69	7.38	11.4	17.4	26	40.2	67.8			
11	Terminal inductance	mH	0.085	0.191	0.34	0.62	0.87	1.04	1.29	2.04	3.16	4.65	6.89	10.3	17.1			
12	Torque constant	mNm/A	19.4	29.2	38.9	52.5	62.2	68	75.8	95.2	119	144	175	214	276			
13	Speed constant	rpm/V	491	328	246	182	154	140	126	100	80.5	66.4	54.6	44.7	34.6			
14	Speed / torque gradient	rpm/mNm	7.93	6.55	7.57	7.05	7.52	7.57	7.79	7.77	7.76	8.01	8.13	8.4	8.49			
15	Mechanical time constant	ms	5.65	5.44	5.4	5.35	5.34	5.35	5.35	5.36	5.36	5.37	5.38	5.39	5.41			
16	Rotor inertia	gcm ²	68.1	79.2	68.1	72.5	67.9	67.4	65.6	65.9	65.9	64	63.2	61.2	60.8			

Specifications

Thermal data			
17	Thermal resistance housing-ambient	6.2 K/W	
18	Thermal resistance winding-housing	2.0 K/W	
19	Thermal time constant winding	30.2 s	
20	Thermal time constant motor	644 s	
21	Ambient temperature	-30...+100°C	
22	Max. permissible winding temperature	+155°C	
Mechanical data (ball bearings)			
23	Max. permissible speed	12000 rpm	
24	Axial play	0.05 - 0.15 mm	
25	Radial play	0.025 mm	
26	Max. axial load (dynamic)	5.6 N	
27	Max. force for press fits (static) (static, shaft supported)	110 N	
28	Max. radial loading, 5 mm from flange	1200 N	
Other specifications			
29	Number of pole pairs	1	
30	Number of commutator segments	13	
31	Weight of motor	340 g	

Operating Range



Comments

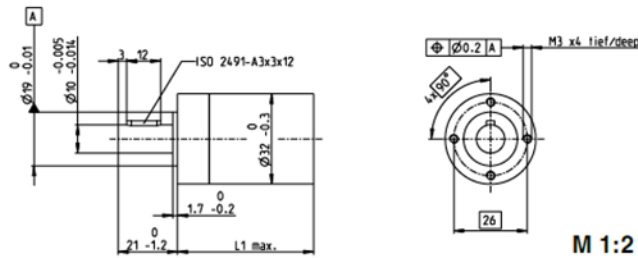
- Continuous operation**
In observation of above listed thermal resistance (lines 17 and 19) the maximum permissible winding temperature will be reached during continuous operation at 25°C ambient.
= Thermal limit.
- Short term operation**
The motor may be briefly overloaded (recurring).
- Assigned power rating**

Figure 79. Maxon Motor RE35 Specifications

Information corresponding to the motor is under part number 273752 column. Adapted from [25]: Maxon Motor (273752), RE 35, 35mm, Graphite Brushes, 90 Watt, Spec sheet. (2015). Maxon motor. [Online]. Available: http://www.maxonmotor.com/medias/sys_master/root/8816798859294/15-140-EN.pdf.

Planetary Gearhead GP 32 HP $\varnothing 32$ mm, 4.0–8.0 Nm

High Power



Technical Data

Planetary Gearhead	straight teeth
Output shaft	stainless steel
Bearing at output	ball bearing
Radial play, 10 mm from flange	max. 0.14 mm
Axial play	max. 0.4 mm
Max. permissible axial load	120 N
Max. permissible force for press fits	120 N
Sense of rotation, drive to output	=
Recommended input speed	< 8000 rpm
Recommended temperature range	-40...+100°C
Number of stages	2 3 4
Max. radial load, 10 mm from flange	200 N 250 N 300 N

maxon gear

	Part Numbers						
	320247	326663	326664	326668	326672	324947	324952
Stock program							
Standard program							
Special program (on request)							
Gearhead Data							
1 Reduction	14:1	33:1	51:1	111:1	190:1	456:1	706:1
2 Reduction absolute	676/43	329/18	17376/543	13824/125	456276/2401	80403/196	158171/224
3 Max. motor shaft diameter	6 mm	3	6	4	6	3	3
Part Numbers	326659		326665	326669	324942	324948	324953
1 Reduction	18:1		66:1	123:1	246:1	492:1	762:1
2 Reduction absolute	624/35		16224/245	6877/56	421824/1715	86112/175	106444/25
3 Max. motor shaft diameter	6 mm		6	3	6	3	4
Part Numbers	326660		326666	326670	324944	324949	324954
1 Reduction	21:1		79:1	132:1	295:1	531:1	913:1
2 Reduction absolute	293/14		3887/49	3312/25	101062/343	321778/625	38305/40
3 Max. motor shaft diameter	6 mm		6	4	6	4	3
Part Numbers	326661		326667	326671	324945	324950	
1 Reduction	23:1		86:1	159:1	318:1	589:1	
2 Reduction absolute	376/25		14076/175	1587/10	389376/1225	20637/35	
3 Max. motor shaft diameter	4 mm		6	3	6	6	
Part Numbers	326662		320297		324946	324951	
1 Reduction	28:1		103:1		411:1	636:1	
2 Reduction absolute	138/5		3388/35		355424/675	79488/125	
3 Max. motor shaft diameter	4 mm		6		6	4	
4 Number of stages	2	2	3	3	4	4	4
5 Max. continuous torque	Nm 4	4	8	8	8	8	8
6 Intermittently permissible torque at gear output	Nm 6	6	12	12	12	12	12
7 Max. efficiency	% 75	75	70	70	60	60	60
8 Weight	g 178	178	213	213	249	249	249
9 Average backlash no load	° 0.8	0.8	1.0	1.0	1.0	1.0	1.0
10 Mass inertia	gcm ² 1.6	0.5	1.5	0.7	1.5	1.5	0.7
11 Gearhead length L1	mm 48.3	48.3	55.0	55.0	61.7	61.7	61.7

Figure 80. Planetary Gearhead GP 32 HP

Information corresponding to the motor is under part number 326661 column. Adapted from [26] Maxon motor Planetary Gearhead (326661) GP 32 HP, 32mm, 4.0-8.9 Nm Spec sheet. (2015). Maxon motor. [Online]. Available: http://www.maxonmotor.com/medias/sys_master/root/8816809115678/15-310-EN.pdf.

D. SPROCKETS

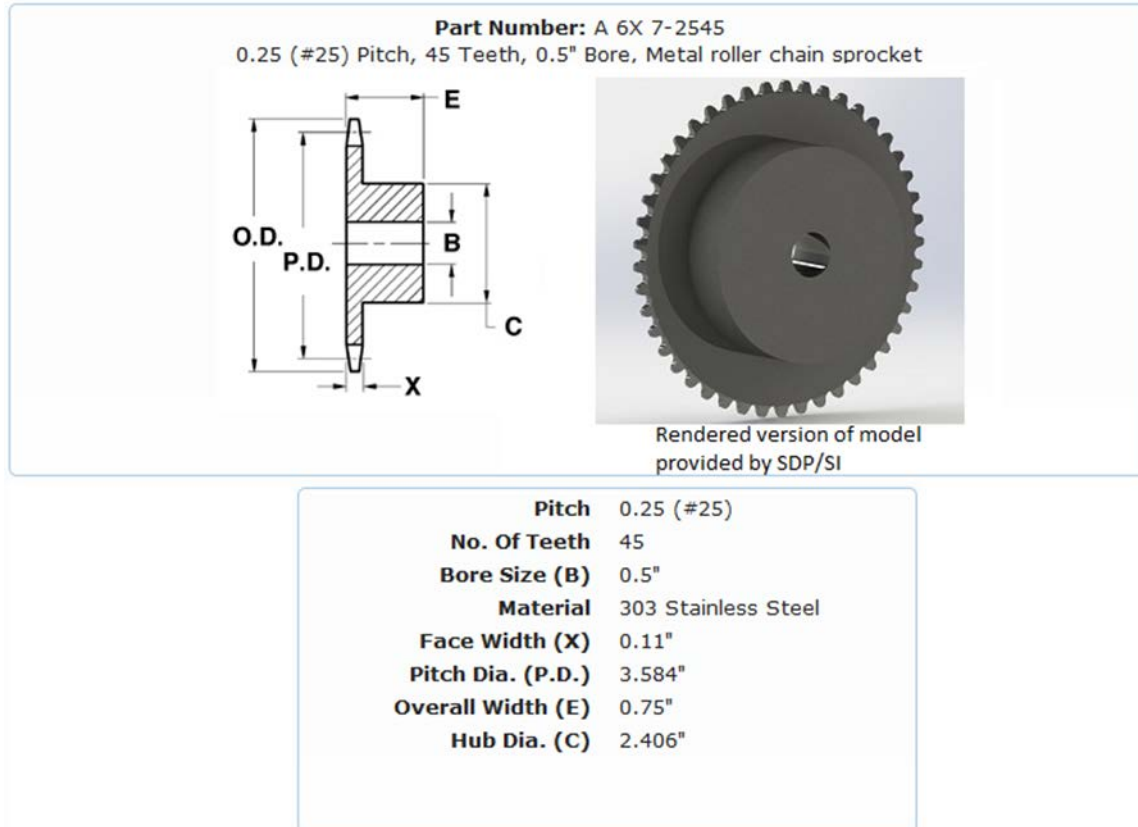
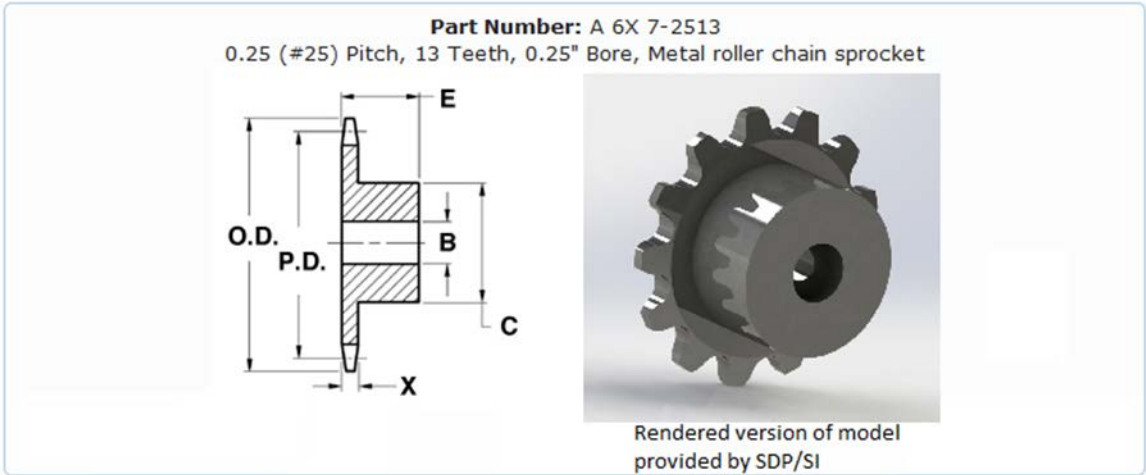


Figure 81. 45 Teeth Sprocket Specifications

Source: [23] 45 teeth sprocket specification (SS 304). (2015). SDP-SI. [Online]. Available: <http://sdp-si.com/eStore/Catalog/Group/585=>.



Pitch	0.25 (#25)
No. Of Teeth	13
Bore Size (B)	0.25"
Material	303 Stainless Steel
Face Width (X)	0.11"
Pitch Dia. (P.D.)	1.045"
Overall Width (E)	0.5"
Hub Dia. (C)	0.719"

Figure 82. 13 Teeth Sprocket Specifications

Source: [24] 13 teeth sprocket specification (SS 304). (2015). SDP-SI. [Online]. Available: <http://sdp-si.com/eStore/Catalog/Group/585=>.

APPENDIX B. SKETCHES

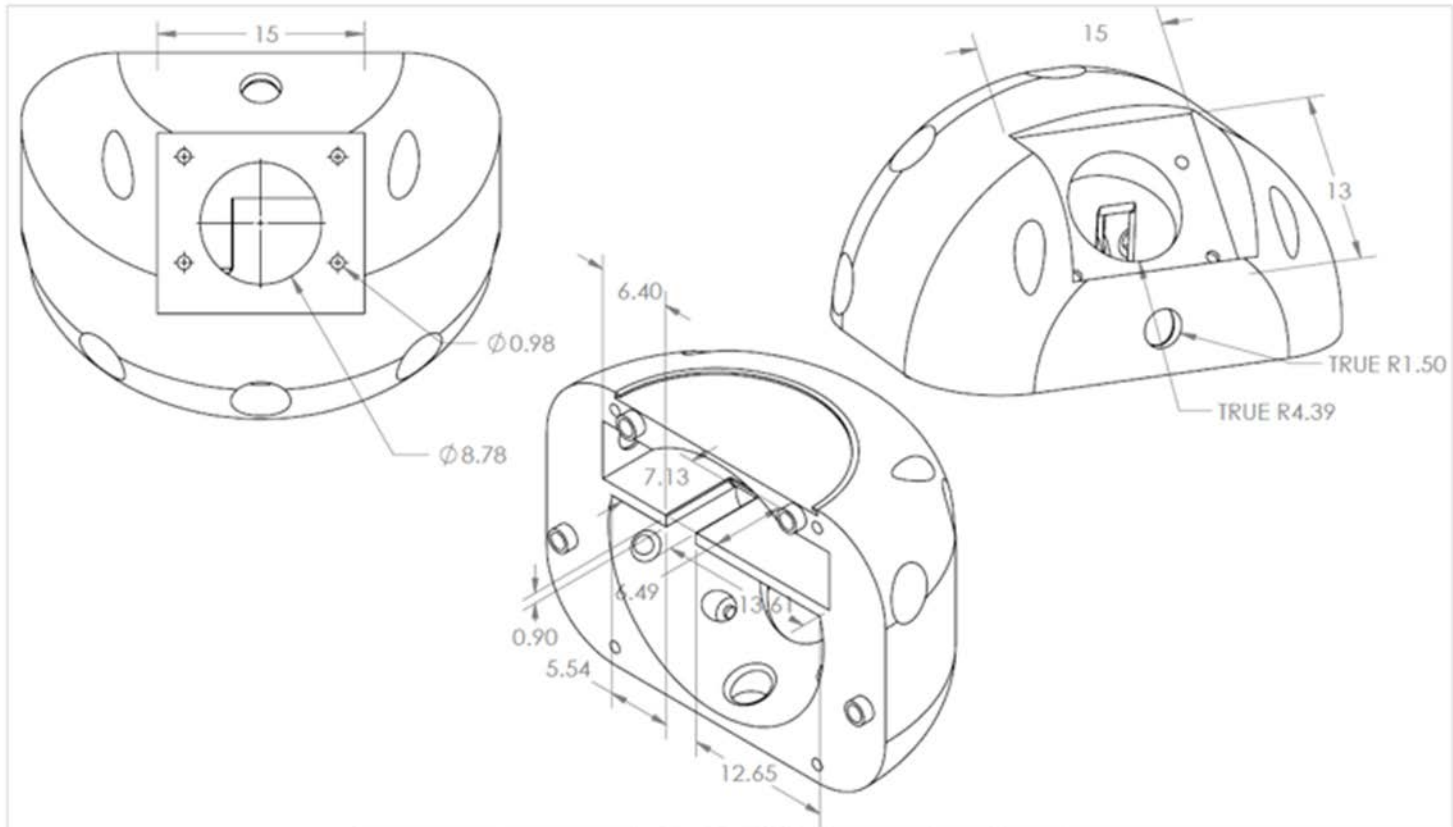
This appendix contains the sketches for all parts designed. These are not meant for replication or used as drawings but to provide general measures on each part. CAD files on Solidworks are part of this research and are kept as part of the theses repository in the AXV-LAB.

All sketches are created using Solidworks 2013–2014 students education edition license.

The sketches are presented in the same order as in the design chapter:

1. Water section
 - Bow end cap
 - Stern end cap
 - Middle section bottom/top
 - Electronics rack
 - Doppler cone
 - Sail

2. Land section
 - Bottom land skid
 - Top land skid
 - Drive train
 - Tail
 - Component holders and mounts



PROPRIETARY AND CONFIDENTIAL
 THE INFORMATION CONTAINED IN THIS DRAWING IS THE SOLE PROPERTY OF NAVAL POSTGRADUATE SCHOOL. ANY REPRODUCTION IN PART OR AS A WHOLE WITHOUT THE WRITTEN PERMISSION OF NPS OR THE AUTHOR IS PROHIBITED.

		UNLESS OTHERWISE SPECIFIED: DIMENSIONS ARE IN CM	DRAWN	NAME	DATE	TITLE: NPS - AXV lab Surfzone Prototype - Bow Endcap
		TOLERANCES: +0.02 CM for clearance and fitting between parts	CHECKED	M.A.		
		INTERPRET GEOMETRIC TOLERANCING PER:	ENG APPR.			
		MATERIAL PC (Styrolux - Polycarbonate)	MFG APPR.			
		FINISH	O.A.			SIZE DWG. NO.
NEXT ASSY	USED ON	DO NOT SCALE DRAWING	COMMENTS: Sparse printed			REV
NPS - AXV lab - SURFZONE PROTOTYPE						SCALE:1:4 WEIGHT: SHEET 3 OF 4

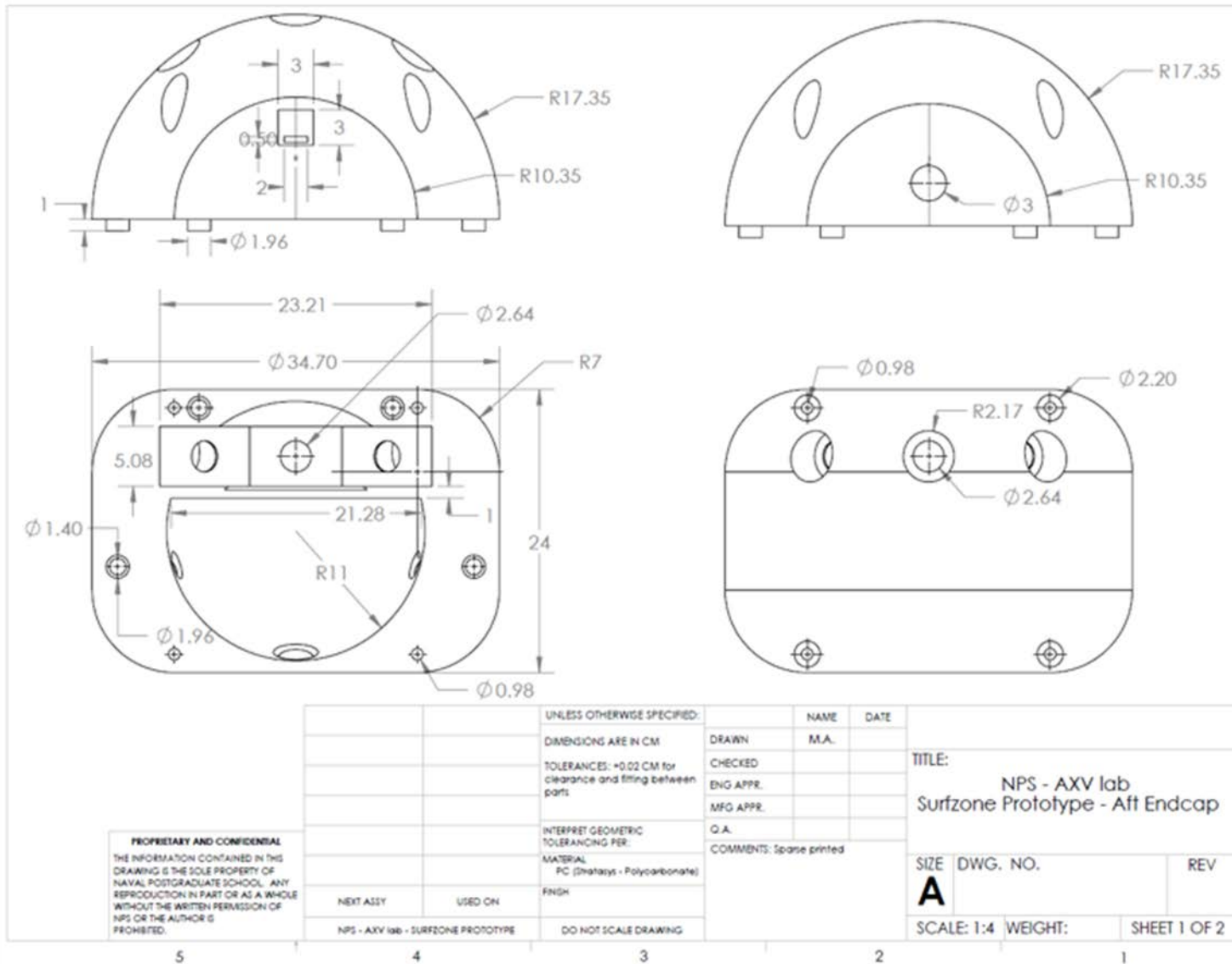
5

4

3

2

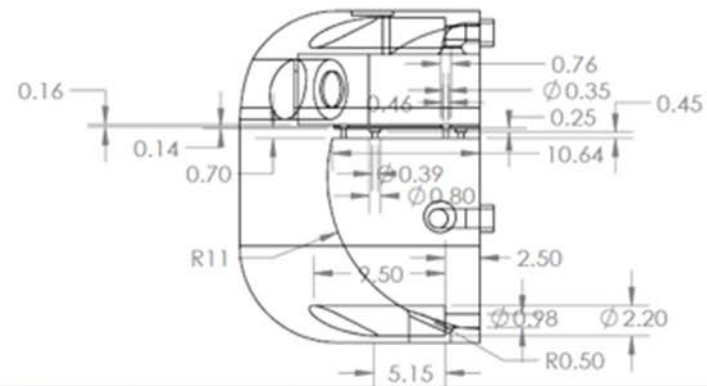
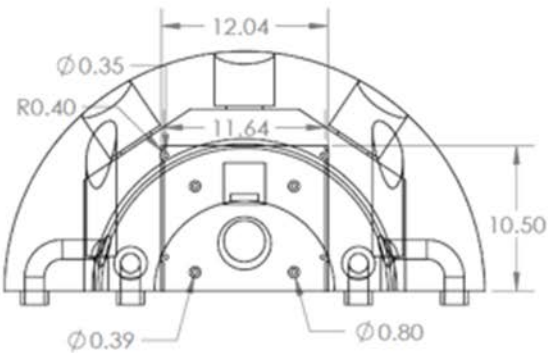
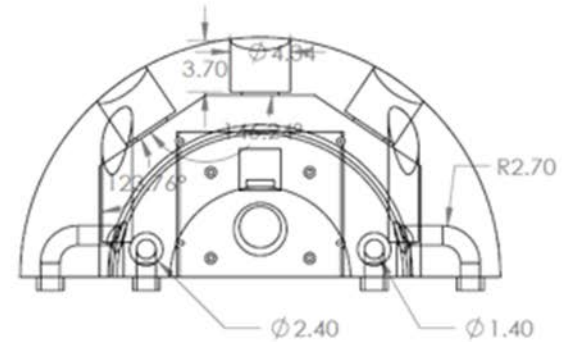
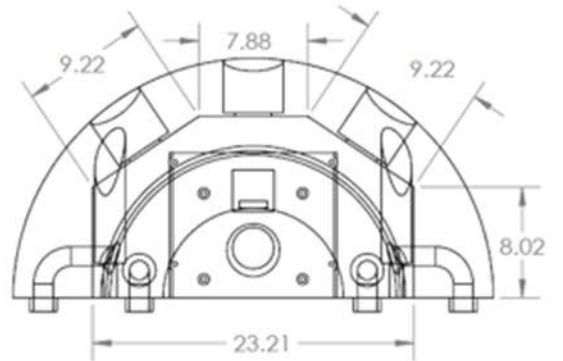
1



PROPRIETARY AND CONFIDENTIAL
 THE INFORMATION CONTAINED IN THIS DRAWING IS THE SOLE PROPERTY OF NAVAL POSTGRADUATE SCHOOL. ANY REPRODUCTION IN PART OR AS A WHOLE WITHOUT THE WRITTEN PERMISSION OF NPS OR THE AUTHOR IS PROHIBITED.

		UNLESS OTHERWISE SPECIFIED:	NAME	DATE
		DIMENSIONS ARE IN CM	DRAWN	M.A.
		TOLERANCES: +0.02 CM for clearance and fitting between parts	CHECKED	
		INTERPRET GEOMETRIC TOLERANCING PER:	ENG APPR.	
		MATERIAL	MFG APPR.	
		PC (Stratagis - Polycarbonate)	Q.A.	
		FINISH	COMMENTS: Sparse printed	
NEXT ASSY	USED ON			
NPS - AXV 198 - SURFZONE PROTOTYPE		DO NOT SCALE DRAWING		

TITLE:		
NPS - AXV lab Surfzone Prototype - Aft Endcap		
SIZE	DWG. NO.	REV
A		
SCALE: 1:4	WEIGHT:	SHEET 1 OF 2



PROPRIETARY AND CONFIDENTIAL
 THE INFORMATION CONTAINED IN THIS DRAWING IS THE SOLE PROPERTY OF NAVAL POSTGRADUATE SCHOOL. ANY REPRODUCTION IN PART OR AS A WHOLE WITHOUT THE WRITTEN PERMISSION OF NPS OR THE AUTHOR IS PROHIBITED.

		UNLESS OTHERWISE SPECIFIED:	NAME	DATE
		DIMENSIONS ARE IN CM	DRAWN	MA.
		TOLERANCES: +0.02 CM for clearance and fitting between parts	CHECKED	
		INTERPRET GEOMETRIC TOLERANCING PER:	ENG APPR.	
		MATERIAL	MFG APPR.	
		PC (Stalays - Polycarbonate)	Q.A.	
		FINISH	COMMENTS: Sparse printed	
NEXT ASSY	USED ON			
NPS - AXV lab - SURFZONE PROTOTYPE		DO NOT SCALE DRAWING		

TITLE:
 NPS - AXV lab
 Surfzone Prototype - Aft Endcap

SIZE	DWG. NO.	REV
A		
SCALE: 1:4	WEIGHT:	SHEET 2 OF 2

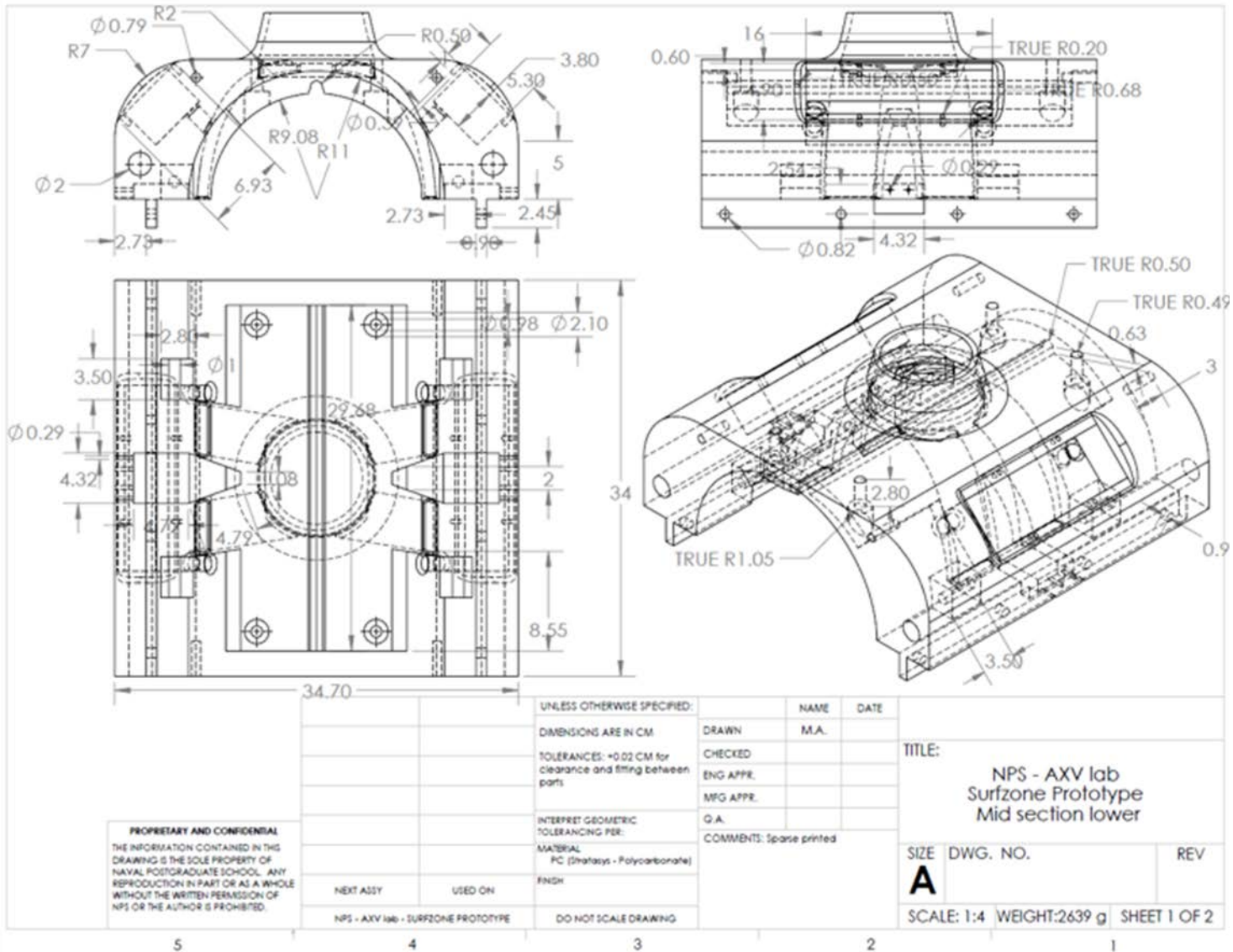
5

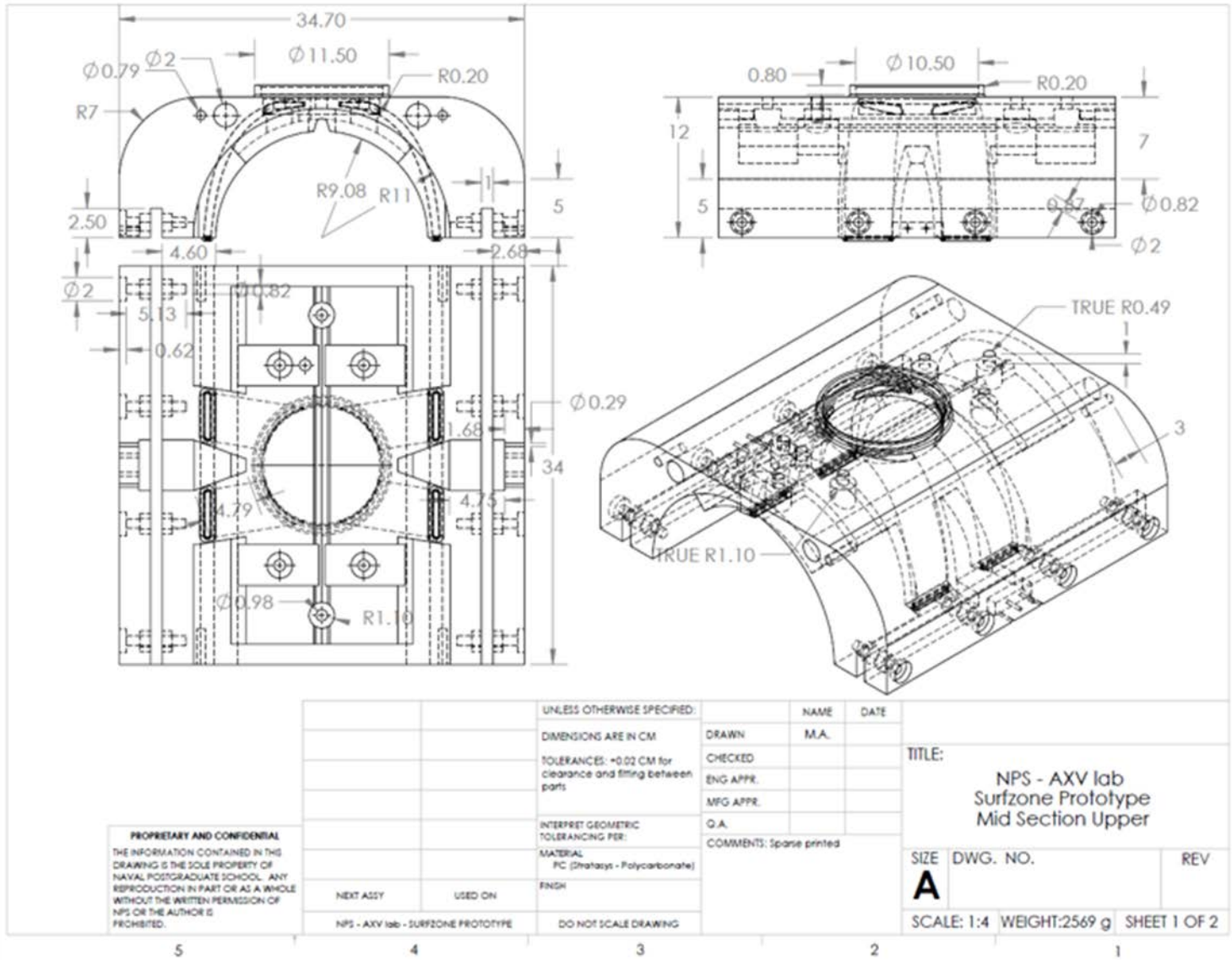
4

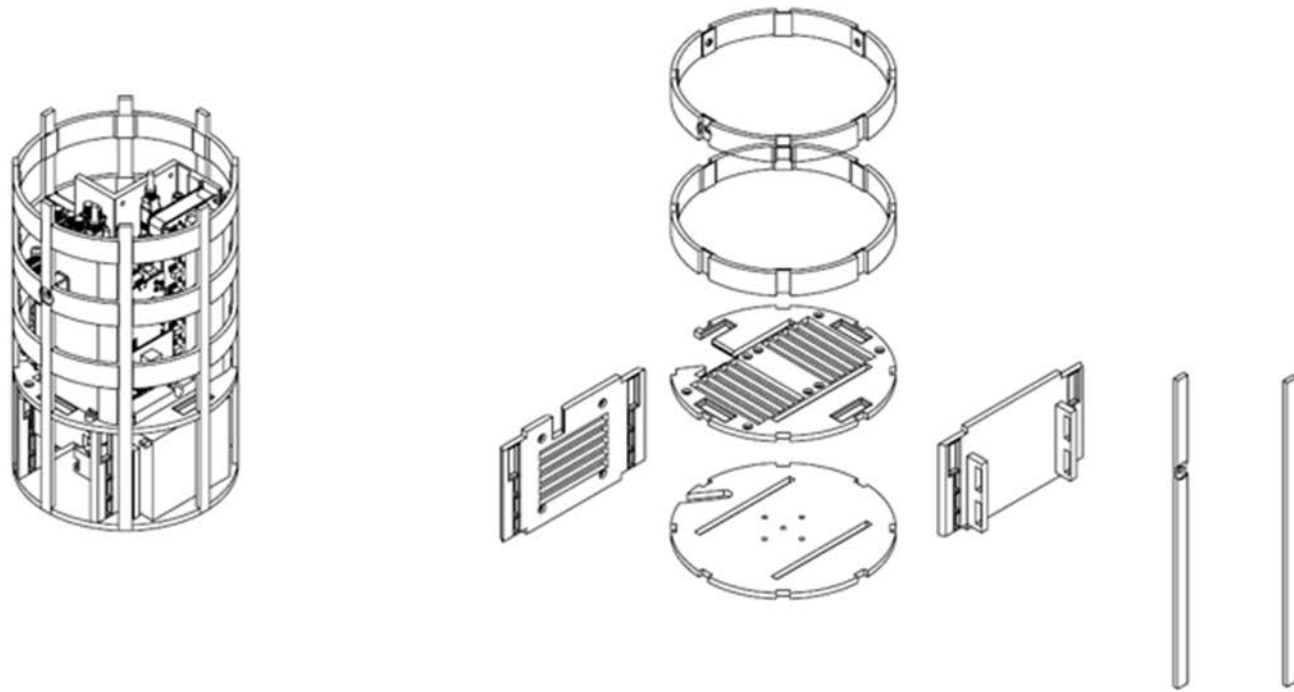
3

2

1







PROPRIETARY AND CONFIDENTIAL
 THE INFORMATION CONTAINED IN THIS DRAWING IS THE SOLE PROPERTY OF NAVAL POSTGRADUATE SCHOOL. ANY REPRODUCTION IN PART OR AS A WHOLE WITHOUT THE WRITTEN PERMISSION OF NPS OR THE AUTHOR IS PROHIBITED.

		UNLESS OTHERWISE SPECIFIED:	NAME	DATE	
		DIMENSIONS ARE IN CM	DRAWN	M.A.	
		TOLERANCES: +0.02 CM for clearance and fitting between parts	CHECKED		
		INTERPRET GEOMETRIC TOLERANCING PER:	ENG APPR.		
		MATERIAL	MFG APPR.		
		PC (Stratagis - Polycarbonate)	Q.A.		
NEXT ASSY	USED ON	Finish	COMMENTS: Sparse printed		TITLE:
NPS - AXV 198 - SURFZONE PROTOTYPE		DO NOT SCALE DRAWING	Weight in this case is the total weight of the assembly		NPS - AXV lab Surfzone Prototype Electronics Cylinder Rack
			SIZE	DWG. NO.	REV
			A		
			SCALE: 1:4	WEIGHT: 821 g	SHEET 1 OF 5

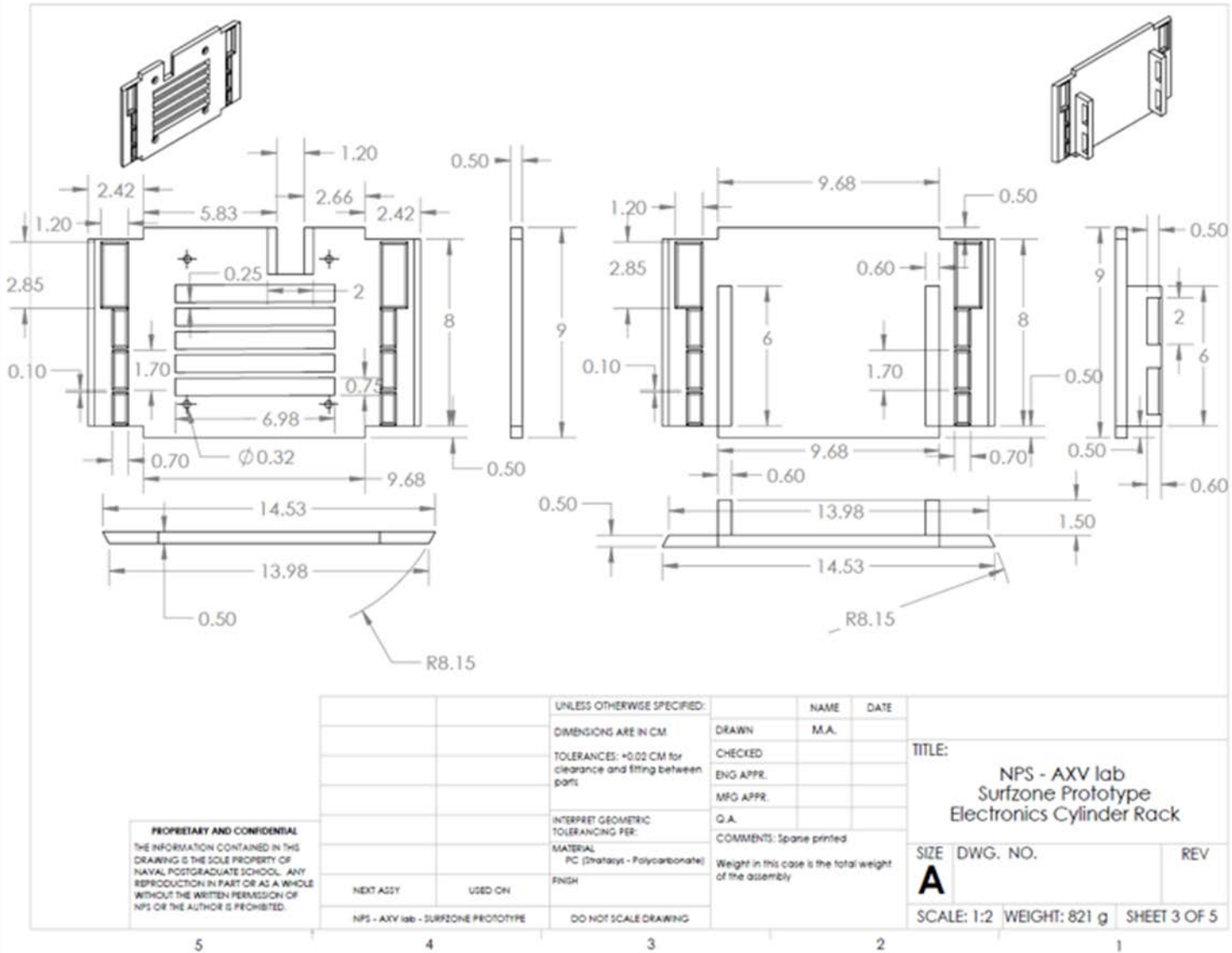
5

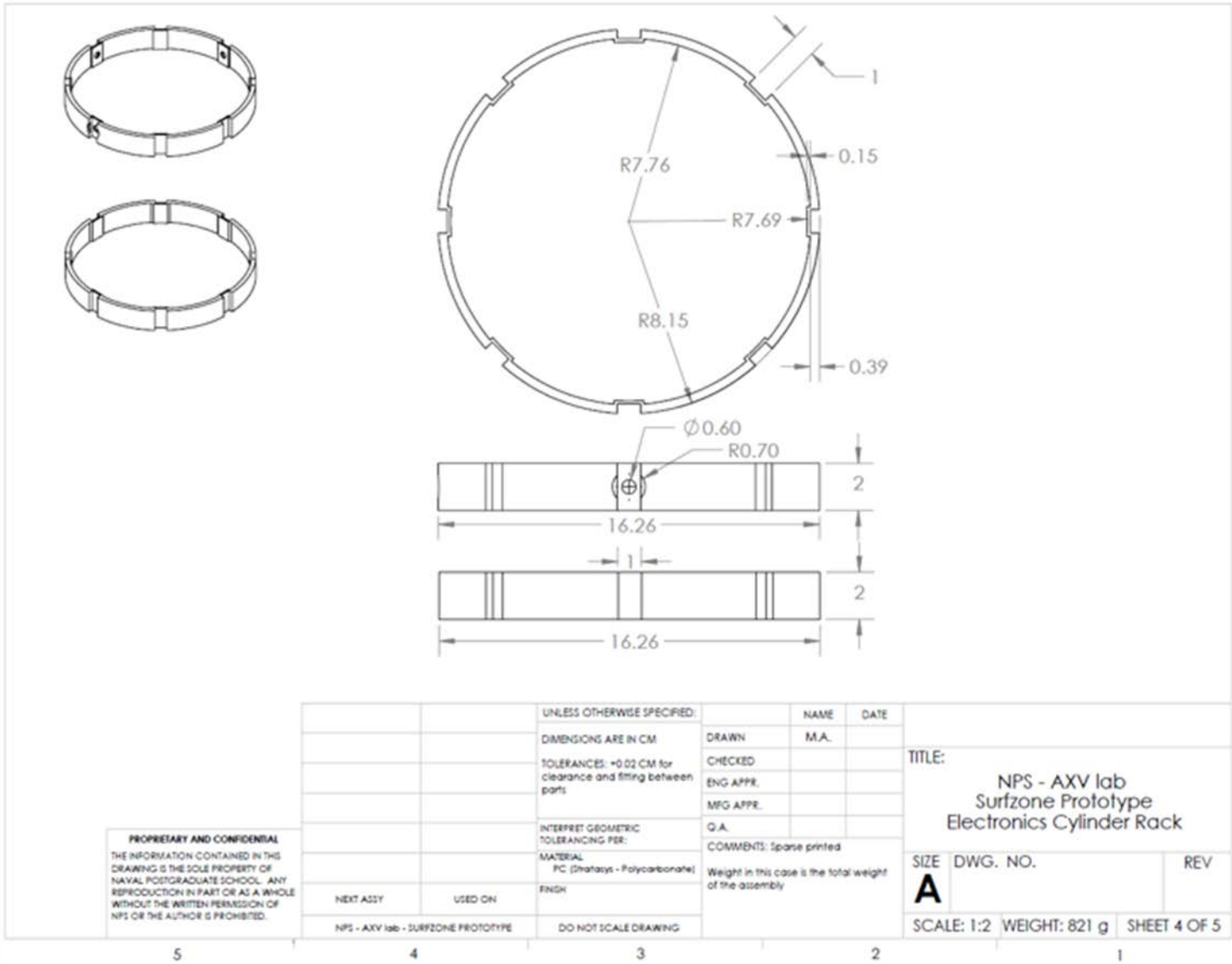
4

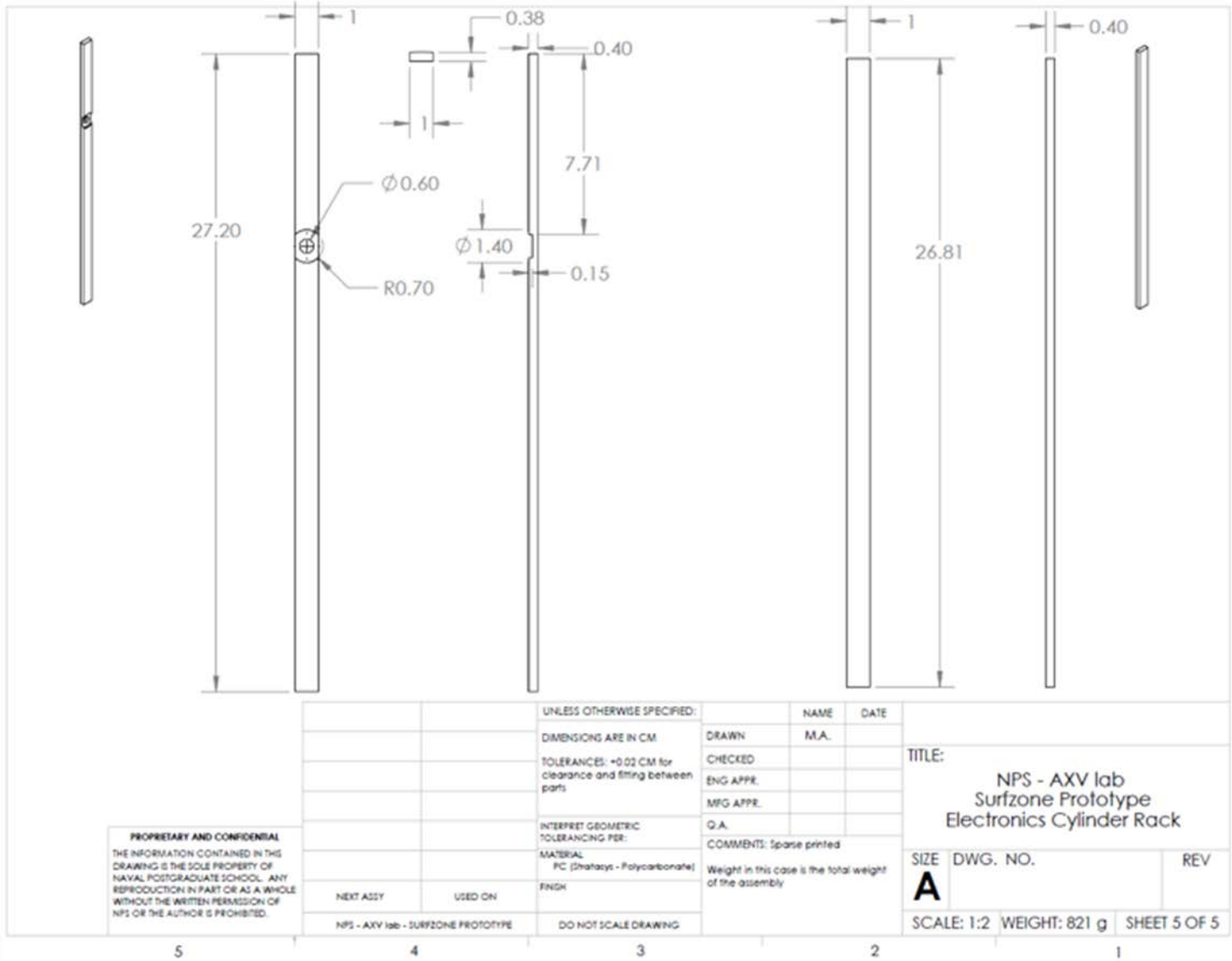
3

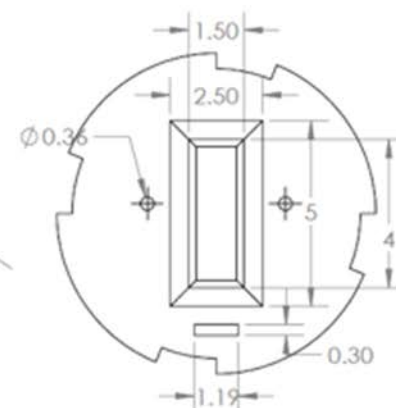
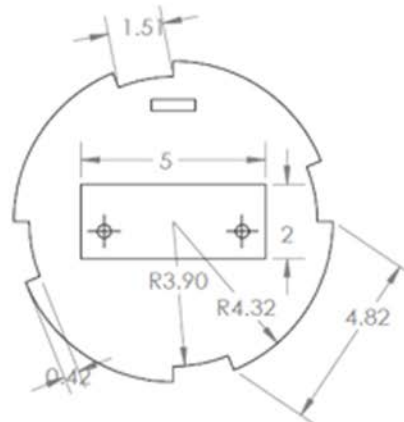
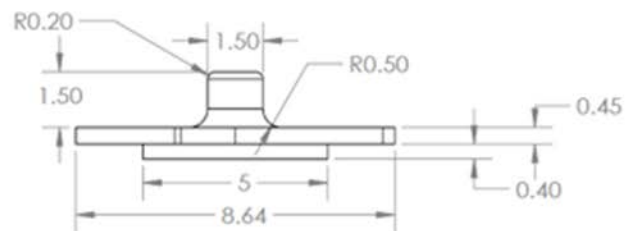
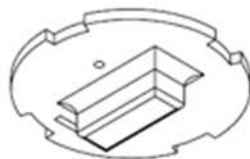
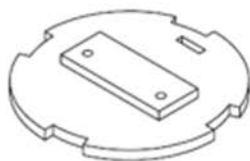
2

1









PROPRIETARY AND CONFIDENTIAL
 THE INFORMATION CONTAINED IN THIS DRAWING IS THE SOLE PROPERTY OF NAVAL POSTGRADUATE SCHOOL. ANY REPRODUCTION IN PART OR AS A WHOLE WITHOUT THE WRITTEN PERMISSION OF NPS OR THE AUTHOR IS PROHIBITED.

		UNLESS OTHERWISE SPECIFIED:		NAME	DATE	
		DIMENSIONS ARE IN CM	DRAWN	M.A.		
		TOLERANCES: +0.02 CM for clearance and fitting between parts	CHECKED			TITLE:
		INTERPRET GEOMETRIC TOLERANCING PER:	ENG APPR.			NPS - AXV lab
		MATERIAL	MFG APPR.			Surfzone Prototype
		PC (Stratyst - Polycarbonate)	O.A.			Doppler mounting base
		FINISH	COMMENTS: Solid printed			SIZE DWG. NO. REV
NEXT ASSY	USED ON					A
NPS - AXV lab - SURFZONE PROTOTYPE		DO NOT SCALE DRAWING				SCALE: 2:3 WEIGHT: 42 g SHEET 1 OF 1

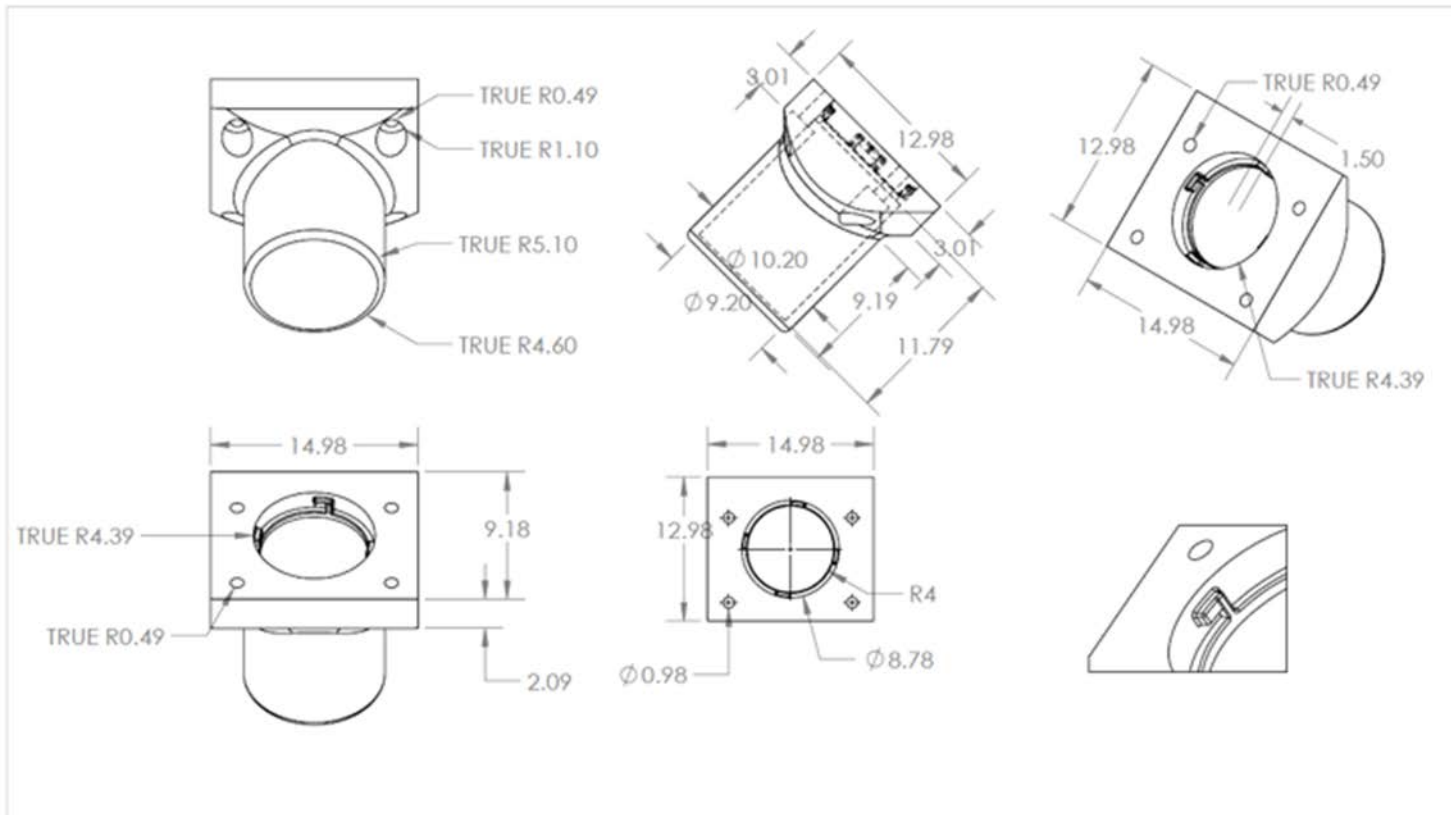
5

4

3

2

1



PROPRIETARY AND CONFIDENTIAL
 THE INFORMATION CONTAINED IN THIS DRAWING IS THE SOLE PROPERTY OF NAVAL POSTGRADUATE SCHOOL. ANY REPRODUCTION IN PART OR AS A WHOLE WITHOUT THE WRITTEN PERMISSION OF NPS OR THE AUTHOR IS PROHIBITED.

		UNLESS OTHERWISE SPECIFIED:		NAME	DATE
		DIMENSIONS ARE IN CM	DRAWN	M.A.	
		TOLERANCES: +0.02 CM for clearance and fitting between parts	CHECKED		
		INTERPRET GEOMETRIC TOLERANCING PER:	ENG APPR.		
		MATERIAL	MFG APPR.		
		PC (Styralyst - Polycarbonate)	Q.A.		
		FINISH	COMMENTS: Solid printed		
NEXT ASSY	USED ON				
NPS - AXV lab - SURFZONE PROTOTYPE		DO NOT SCALE DRAWING			

TITLE:		
NPS - AXV lab Surfzone Prototype Bow endcap cylinder for doppler		
SIZE	DWG. NO.	REV
A		
SCALE: 1:5		WEIGHT: 916 g
SHEET 1 OF 1		

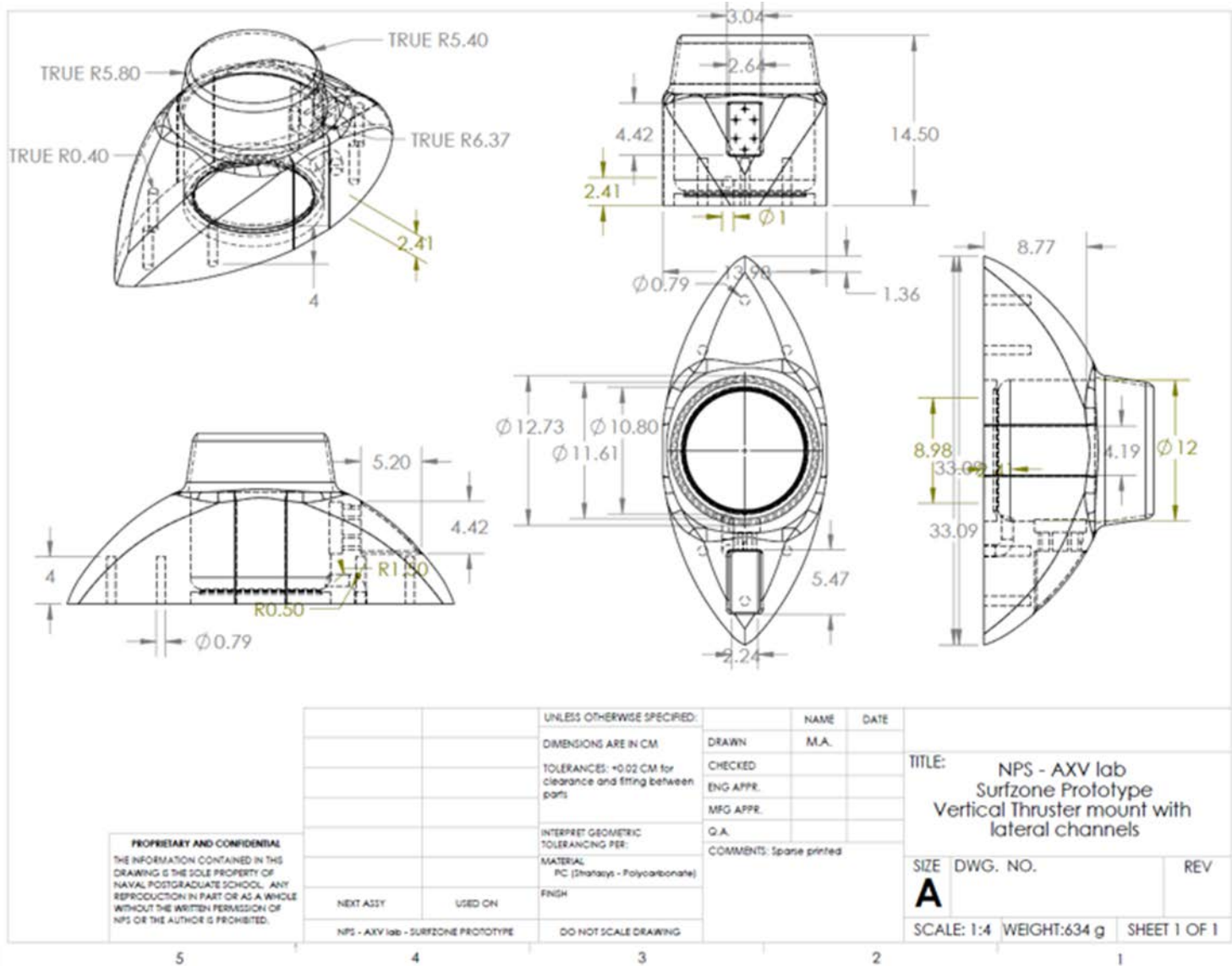
5

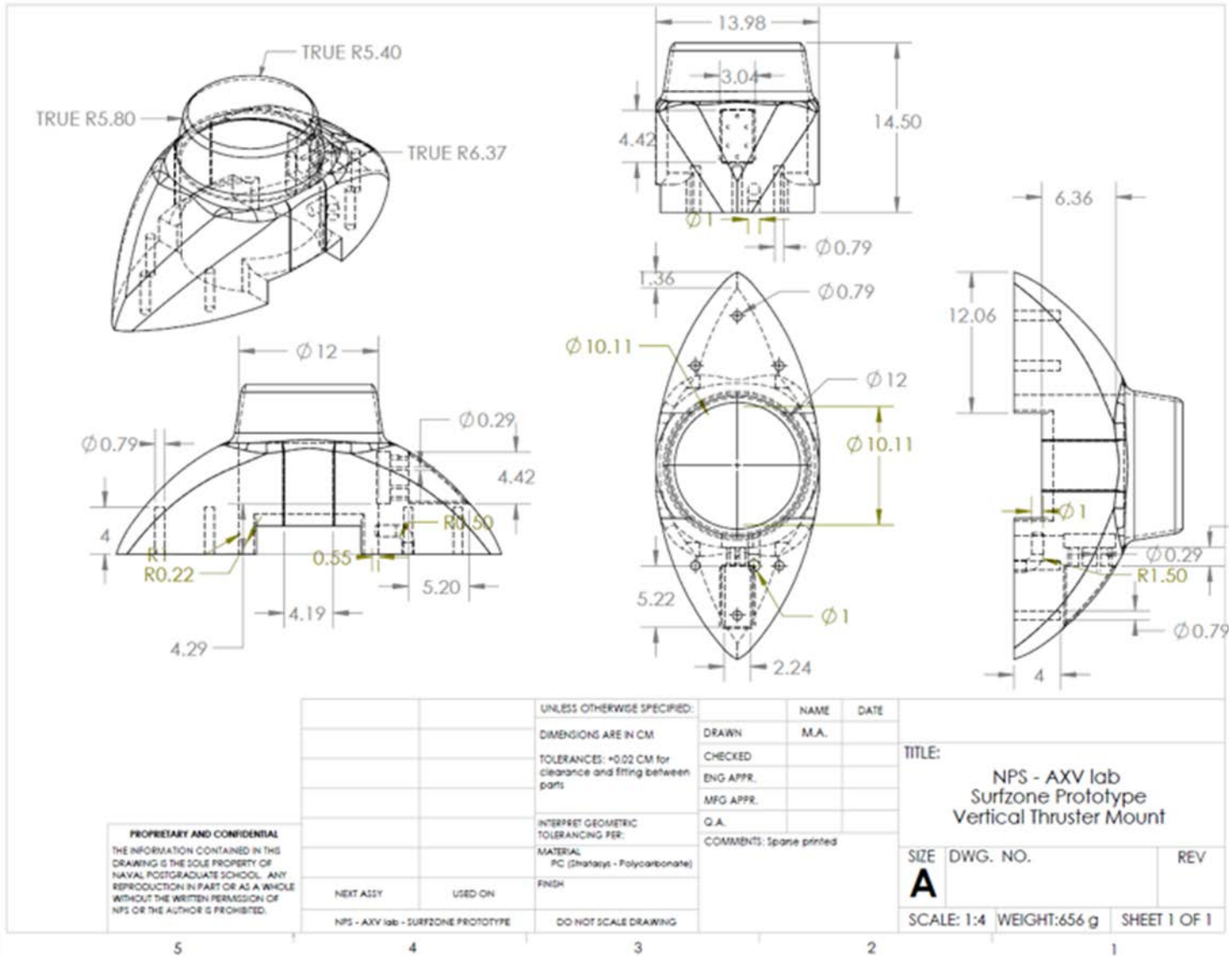
4

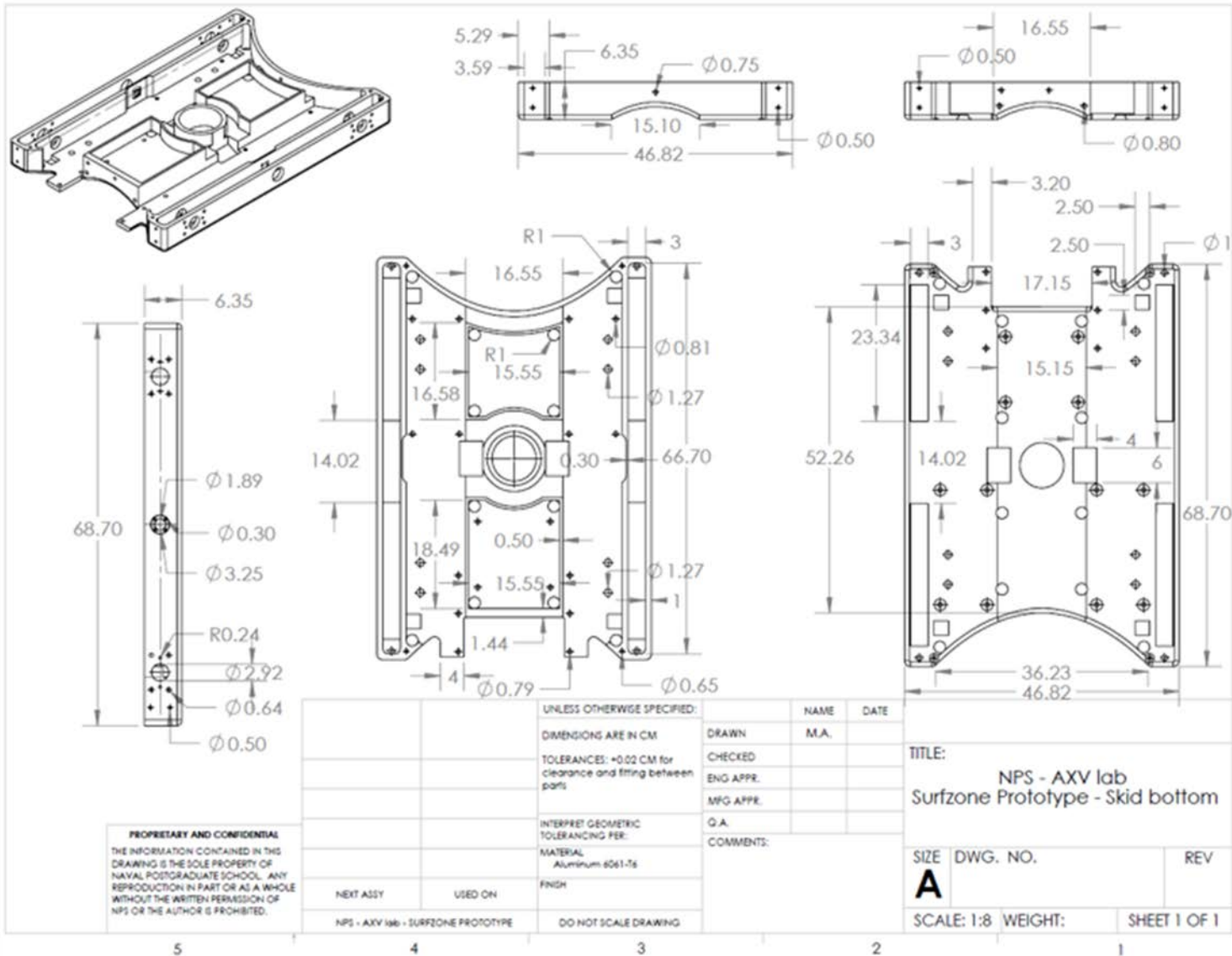
3

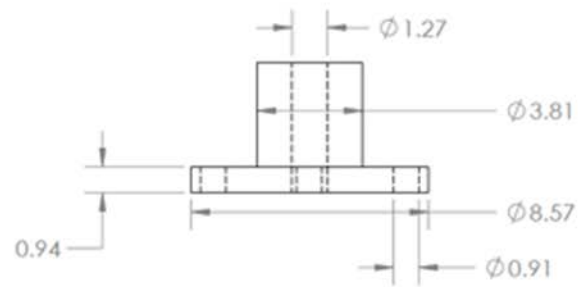
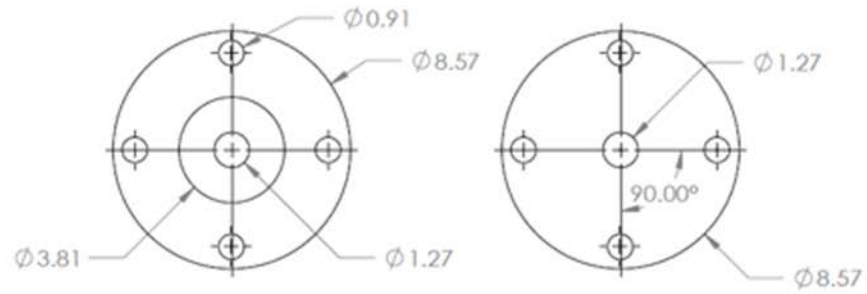
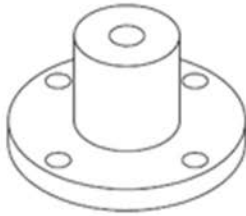
2

1







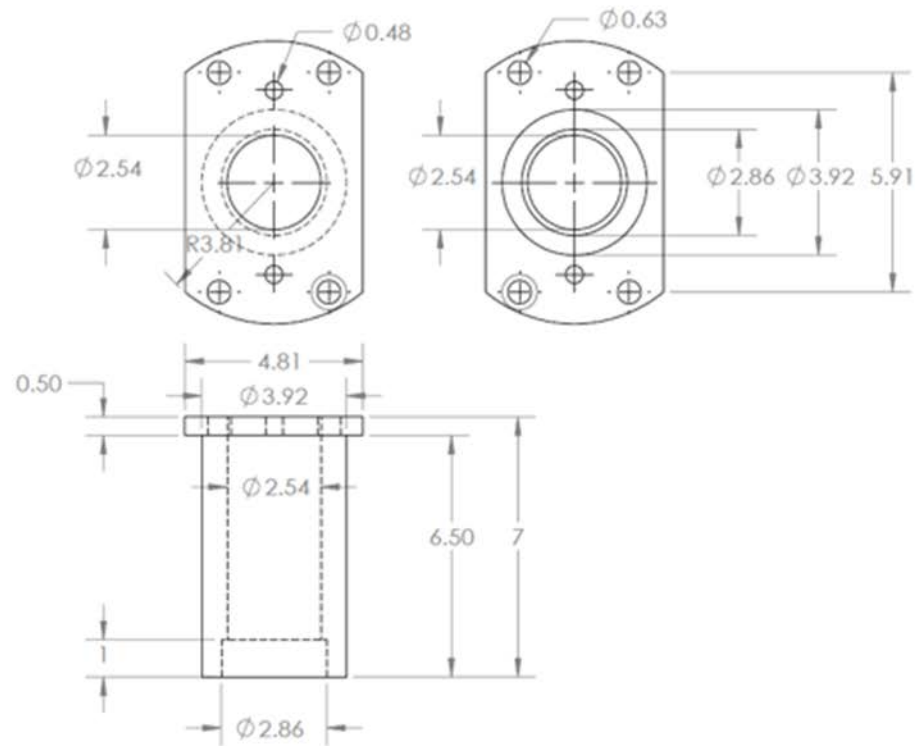
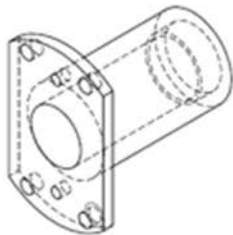


PROPRIETARY AND CONFIDENTIAL
 THE INFORMATION CONTAINED IN THIS DRAWING IS THE SOLE PROPERTY OF NAVAL POSTGRADUATE SCHOOL. ANY REPRODUCTION IN PART OR AS A WHOLE WITHOUT THE WRITTEN PERMISSION OF NPS OR THE AUTHOR IS PROHIBITED.

		UNLESS OTHERWISE SPECIFIED:	NAME	DATE	
		DIMENSIONS ARE IN CM	DRAWN	M.A.	
		TOLERANCES: ± 0.02 CM for clearance and fitting between parts	CHECKED		
		INTERPRET GEOMETRIC TOLERANCING PER:	ENG APPR.		
		MATERIAL	MFG APPR.		
		Aluminum 6061-T6	G.A.		
		FINISH	COMMENTS:		
NEXT ASSY	USED ON				TITLE: NPS - AXV lab Surfzone Prototype Wheg hub
NPS - AXV 198 - SURFZONE PROTOTYPE		DO NOT SCALE DRAWING			SIZE DWG. NO. REV
					A
					SCALE: 1:2 WEIGHT: SHEET 1 OF 1

5

4



PROPRIETARY AND CONFIDENTIAL
 THE INFORMATION CONTAINED IN THIS DRAWING IS THE SOLE PROPERTY OF NAVAL POSTGRADUATE SCHOOL. ANY REPRODUCTION IN PART OR AS A WHOLE WITHOUT THE WRITTEN PERMISSION OF NPS OR THE AUTHOR IS PROHIBITED.

		UNLESS OTHERWISE SPECIFIED:	NAME	DATE	TITLE: NPS - AXV lab Surfzone Prototype Support shaft and bearings
		DIMENSIONS ARE IN CM	DRAWN	M.A.	
		TOLERANCES: ± 0.02 CM for clearance and fitting between parts	CHECKED		
		INTERPRET GEOMETRIC TOLERANCING PER:	ENG APPR.		
		MATERIAL Aluminum 6061-T6 (55)	MFG APPR.		
NEXT ASSY	USED ON	FIND#	O.A.		SIZE
NPS - AXV lab - SURFZONE PROTOTYPE		DO NOT SCALE DRAWING	COMMENTS: Machined		A
					DWG. NO.
					REV
					SCALE: 1:2
					WEIGHT: 155 g
					SHEET 1 OF 1

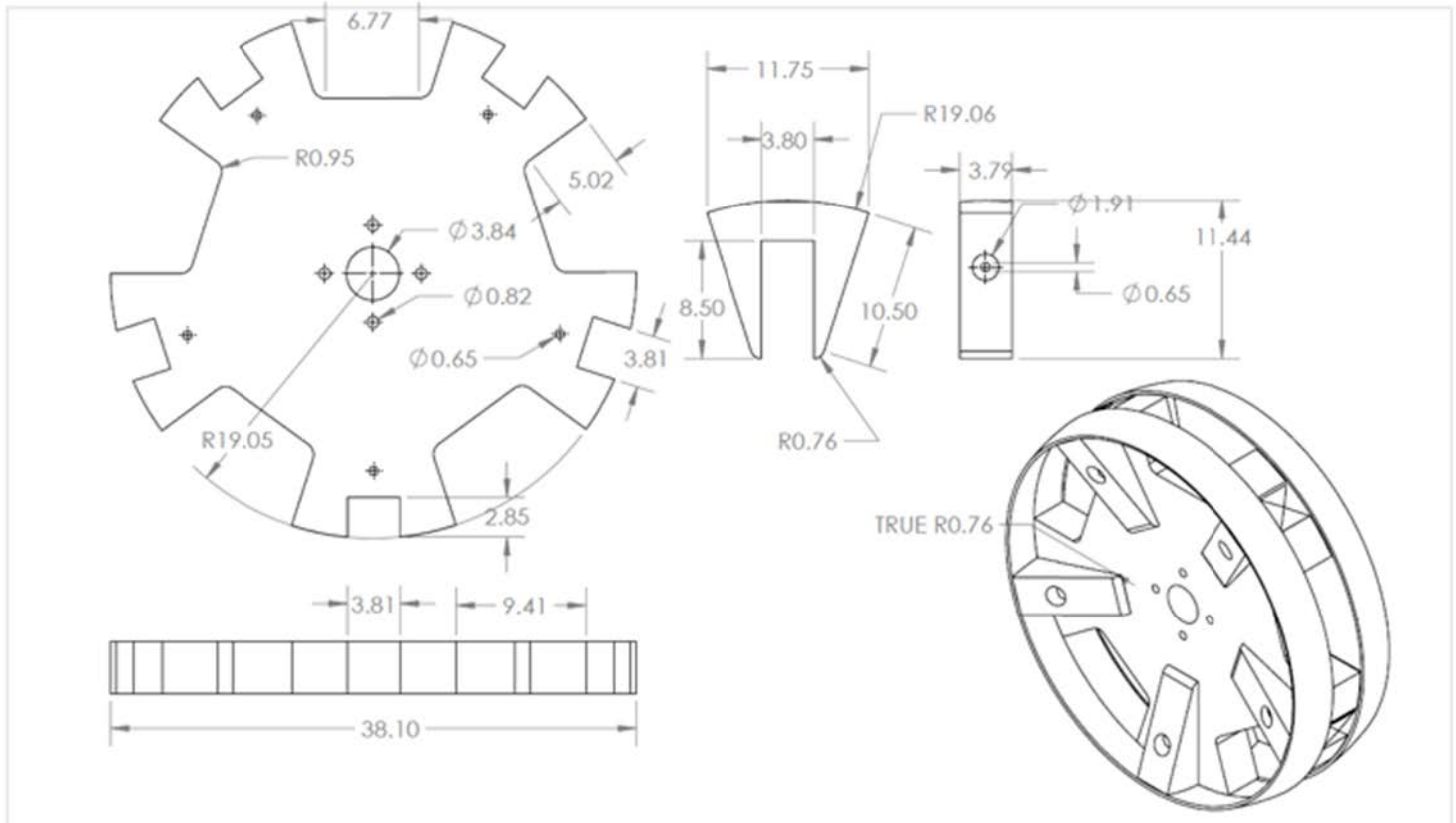
5

4

3

2

1



PROPRIETARY AND CONFIDENTIAL
 THE INFORMATION CONTAINED IN THIS DRAWING IS THE SOLE PROPERTY OF NAVAL POSTGRADUATE SCHOOL. ANY REPRODUCTION IN PART OR AS A WHOLE WITHOUT THE WRITTEN PERMISSION OF NPS OR THE AUTHOR IS PROHIBITED.

		UNLESS OTHERWISE SPECIFIED:	NAME	DATE	TITLE: NPS - AXV lab Surfzone Prototype - Whegs
		DIMENSIONS ARE IN CM	DRAWN	M.A.	
		TOLERANCES: +0.02 CM for clearance and fitting between parts	CHECKED		
		INTERPRET GEOMETRIC TOLERANCING PER:	ENG APPR.		
		MATERIAL	MFG APPR.		Q.A.
		PC (Stratasis - Polycarbonate)			COMMENTS: Sparse printed
		FINISH			Ruber tires around whegs paddles to give better performance on hard surfaces
		DO NOT SCALE DRAWING			Weight only for 3D printed parts
	NEXT ASSY	USED ON			SIZE DWG. NO. REV
	NPS - AXV 198 - SURFZONE PROTOTYPE				A SCALE: 1:5 WEIGHT: 1590 SHEET 1 OF 1

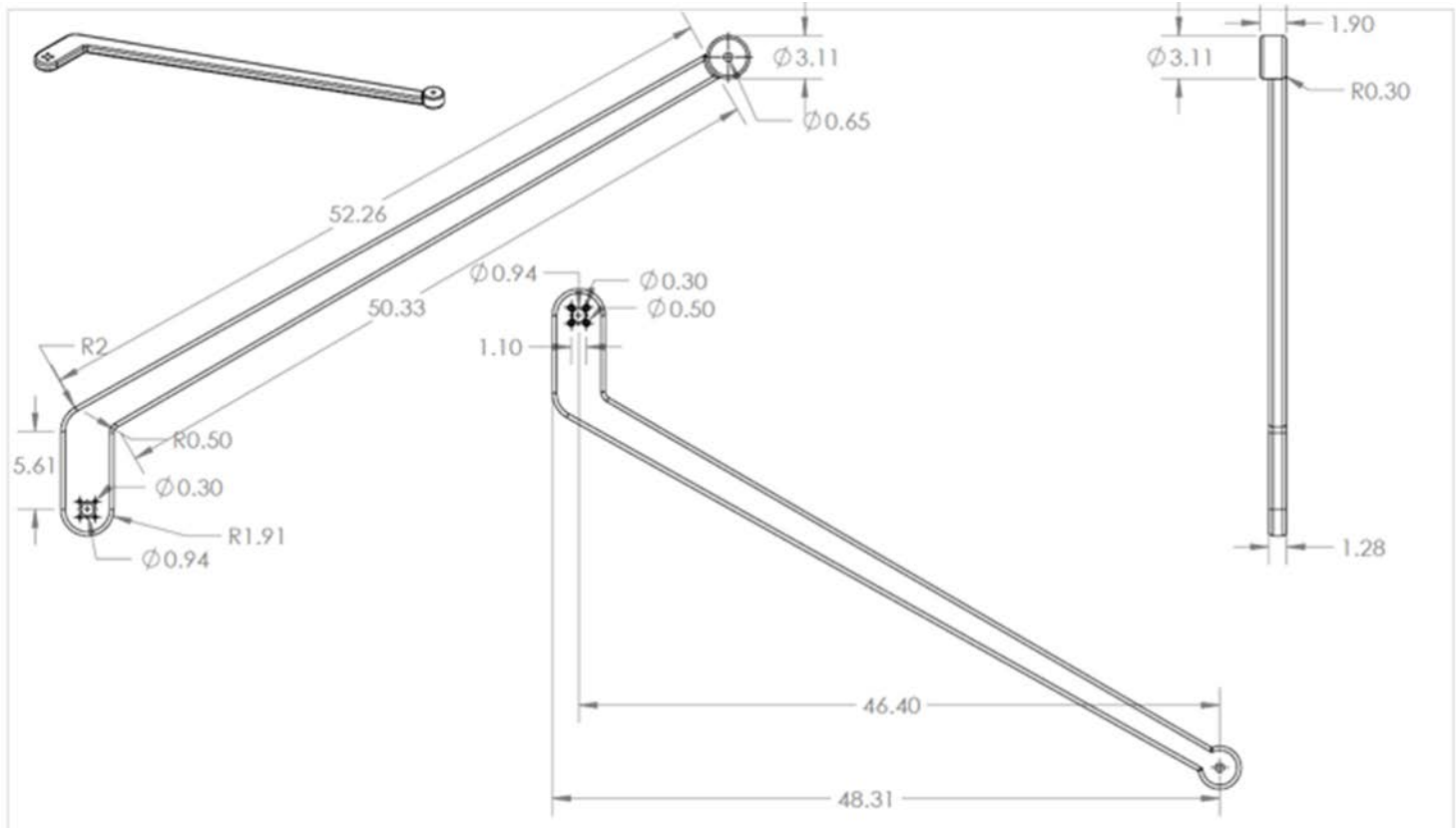
5

4

3

2

1



PROPRIETARY AND CONFIDENTIAL
 THE INFORMATION CONTAINED IN THIS DRAWING IS THE SOLE PROPERTY OF NAVAL POSTGRADUATE SCHOOL. ANY REPRODUCTION IN PART OR AS A WHOLE WITHOUT THE WRITTEN PERMISSION OF NPS OR THE AUTHOR IS PROHIBITED.

UNLESS OTHERWISE SPECIFIED:		NAME	DATE
DIMENSIONS ARE IN CM		DRAWN	M.A.
TOLERANCES: +0.02 CM for clearance and fitting between parts		CHECKED	
INTERPRET GEOMETRIC TOLERANCING PER:		ENG APPR.	
MATERIAL		MFG APPR.	
Aluminum 6061-T6		Q.A.	
FINISH		COMMENTS:	
NEXT ASSY	USED ON		
NPS - AXV lab - SURFZONE PROTOTYPE	DO NOT SCALE DRAWING		

TITLE:		
NPS - AXV lab Surfzone Prototype - Tail port		
SIZE	DWG. NO.	REV
A		
SCALE: 1:4	WEIGHT:	SHEET 1 OF 1

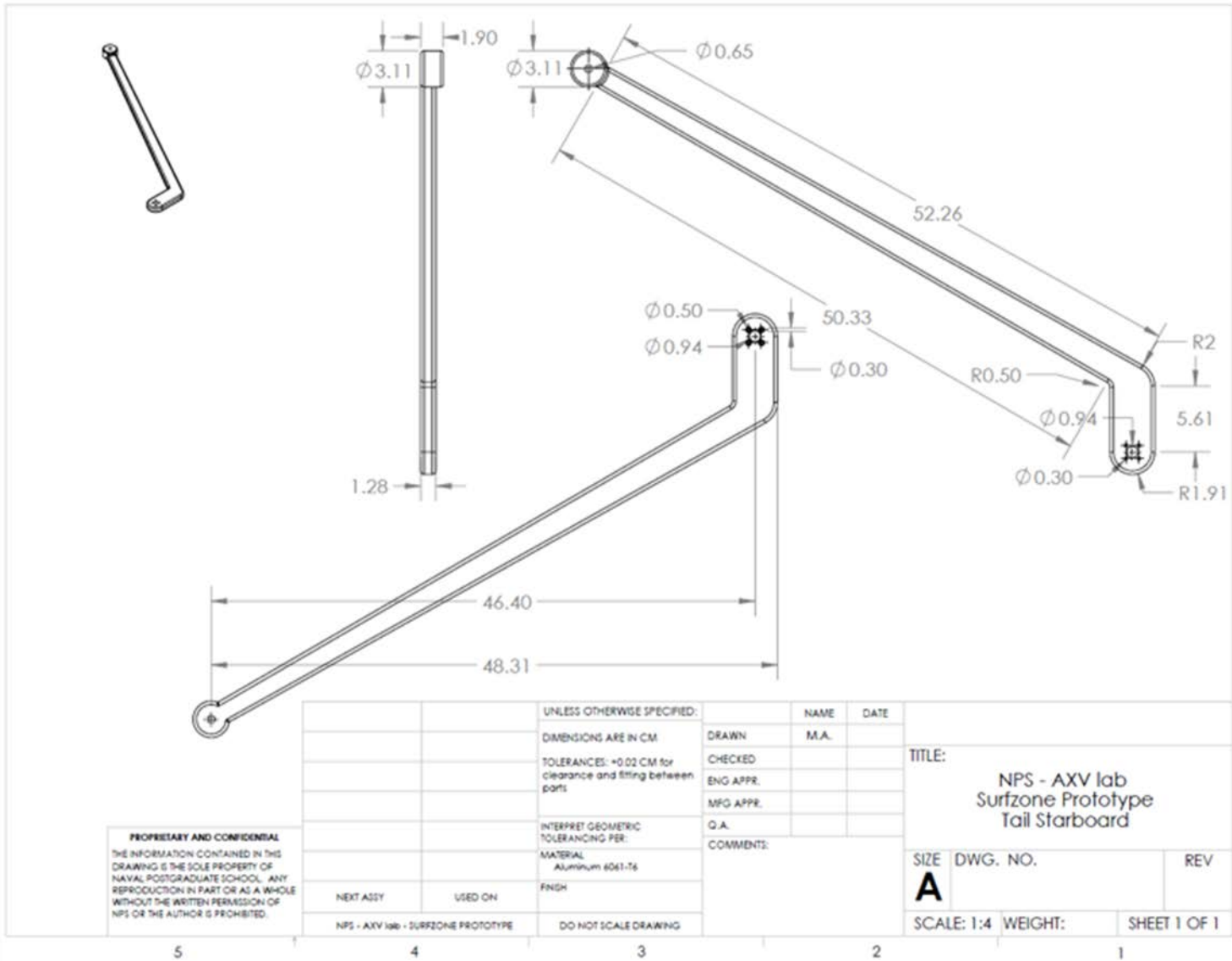
5

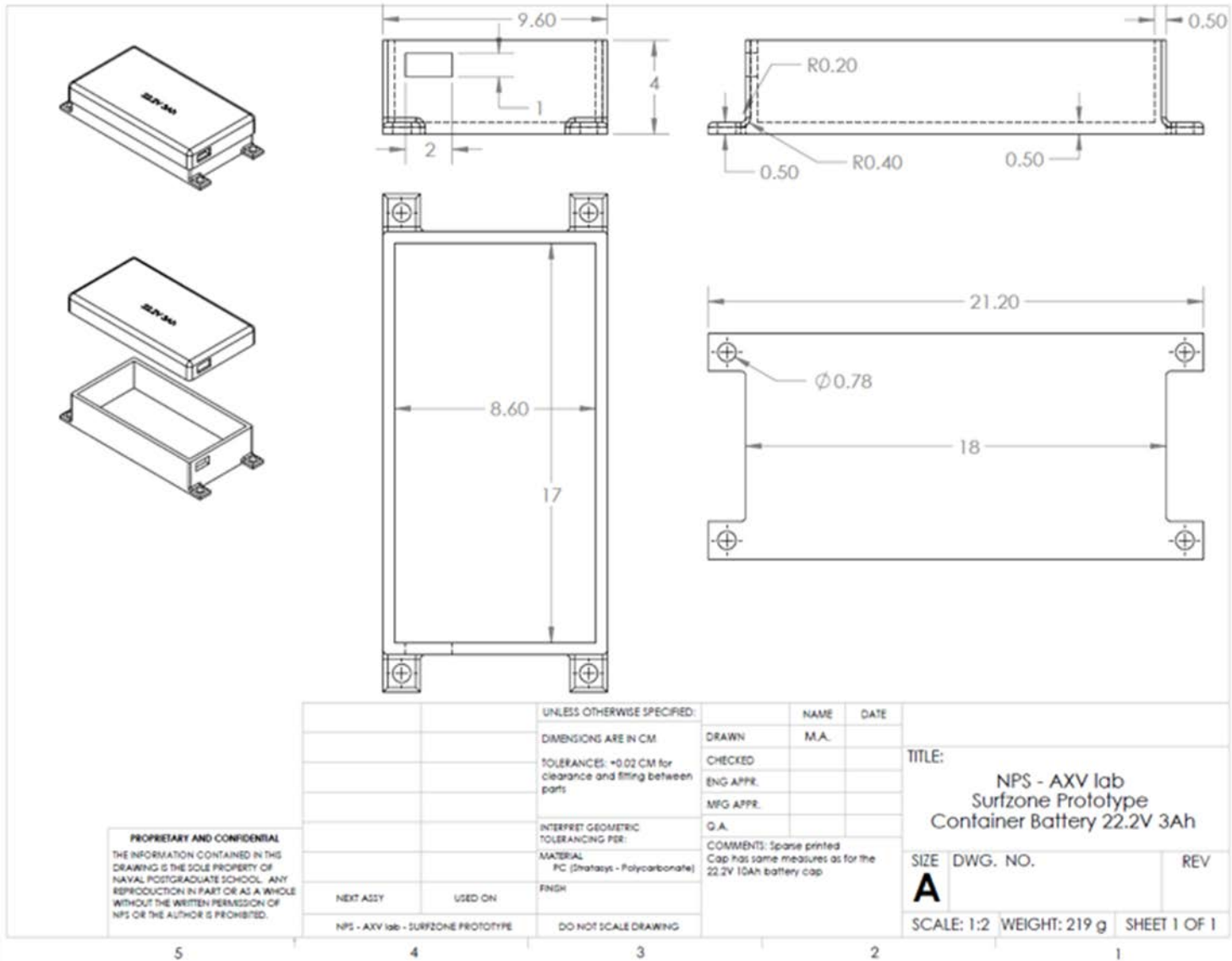
4

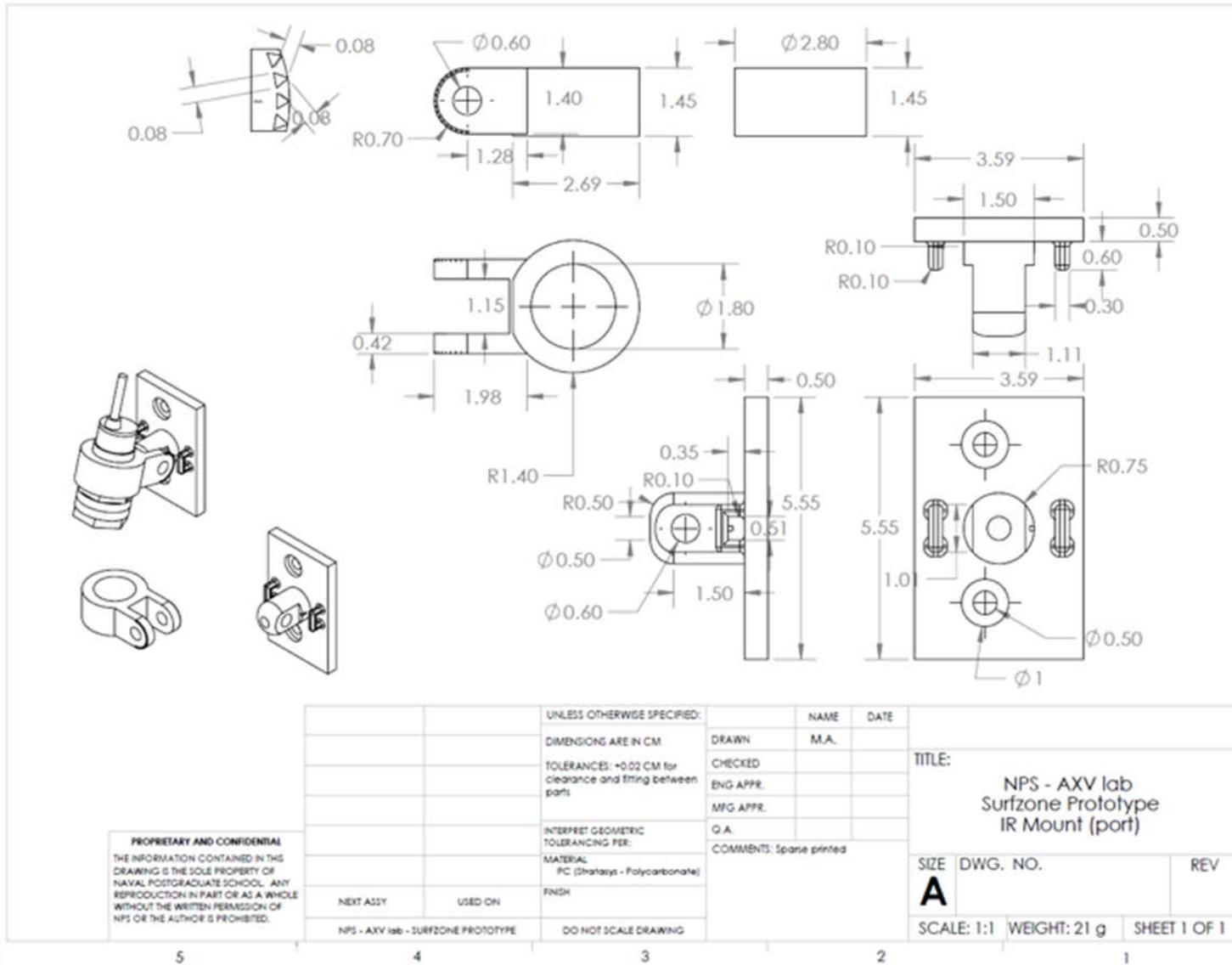
3

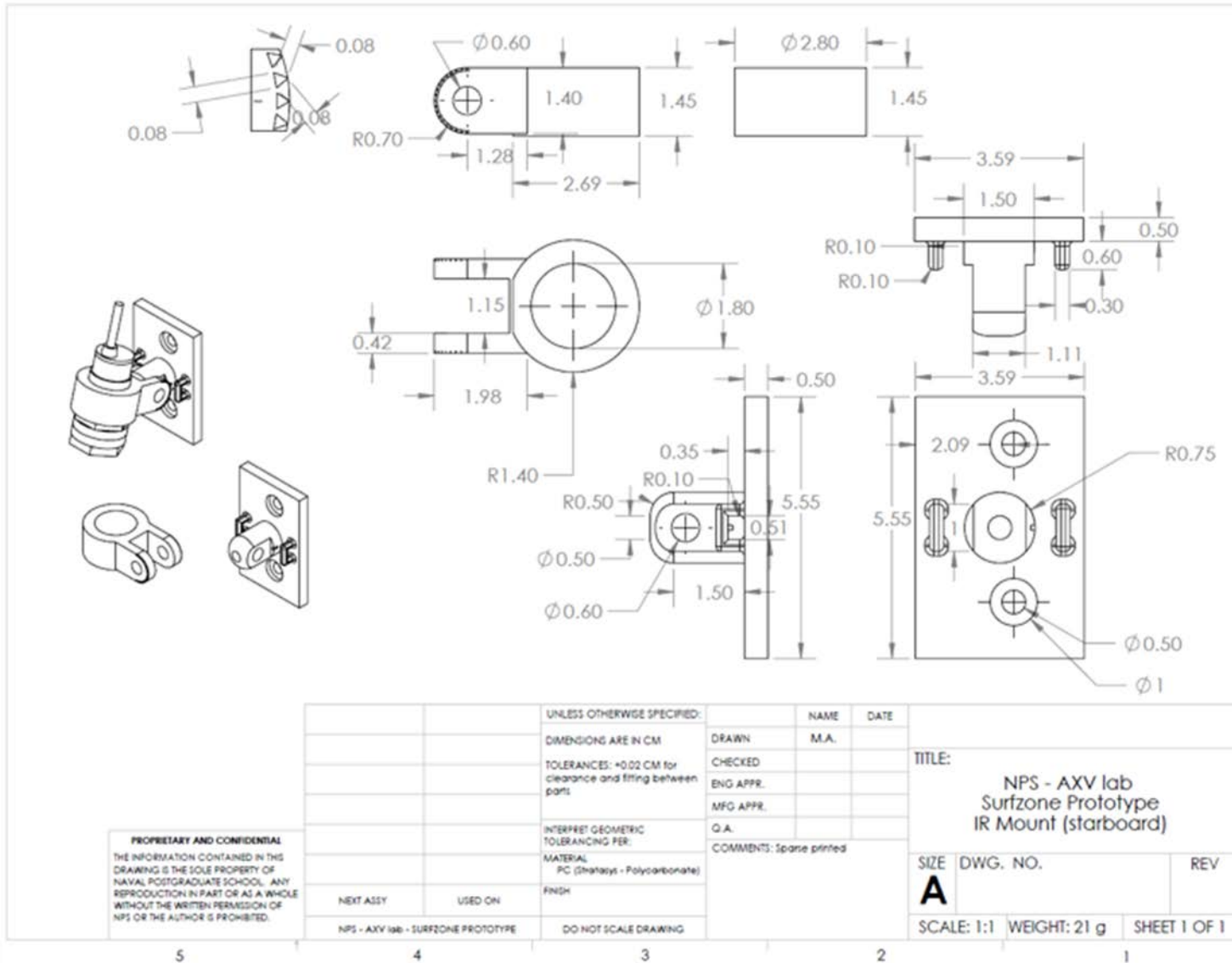
2

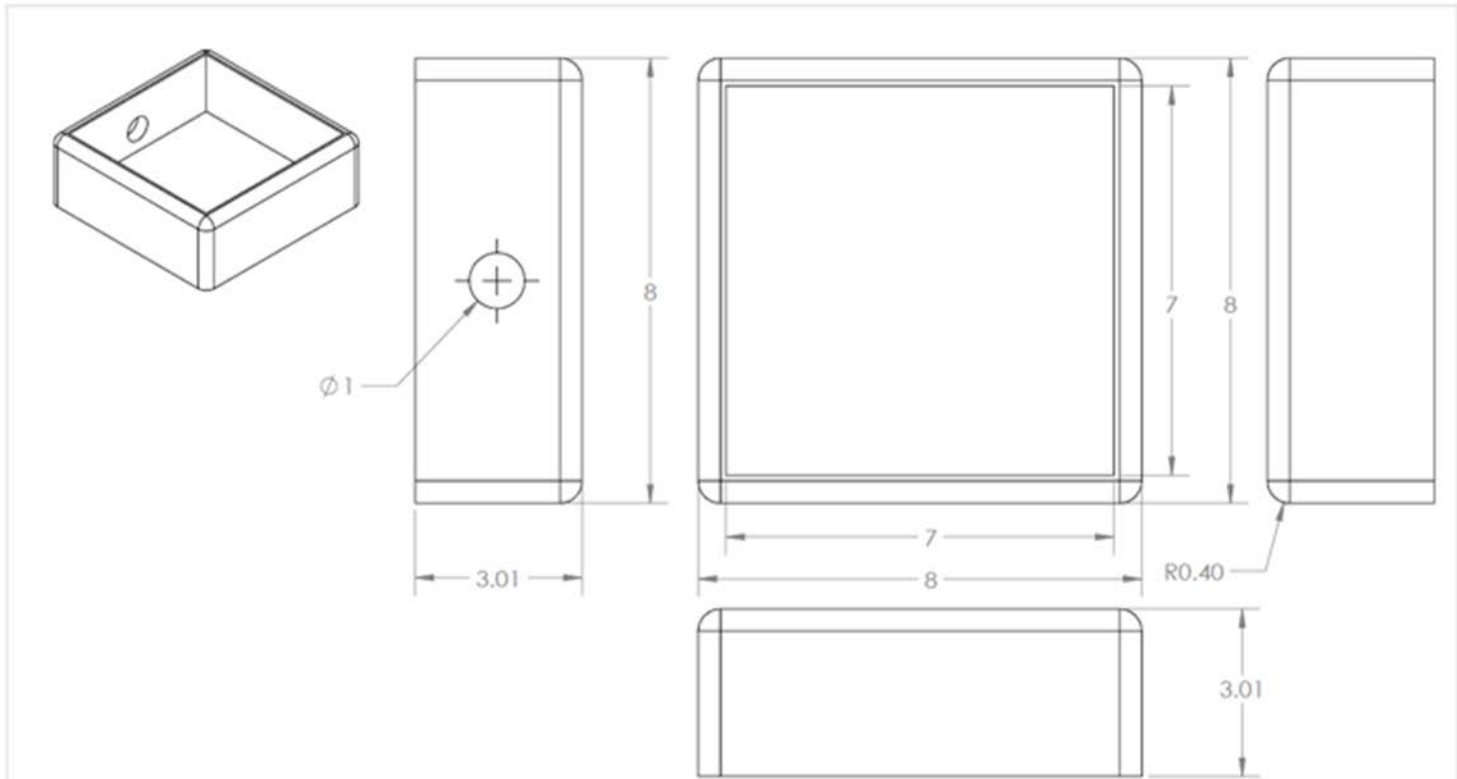
1











PROPRIETARY AND CONFIDENTIAL
 THE INFORMATION CONTAINED IN THIS DRAWING IS THE SOLE PROPERTY OF NAVAL POSTGRADUATE SCHOOL. ANY REPRODUCTION IN PART OR AS A WHOLE WITHOUT THE WRITTEN PERMISSION OF NPS OR THE AUTHOR IS PROHIBITED.

		UNLESS OTHERWISE SPECIFIED:		NAME	DATE	
		DIMENSIONS ARE IN CM	DRAWN	M.A.		
		TOLERANCES: +0.02 CM for clearance and fitting between parts	CHECKED			TITLE:
		INTERPRET GEOMETRIC TOLERANCING PER:	ENG APPR.			NPS - AXV lab
		MATERIAL	MFG APPR.			Surfzone Prototype - Junction Box
		PC (Stratagis - Polycarbonate)	G.A.			SIZE DWG. NO. REV
NEXT ASSY	USED ON	FINISH	COMMENTS: sparse printed			A
NPS - AXV lab - SURFZONE PROTOTYPE		DO NOT SCALE DRAWING				SCALE: 1:2 WEIGHT: SHEET 1 OF 1

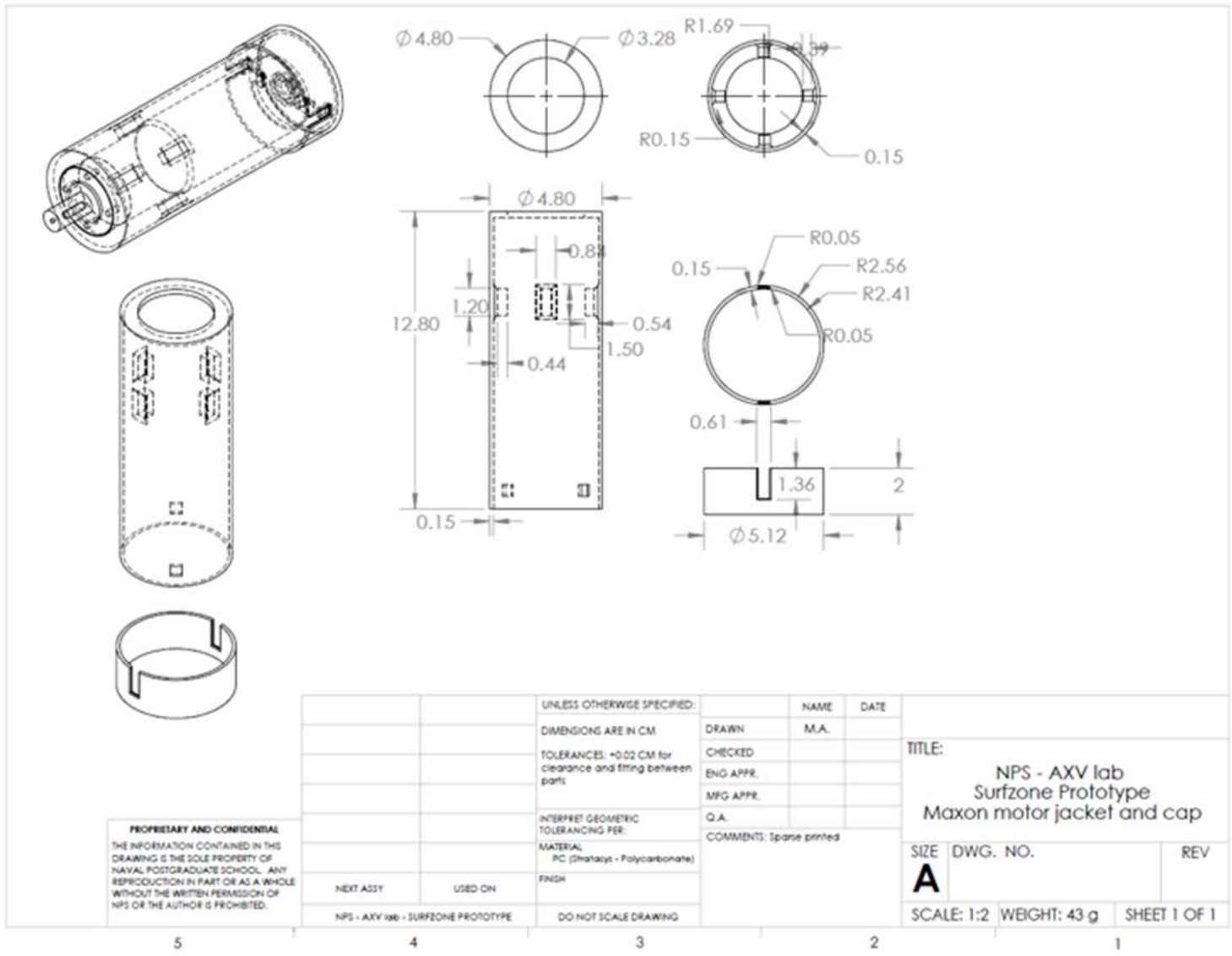
5

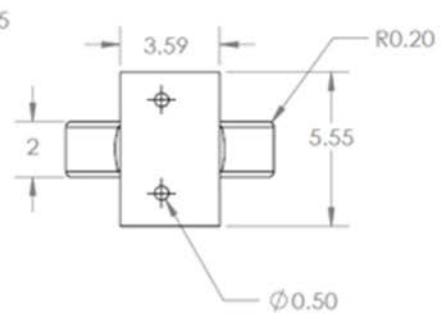
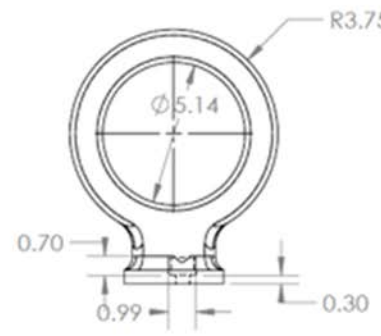
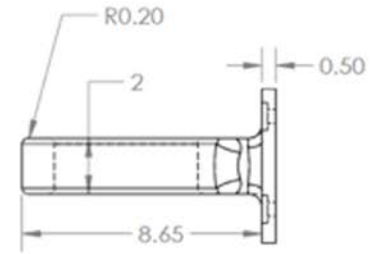
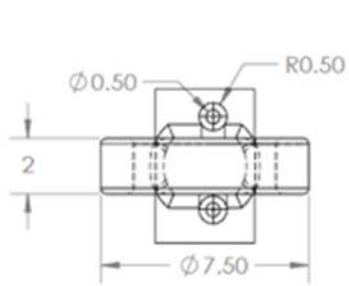
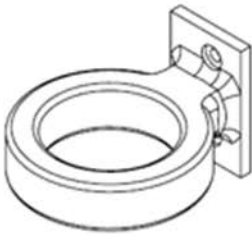
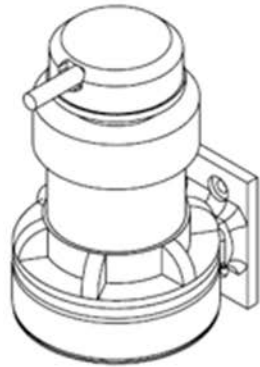
4

3

2

1





PROPRIETARY AND CONFIDENTIAL
 THE INFORMATION CONTAINED IN THIS DRAWING IS THE SOLE PROPERTY OF NAVAL POSTGRADUATE SCHOOL. ANY REPRODUCTION IN PART OR AS A WHOLE WITHOUT THE WRITTEN PERMISSION OF NPS OR THE AUTHOR IS PROHIBITED.

		UNLESS OTHERWISE SPECIFIED:	NAME	DATE
		DIMENSIONS ARE IN CM	DRAWN	M.A.
		TOLERANCES: +0.02 CM for clearance and fitting between parts	CHECKED	
		INTERPRET GEOMETRIC TOLERANCING PER:	ENG APPR.	
		MATERIAL	MFG APPR.	
		PC (Stratagis - Polycarbonate)	Q.A.	
		FINISH	COMMENTS: sparse printed	
NEXT ASSY	USED ON	DO NOT SCALE DRAWING		
NPS - AXV lab - SURFZONE PROTOTYPE				

TITLE: NPS - AXV lab Surfzone Prototype Sonar sensor mount		
SIZE	DWG. NO.	REV
A		
SCALE: 1:2	WEIGHT: 36 g	SHEET 1 OF 1

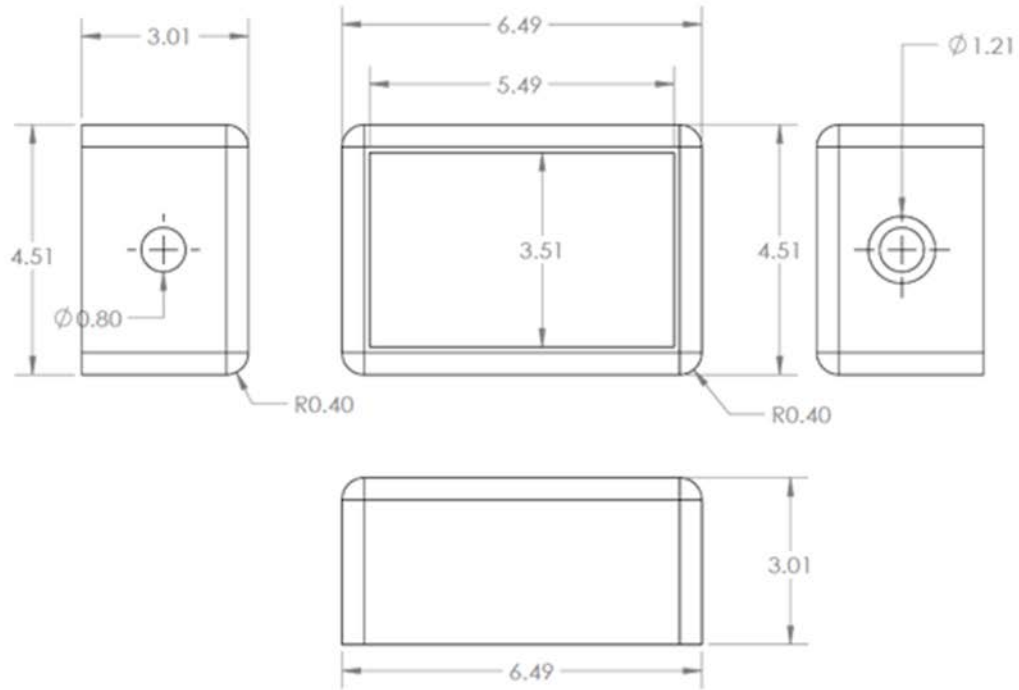
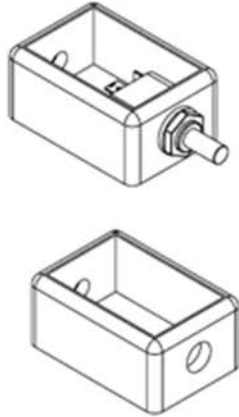
5

4

3

2

1



PROPRIETARY AND CONFIDENTIAL
 THE INFORMATION CONTAINED IN THIS DRAWING IS THE SOLE PROPERTY OF NAVAL POSTGRADUATE SCHOOL. ANY REPRODUCTION IN PART OR AS A WHOLE WITHOUT THE WRITTEN PERMISSION OF NPS OR THE AUTHOR IS PROHIBITED.

		UNLESS OTHERWISE SPECIFIED:		NAME	DATE	
		DIMENSIONS ARE IN CM	DRAWN	M.A.		
		TOLERANCES: +0.02 CM for clearance and fitting between parts	CHECKED			TITLE:
		INTERPRET GEOMETRIC TOLERANCING PER:	ENG APPR.			NPS - AXV lab
		MATERIAL	MFG APPR.			Surfzone Prototype - Thrusters
		PC (Styralys - Polycarbonate)	Q.A.			on/off switch holder
		FINISH	COMMENTS: Sparse printed			SIZE DWG. NO. REV
NEXT ASSY	USED ON					A
NPS - AXV lab - SURFZONE PROTOTYPE		DO NOT SCALE DRAWING				SCALE: 1:1 WEIGHT: SHEET 1 OF 1

5 4 3 2 1

LIST OF REFERENCES

- [1] 1 S. Halle, J. Hickie, "The design and implementation of a semi-autonomous surf-zone robot using advanced sensors and a common robot operating system," M.S. thesis, Dept. of Physics, Naval Postgraduate School, Monterey, CA, 2011.
- [2] 2 M. Slatt, "Development and testing of a hybrid wheg mobile platform for Autonomous surf-zone operations," M.S. thesis, Dept. of Physics, Naval Postgraduate School, Monterey, CA, 2011.
- [3] 3 J. Fitzgerald, "Characterization parameters for a three degree of freedom mobile robot," M.S. thesis, Dept. of Physics, Naval Postgraduate School, Monterey, CA, 2013.
- [4] 4 E. Shuey, M. Shuey, "Model and simulation for a surf-zone robot," M.S. thesis, Dept. of Physics, Naval Postgraduate School, Monterey, CA, 2012.
- [5] T. Bell, "Sea-shore interface robotic design," M.S. thesis, Dept. of Physics, Naval Postgraduate School, Monterey, CA, 2014.
- [6] LBC - Little Benthic Crawler. (n.d.). Teledyne SeaBotix. [Online]. Available: <http://www.seabotix.com/products/lbc.htm>. Accessed Oct. 23, 2015.
- [7] vLBC - vectored Little Benthic Crawler. (n.d.). Teledyne SeaBotix. [Online]. Available: <http://www.seabotix.com/products/vlbc.htm>. Accessed Oct. 23, 2015.
- [8] Product Overview - C-TALON Submersible Crawling Robot for Surf Zone, Riverine Environments and Limited-Access Harbor Areas. (n.d.). QinetiQ North America. [Online]. Available: <https://www.qinetiq-na.com/products/unmanned-systems/talon/c-talon/>. Accessed Oct. 23, 2015.
- [9] DOD, (2010, Nov. 8). Joint Publication 1-02, *DOD Dictionary of Military and Associated Terms*. [Online]. Available: http://www.dtic.mil/doctrine/new_pubs/jp1_02.pdf
- [10] The University Corporation for Atmospheric Research. (2004). The Comet Program. Rip Currents: Nearshore Fundamentals. [Online]. Available: http://www.cityoforangebeach.com/pages/know_your_beach/ripcurrents/near_shore_formation/print.htm#21

- [11] DOD - CJCS. (2015, Jan. 23). *Joint Capabilities Integration and Development System (JCIDS)*. [Online]. Available: <http://acqnotes.com/wp-content/uploads/2014/09/CJCS-Instruction-3170-01I-Joint-Capabilities-Integration-and-Development-System-23-Jan-15.pdf>
- [12] O. Garcia, "Sensors and algorithms for an unmanned surf zone robot," unpublished.
- [13] R. D. Christ and R. L. Wernli, *The ROV Manual, A User Guide for Remotely Operated Vehicles*. Oxford, England, Butterworth-Heinemann, 2013.
- [14] A. Dirks. (2015, June 15). Waterproof Vessel - Technical Guide. [Online]. Available: <http://crustcrawler.com/products/Waterproof%20Enclosure/>
- [15] PC (polycarbonate), production-grade thermoplastic for FORTUS 3D production systems (Spec sheet). (2015). Stratasys. [Online]. Available: <http://www.stratasys.com/materials/fdm/pc>
- [16] ABSplus-P430, production-grade thermoplastic for DESIGN series 3D printers (Spec sheet). (2015). Stratasys. [Online]. Available: <http://www.stratasys.com/materials/fdm/absplus>
- [17] Sealing FDM parts. (2015). Stratasys. [Online]. Available: <http://www.stratasys.com/solutions/finishing-processes/sealing-fdm-parts>
- [18] R. Butcher and L. Rydill. *Concepts in Submarine Design*, Illustrated edition ed. New York, Cambridge University Press, 1994.
- [19] 400HFS-L Hi-Flow Thruster - Data Sheet. (2015). CrustCrawler. [Online]. Available: <http://crustcrawler.com/products/urov2/index.php>
- [20] R. D. Christ and R. L. Wernli, *The ROV Manual: A User Guide for Observation-Class Remotely Operated Vehicles*. Amsterdam, Holland, Butterworth-Heinemann, 2007.
- [21] A. Ugural, "Chapter 13: Belts, chains, clutches, and brakes," in *Mechanical Design: An Integrated Approach*, MacGraw-Hill, New York, NY, 2004. pp. 507–558.
- [22] 45 teeth sprocket specification (SS 304). (2015). SDP-SI. [Online]. Available: <http://sdp-si.com/eStore/Catalog/Group/585=>
- [23] 13 teeth sprocket specification (SS 304). (2015). SDP-SI. [Online]. Available: <http://sdp-si.com/eStore/Catalog/Group/585=>

- [24] National Institute of Standards and Technology (NIST). (2008). *Autonomy Levels for Unmanned Systems (ALFUS) Framework*. [Online]. Available: http://www.nist.gov/el/isd/ks/upload/NISTSP_1011-I-2-0.pdf
- [25] Maxon Motor (273752), RE 35, 35mm, Graphite Brushes, 90 Watt, Spec sheet. (2015). Maxon motor. [Online]. Available: http://www.maxonmotor.com/medias/sys_master/root/8816798859294/15-140-EN.pdf
- [26] Maxon Motor Planetary Gearhead (326661) GP 32 HP, 32mm, 4.0-8.9 Nm Spec sheet. (2015). Maxon motor. [Online]. Available: http://www.maxonmotor.com/medias/sys_master/root/8816809115678/15-310-EN.pdf

THIS PAGE INTENTIONALLY LEFT BLANK

INITIAL DISTRIBUTION LIST

1. Defense Technical Information Center
Ft. Belvoir, Virginia
2. Dudley Knox Library
Naval Postgraduate School
Monterey, California